8-13-2024 5:00 PM

Analysis of Healthy Glenohumeral Arthrokinematics and Anatomic Shoulder Implant Subluxation Using 4DCT

Kylie Kiera Paliani, *Western University*

Supervisor: Lalone, Emily A., *The University of Western Ontario*
Co-Supervisor: Johnson, James A., *The University of Western Ontario*
A thesis submitted in partial fulfillment of the requirements for the Master of Engineering Science degree in Biomedical Engineering

Abstract

The shoulder is the most mobile joint in the human body, with the glenohumeral joint specifically allowing a wide range of motion and a high incidence of instability due to its ability to translate, as well as rotate in its socket. However, the extent of translation in a healthy glenohumeral joint is not well-established. Additionally, it is unclear if subluxation correction after anatomic total shoulder arthroplasty (TSA) with posterior augmented glenoid (PAG) implants remains consistent throughout active motion. This thesis aimed to evaluate healthy glenohumeral arthrokinematics to benchmark normal joint proximity and translation, and to assess if a TSA with PAG implants correct subluxation and maintain joint mechanics throughout motion post-surgery. Using four-dimensional computed tomography, 3D Slicer, and ICP registration, the study found that healthy glenohumeral proximity and translation were mostly consistent across ages and that a TSA with PAG implants effectively restored and maintained corrected joint mechanics throughout active motion.

Keywords

Glenohumeral Joint, Shoulder Osteoarthritis, Arthrokinematics, Joint Translation, Anatomic Total Shoulder Arthroplasty, Walch Type B2 Glenoid, Subluxation, Internal Rotation, Forward Elevation, Four-Dimensional Computed Tomography (4DCT)

Summary for Lay Audience

The shoulder joint, also known as the glenohumeral joint (articulation between the humeral head and glenoid) is the most mobile joint in the human body and enables people to move their arms freely in many directions. Due to the unique makeup of the shoulder joint, it can slide (translate) in addition to rotate in its socket. This makes the joint prone to instability, which can eventually lead to a greater chance of needing a shoulder replacement. Currently, it is not well-established how much translation occurs in the healthy glenohumeral joint and how that changes overtime as people age. Additionally, it is unknown if shoulder stability, corrected by a specific type of shoulder replacement surgery (anatomic total shoulder arthroplasty) using special implants (posterior augmented glenoid implants), stays consistent during activities of daily living.

This thesis aimed to understand how a healthy shoulder joint moves throughout different motions and to determine if these special implants can correct shoulder displacement and keep the joint stable during movement after surgery. Advanced imaging techniques, such as four-dimensional computed tomography (4DCT), were used to observe these movements in detail. Three-dimensional bone models were made from these scans and were used in the analyses to see how the glenohumeral joint moves within different people.

In the first study, the research findings highlighted the importance of translation within the joint during movements of daily living, which can then be used in the design and optimization of shoulder implants. In the second study, patients who received the shoulder replacement, due to conditions like osteoarthritis (where the shoulder joint erodes and becomes unstable), found the implants to be effective. These implants corrected the dislocation and kept the shoulder stable throughout movement.

Overall, the findings in this thesis showcased how important translation is within the healthy glenohumeral joint to achieve good functional movement. As well, this work demonstrated that the special shoulder implants are effective at restoring and maintaining proper shoulder alignment during daily movements. These results allow for better-informed clinical decisions, improved patient care, and enhanced outcomes in treatment of shoulder instability.

Co-Authorship Statement

Chapter 1:

Sole Author: Kylie Paliani

Manuscript Reviewers: James Johnson, and Emily Lalone

Chapter 2:

Study Design: George Athwal, James Johnson, Emily Lalone, and Kylie Paliani

Data Collection: Baraa Daher, James Hunter, and Emily Lalone

Statistical Analysis: Kylie Paliani

Manuscript Writer: Kylie Paliani

Manuscript Reviewers: George Athwal, James Johnson, and Emily Lalone

Special Contribution: Analysis of joint proximity and translation for the first seven participants was previously completed and published in Baraa Daher's thesis.

Chapter 3:

Study Design: George Athwal, James Johnson, Emily Lalone, and Kylie Paliani

Data Collection: Emily Lalone, James Hunter, and Kylie Paliani

Statistical Analysis: Kylie Paliani

Manuscript Writer: Kylie Paliani

Manuscript Reviewers: George Athwal, James Johnson, and Emily Lalone

Chapter 4:

Sole Author: Kylie Paliani

Manuscript Reviewers: James Johnson, and Emily Lalone

Acknowledgements

I want to recognize and thank everyone who made the work in this thesis possible. To my supervisor, Dr. Emily Lalone, I simply do not have enough words for all the support you have given me throughout this entire process and for your constant kindness. You have been there for me, every step of the way, to encourage me to always do my best work. You have truly inspired me as a woman in engineering to continue to do great things within this industry. To my other supervisor, Dr. Jim Johnson, since meeting you in my undergraduate degree here at Western University, you lit the passion within me to pursue Biomedical Engineering and for that I am thankful to have had a professor and supervisor as caring and as brilliant as you.

I would also like to thank my advisory committee member, medical mentor and shoulder expert, Dr. George Athwal. It was clear early on that you have had an incredible impact on your patients through the stories that they shared about you as a surgeon. Your passion and excitement in your field were evident in every meeting that I had with you about my work and its findings. Your feedback and mentorship have meant so much to me and I feel lucky to have been able to work alongside you and learn from your expertise.

Thank you to all my past and present labmates: Carla, Lauren, Elizabeth, James, Max, Megan, Randa, Christian, Jennifer, Marie, and Laura. You have truly been the most incredible people to work with and I have learned something from every single one of you. A special thank you to my one and only 'Team Shoulder' member, James Hunter. It has been a pleasure to work and learn from you and I am beyond thankful for all your mentorship.

Lastly, I would like to thank my family, friends, and boyfriend. Mom, thank you for being my "Western Uber" and driving me to lectures, meetings, exams, conferences, etc., as well as being the best writing coach through the years. Dad, you have always been a true inspiration of what hard work looks like and I'll never forget all the hours you spent teaching me Math and Science growing up. Grandma, you have shown me that if you know who you are, you will be successful at anything in life. To my older brothers, Kian and Keelan, I am grateful to have had academic support and guidance from you throughout the years. To my boyfriend Adrian, thank you for your constant and unwavering support for me to pursue my passion and dreams. I simply would not be the person I am today without all of you, so thank you.

Table of Contents

List of Tables

List of Figures

List of Appendices

Chapter 1

1 Introduction

The shoulder is an incredibly complex and mobile joint, that when subjected to everyday use, often leads to lingering shoulder issues over time. Many people endure shoulder pain for far too long, and even after receiving a shoulder replacement, they often do not regain their full range of motion. This chapter introduces the main topic of this thesis: the shoulder. It starts with outlining shoulder anatomy, exploring how the shoulder joint moves and then compares how different imaging modalities have been used to assess the shoulder. It then delves into various shoulder pathologies, how they cause pain, and how they affect shoulder range of motion during different movements. Additionally, this chapter examines the role of shoulder replacements in addressing these issues. Finally, a summary of the thesis motivation, objectives, and hypotheses are outlined.

1.1 Shoulder Anatomy

The shoulder is the most mobile joint in the human body and is considered part of the shoulder girdle within the appendicular skeleton.[1] The shoulder girdle serves as the primary connection between the upper limbs of the appendicular skeleton and the thoracic cage of the axial skeleton. It consists of three bones: the humerus (upper arm bone), scapula (shoulder blade), and clavicle (collar bone) (Figure 1-1). These bones interact to form four main joints/articulations of the shoulder: the glenohumeral (GH) joint, acromioclavicular (AC) joint, sternoclavicular (SC) joint, and scapulothoracic (SC) joint.[2] The subsequent sections will delve into the anatomy of these shoulder bones, joints, and their associated muscles, ligaments, and tendons.*

---

*All anatomical terms and definitions were referenced using the same resources.[3–5]

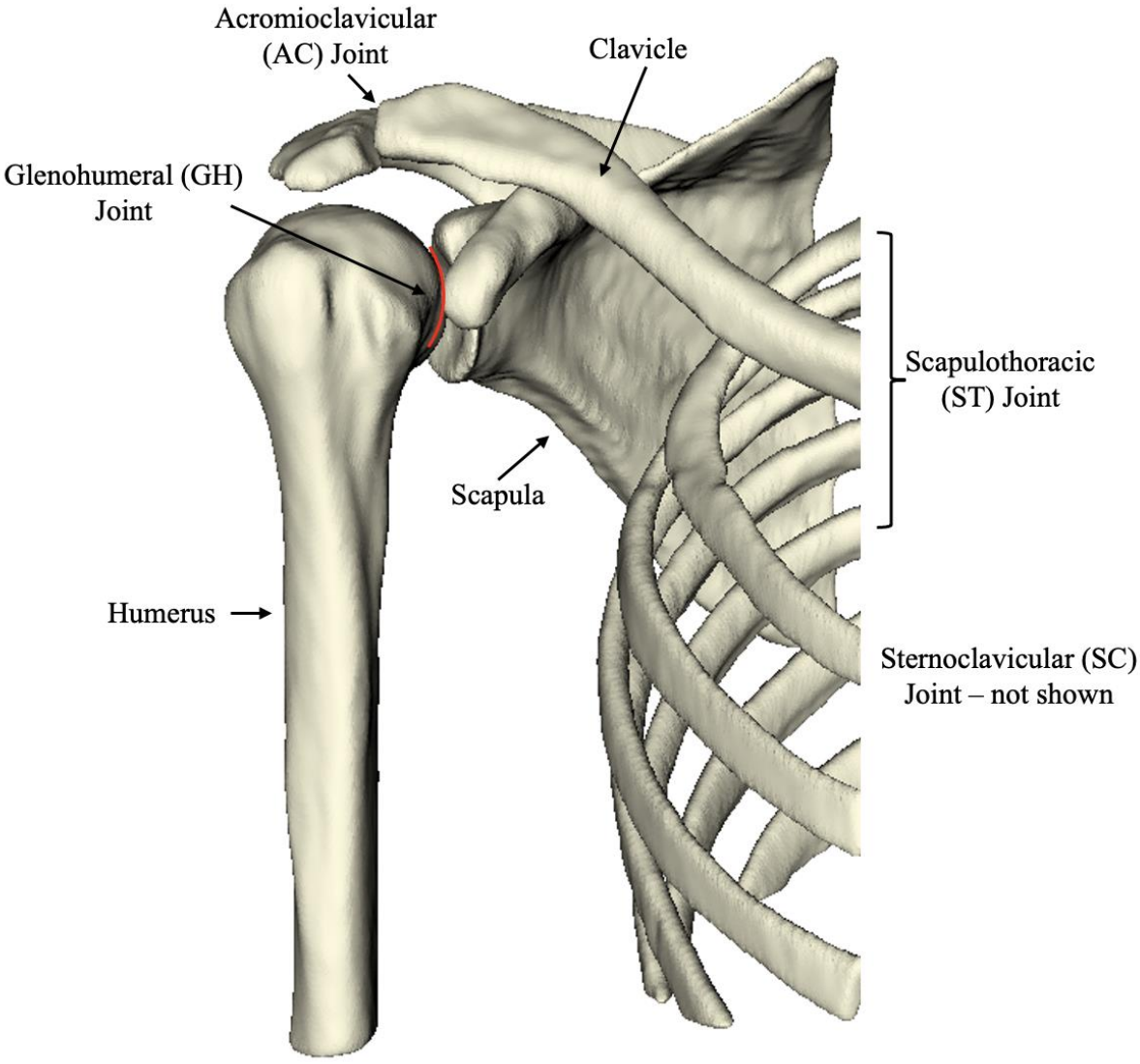

Figure 1-1: Shoulder Bones and Joints

Anterior view of the shoulder joint. Note that the glenohumeral joint is outlined by the red line and that the sternoclavicular joint is not shown on the figure.

1.1.1 Osteology

The following section will highlight the three shoulder bones associated with the shoulder complex. These three bones (i.e., humerus, scapula and clavicle) all play an important role in providing the shoulder with the movement and range of motion that it exhibits.

1.1.1.1 Humerus

The humerus, otherwise known as the upper arm bone, is a long bone that plays a very important role in the shoulder joint.

The proximal end of the humerus contains many significant bony landmarks. On the medial side sits one of the most remarkable bony landmarks, the humeral head, which is a spherical shaped bone that sits into the glenoid cavity of the scapula (Figure 1-2). The articulation between these two bones creates the glenohumeral joint, which is the main focus of this thesis. The more lateral side of the humeral head is used as the attachment point for all four rotator cuff muscles, in addition to three other upper extremity muscles, and contains two main distinguishing points, the greater and lesser tubercules.

The greater tubercule, a large bony protrusion located posteriorly on the head, is imperative to the shoulder joint because three of the four rotator cuff muscles, for example, the supraspinatus, infraspinatus, and teres minor, insert into the superior, middle, and inferior facet of the greater tubercule, respectively. The lesser tubercule, located anteriorly on the head, is a smaller version of the greater tubercule and is the insertion of the fourth rotator cuff muscle, the subscapularis. Within the middle of these two tubercules is the intertubercular sulcus (i.e., bicipital groove), which is a valley that the deltoid muscle extends through. Superior to these tubercules sits the anatomical neck, and inferior to these tubercules sits the surgical neck, which is where the tubercules merge distally into the starting point of the long, cylindrical shaft of the humerus.

On the shaft of the humerus, about one-third of the way to the elbow, is a roughened portion of the shaft called the deltoid tuberosity, which serves as the attachment point for the deltoid muscle. Finally, at the distal end of the humerus are the articulations between the humerus and the radius and ulna, creating the elbow joint.

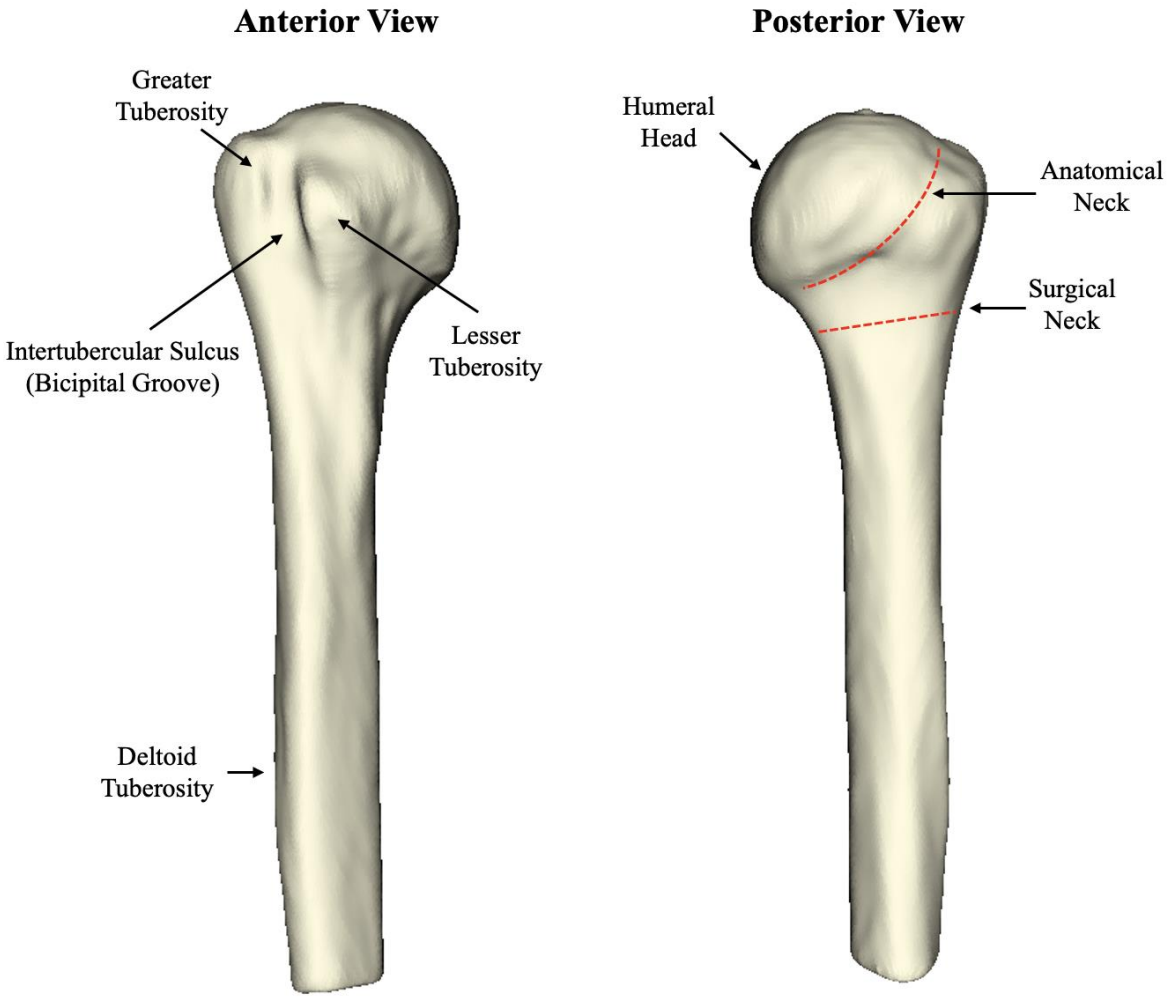

Figure 1-2: Bony Anatomy of the Humerus

Anterior (left) and posterior (right) view of the proximal humerus.

1.1.1.2 Scapula

The scapula, colloquially known as the shoulder blade, is a strong, flat, triangular bone that connects the clavicle to the humerus and contains three of the four shoulder articulations including, the glenohumeral, acromioclavicular and scapulothoracic joints (Figure 1-3). Overall, the scapula consists of two surfaces (e.g., anterior/costal, and posterior), three borders (e.g., superior, lateral and medial), three angles (e.g., superior, inferior, and lateral), three processes (e.g., coracoid, spinous, and acromion) and four fossas (e.g., supraspinous fossa, infraspinous fossa, subscapular fossa, and glenoid fossa). The scapula is vital to the function of the shoulder, since it acts as the attachment bone for various important muscles, including the rotator cuff muscles. These 17 different muscle attachments stabilize the scapula, causing minimal chance of fracture of this bone.[6]

Due to the scapula's unique triangular shape, it consists of three borders and three angles. The lateral border is the thickest and strongest of the three borders and includes the glenoid cavity, which articulates with the humeral head, forming the glenohumeral joint. Following the lateral border inferiorly is the inferior angle, which connects the lateral border and medial border. The medial border is a thin border that runs parallel to the spine. Following the medial border superiorly is the superior angle, which connects the medial border to the superior border. The superior border is the thinnest and shortest border. Following it laterally, the scapular notch can be found at the beginning of the lateral angle. The lateral angle connects the superior border back to the lateral border. The entirety of the body of the scapula articulates with the thorax to create the scapulothoracic (ST) joint.

The body of the scapula includes a posterior side and anterior/costal side of the scapula. The posterior side of the scapula is concave, and its most prominent feature is the spinous process, which is more commonly known as the spine of the scapula. The spine is a triangular bony protrusion that spans transversely across the posterior side of the scapula, dividing it into two fossae, and eventually turns into the acromion. Superior to the spine is the supraspinous fossa, which is a smooth, convex surface that is larger at its lateral end, and is the origin for one of the four rotator cuff muscles, the supraspinatus. Inferior to the spine is the infraspinous fossa, which is the larger of the two fossae but not as convex, and is the origin for two rotator cuff muscles, the infraspinatus, and teres minor. The entire

anterior or costal side of the scapula is a concave, smooth surface called the subscapular fossa, which is the origin of the large subscapularis muscle.

The lateral end of the scapula also includes some of the most important bony landmarks including, the glenoid fossa or glenoid cavity, coracoid process, and acromion. The most important to this thesis is the glenoid fossa, which is a smooth shallow, concave, pear-shaped surface that articulates with the humeral head, forming the glenohumeral (GH) joint.[7] The glenoid is considered pear-shaped due to it having a larger anterior-posterior diameter inferiorly than superiorly. Its concave surface is also very shallow, allowing it to articulate with 25% of the humeral head,[6] which gives rise to an unstable articulation causing translations in the joint and making it unable to act like a true ball and socket joint.[8–10] Superior to the glenoid is the supraglenoid tubercle, and inferior to the glenoid fossa is the infraglenoid tubercle, which are important attachment points for the bicep and tricep muscles, respectively. Extending from the superior-anterior part of the lateral edge of the scapula is the acromion process, which is a hook-like bony protrusion that points laterally forward. The acromion is an important attachment point for muscles and ligaments of the shoulder, especially between the scapula and clavicle. The acromion extends from the spine of the scapula on the posterior side and arches anteriorly towards the glenoid. The acromion articulates with the clavicle to form the acromioclavicular (AC) joint.

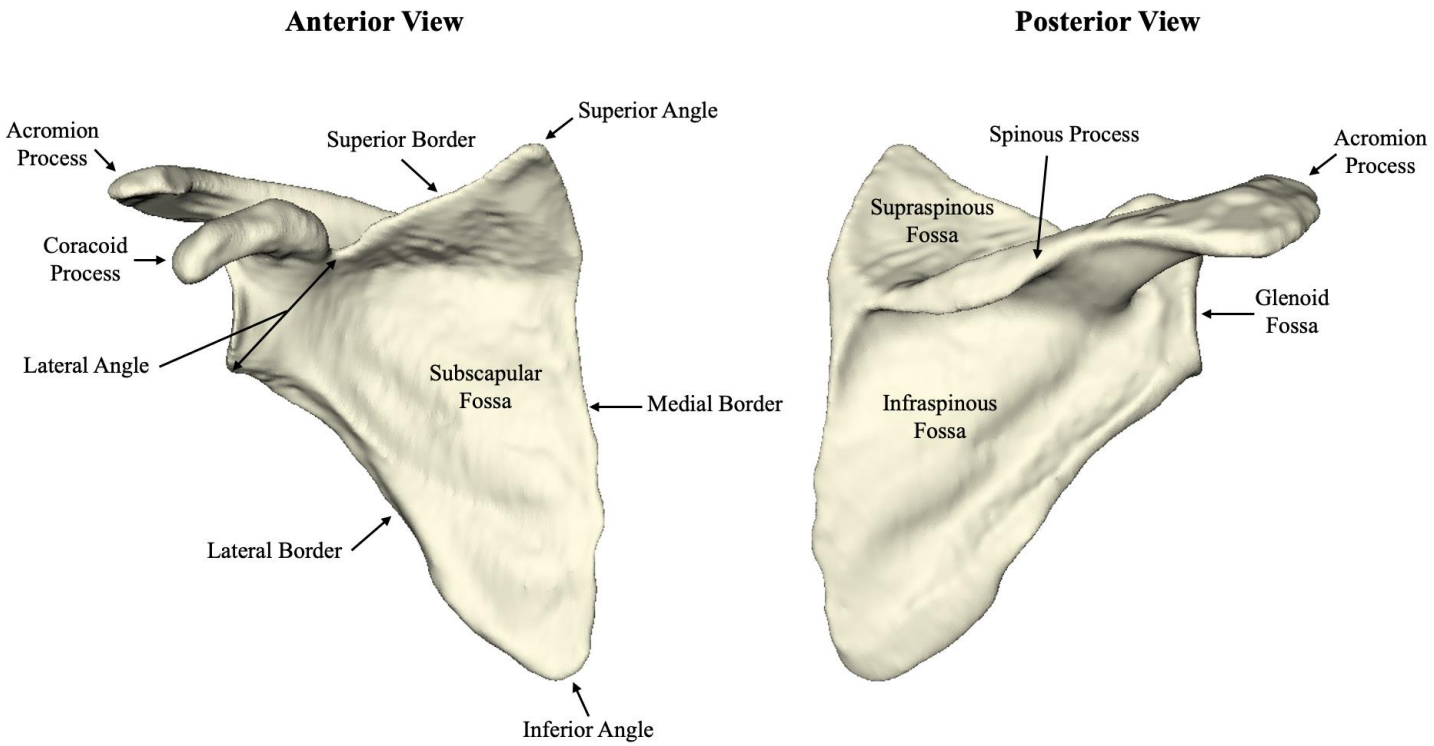

Figure 1-3: Bony Anatomy of the Scapula

Anterior (left) and posterior (right) views of the scapula including all important bony landmarks.

1.1.1.3 Clavicle

The clavicle, also known as the collar bone, is one of the three bones that exist in the shoulder. The clavicle is an ‘S’ or crank-shaped bone (as viewed from above or below) that connects the manubrium of the sternum to the acromion of the scapula, being a prime component in supporting the forces that act from the upper limbs into the thorax (Figure 1-4). Due to this, it is also one of the most frequently broken bones in the human body.

The sternal or medial end is thicker, more cylindrical, and contains the sternal facet which is the articulation of the scapulothoracic (SC) joint. On the inferior side of the sternal end is a rough, oval impression for the costoclavicular ligament attachment. The shaft of the clavicle is an important attachment point for numerous muscles contributing to shoulder function.

The acromial or lateral end is more flattened and contains an acromial facet, which is the articulation of the acromioclavicular (AC) joint. On the inferior side of the acromial end is the conoid tubercle, which is the attachment point for the conoid ligament.

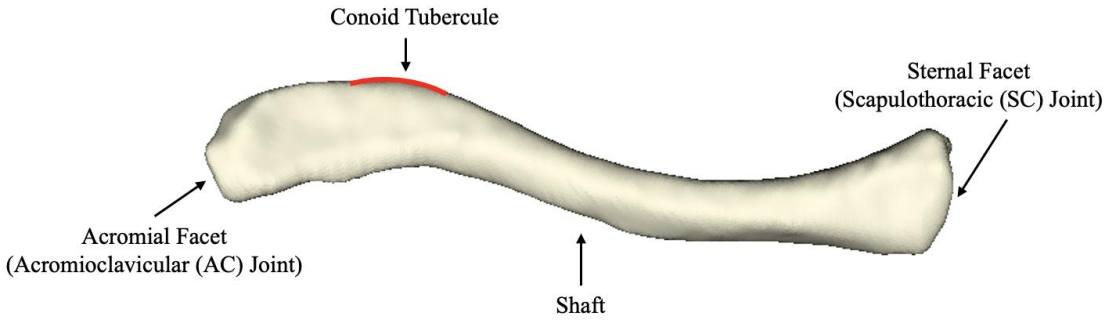

Figure 1-4: Bony Anatomy of the Clavicle

Superior view of the clavicle. Note the conoid tubercule is highlighted in red.

1.1.2 Articulations

The three shoulder bones described in detail in Section 1.1.1 make up the four unique shoulder articulations: the glenohumeral (GH) joint, acromioclavicular (AC) joint, sternoclavicular (SC) joint, and scapulothoracic (ST) joint. These joints all play a vital role in shoulder movement, but the focus of this thesis is the glenohumeral joint.

1.1.2.1 Glenohumeral Joint

The glenohumeral joint, which is the centre of movement at the shoulder complex, is considered a synovial, ball-and-socket joint.[11] A ball-and-socket joint is the type of joint in the body that allows for the largest range of motion (ROM) due to the ability to rotate (3 degrees of freedom (DOF)) in its socket. The humeral head of the humerus sits into the scapula through a socket, known as the glenoid cavity. The glenoid cavity is very shallow in comparison to the humeral head curvature, meaning only a portion of the humeral head is in contact with the glenoid cavity at any given time. This allows the glenohumeral joint to have a wide range of motion due to the ability to not only rotate, but also translate in its socket. Besides the shoulder, the hip is the only other ball-and-socket joint in the human body. Synovial joints are the most common type of joint in the human body and allow for the smooth gliding of the bones over one another.[12] They consist of smooth articular cartilage that lines the bones on either side of the articulation and synovial fluid within the joint cavity, encapsuled by a synovial membrane. Overall, the glenohumeral joint is a complex joint that employs multiple unique mechanisms to achieve full functionality.

1.1.2.2 Acromioclavicular, Scapulothoracic, and Sternoclavicular Joints

The acromioclavicular (AC) joint functions as a plane synovial joint and connects the acromion of the scapula to the clavicle. Various ligaments including the coracoclavicular ligament, superior and inferior acromioclavicular ligaments all act as important stabilizers for this joint.

The scapulothoracic (ST) joint, although not technically classified as a true joint, acts as one as the anterior part of the scapula glides over the posterior thoracic cage.

The sternoclavicular (SC) joint is a synovial saddle joint. It is the only joint that attaches the upper limb to the axial skeleton by connecting the clavicle to the sternum.

1.1.3 Passive Soft Tissue

Due to the shoulder being a complex joint, there are many specific shoulder muscles, ligaments, and tendons that work together to provide this joint with its extensive range of motion, as well as, to help stabilize the joint.

1.1.3.1 Ligaments

Ligaments, otherwise known as passive soft tissue, are fibrous connective tissues that connect a bone to another bone. They are so important within the joint to keep it stabilized so that it does not twist too much or move too far apart and become dislocated, which is a big issue at the glenohumeral joint. The joint capsule, glenoid labrum and associated ligaments are all important soft tissue structures that provide stability to the joint (Figure 1-5).

The shoulder joint capsule is a watertight sack that surrounds the glenohumeral joint and is considered the main source of stability at the shoulder. It is moderately loose throughout normal motion to allow for a wide ROM, but becomes tensioned near the extremes of motion to stabilize the joint and permit large translations of the humeral head.[13] The capsule is thin and connects the rim of the glenoid to the anatomical neck of the humerus. It is formed by an outer fibrous membrane and an inner synovial membrane. Located on the anterior part of the joint sack are three of the glenohumeral ligaments: superior glenohumeral ligament, middle glenohumeral ligament, and inferior glenohumeral ligament. Although not well-defined ligaments, these ‘pleated folds’ of the capsule help hold the shoulder in place and stop it from dislocating.

There are two other important ligaments surrounding the glenohumeral joint: the transverse humeral ligament, which originates at the lesser tubercule and inserts at the greater tubercule, and the coracohumeral ligament, which originates from the coracoid process and inserts on the humeral head near the lesser and greater tubercules. The coracohumeral ligament supports the upper part of the joint capsule.

Other important ligaments that stabilize the joint include the coracoacromial ligament and the coracoclavicular ligament. The coracoacromial ligament connects the coracoid process to the acromial process and forms a ‘roof’ over the humeral head to provide support when an upward facing force is applied to the humerus. The coracoclavicular ligament is made up of two smaller ligaments, the trapezoid ligament and the conoid ligament, that connect the coracoid process to the clavicle. These ligaments are strong vertical stabilizers of the AC joint, preventing against superior dislocation of the AC joint and excessive rotation of the scapula and clavicle.

Another structure that contributes to the stability of the shoulder joint is the glenoid labrum. It is a fibrocartilaginous ring that fully surrounds the edge of the glenoid, deepening the socket to better accommodate the humeral head, since the glenoid socket is quite shallow in nature. This provides added stability and securement for humeral head movement.

1.1.3.2 Tendons

Tendons are sturdy bands of connective tissue that connect muscle to bone. Comprised of collagen, much like ligaments, they have the capacity to withstand heightened tension. Tendons play a pivotal role in enabling muscle contraction to move the bones within the body. Important tendons that exist in the shoulder complex include the long head of biceps tendon (which connects directly to the glenoid labrum) and the four rotator cuff tendons: subscapularis tendon, infraspinatus tendon, teres minor tendon, and subscapularis tendon.

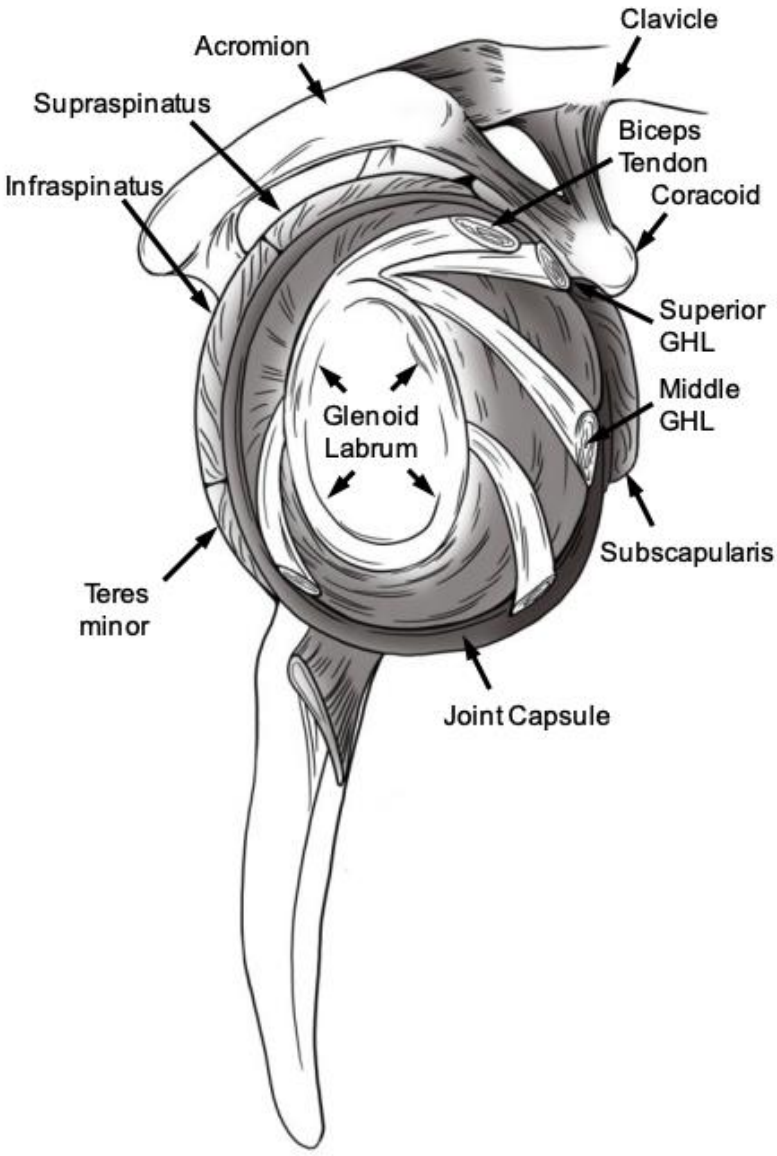

Figure 1-5: Lateral View of the Glenohumeral Joint and Associated Soft Tissue Structures

Important soft tissue structures to note in this illustration are the glenoid labrum that borders the glenoid, the joint capsule that encompasses the entire joint, the three glenohumeral ligaments (superior, middle and inferior glenohumeral ligaments), the biceps tendon, as well as the four rotator cuff tendons (supraspinatous tendon, infraspinatus tendon, teres minor tendon, and subscapularis tendon).

1.1.4 Muscles

Muscles, otherwise known as active soft tissue, are present in the shoulder for numerous reasons including, holding the joint in place, assisting in a variety of movements (e.g., raising and rotating the arm), and providing structural support and stability to the joint. Due to the passive soft tissues (ligaments and tendons) not being able to actively guide motion in the shoulder, the muscles in the shoulder are required to aid in the dynamic stability of the glenohumeral joint. There are many muscles in the shoulder that assist with shoulder range of motion, but for the purpose of this work, only the ones that contribute mostly to glenohumeral movement will be discussed (Figure 1-6).

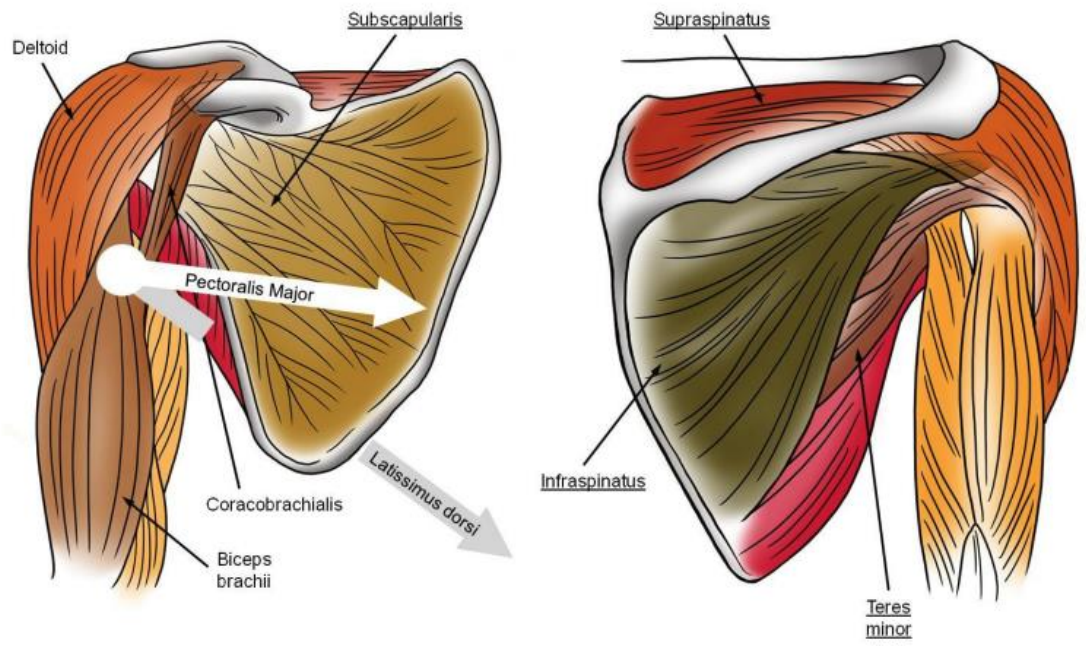

Figure 1-6: Scapulohumeral Shoulder Muscles

Anterior (left) and posterior (right) view of the scapulohumeral shoulder muscles. Note: the four rotator cuff muscles (subscapularis, infraspinatus, teres minor, and subscapularis) are underlined and the arrows indicate the direction of pull of the latissimus dorsi and pectoralis major muscles that are not shown.

1.1.4.1 Rotator Cuff Muscles

Some of the most important muscles in the shoulder joint are the four rotator cuff muscles: supraspinatus, infraspinatus, teres minor and subscapularis. The rotator cuff muscles are known for providing the shoulder with its motion and add stability. The supraspinatus, infraspinatus, and teres minor muscles are located on the posterior side of the scapula, and the subscapularis muscle is located on the anterior side of the scapula.

The supraspinatus is located superior to the spine of the scapula. It originates from the supraspinous fossa, wrapping superiorly over the humeral head and inserting on the superior facet of the greater tuberosity of the humerus. The supraspinatus is responsible mainly for abduction of the shoulder and gets protection from the subacromial bursa to avoid impingement with the acromion.

The infraspinatus muscle is located below the spine of the scapula. It originates from the infraspinatus fossa, wraps around the posterosuperior part of the humeral head and inserts into the middle facet of the greater tuberosity of the humerus. The infraspinatus is responsible mainly for external rotation of the shoulder and aids in providing support to the posterior side of the joint capsule, while ensuring no posterior dislocation occurs.

The teres minor is located inferior to the infraspinatus. It originates from the lateral scapula border and inserts into the inferior facet of the greater tuberosity of the humerus. In addition to the infraspinatus, the teres minor also assists in external rotation of the shoulder while providing support to avoid posterior dislocation.

The subscapularis is located and originates on the subscapular fossa, wrapping anteriorly around the humeral head and inserts into the lesser tuberosity of the humerus. This muscle is the largest and strongest rotator cuff muscle, equaling around 50% of rotator cuff strength output. The subscapularis is responsible mainly for internal rotation of the shoulder.

1.1.4.2 Deltoid

Other than the rotator cuff muscles, one other important muscle that aids in glenohumeral stability and movement is the deltoid. The deltoid is a superficial muscle that is triangular in shape and covers the shoulder on three sides, giving the shoulder its rounded shape. The deltoid muscle has the largest moment of all shoulder muscles during elevation, is the largest in cross section and is the primary elevator of the shoulder. Due to the large cross section, the deltoid is separated into three separate parts (or heads): anterior, middle, and posterior deltoid muscles. These three parts of the deltoid have various locations of origin including, the outer third of the clavicle (anterior), lateral side of the acromion process (middle), and spine of the scapula (posterior), but all insert into one common location, the deltoid tuberosity. All three parts of the deltoid are effective in aiding the joint in abduction, however, due to its vertical line of pull being lateral to the joint axis, the middle deltoid contributes the most to this movement.

The pectoralis major and latissimus dorsi are two other muscles that contribute largely to the abduction of the shoulder. They both originate on the torso and insert on the humerus. The pectorals major muscle along with the anterior deltoid muscle contribute mostly to forward elevation and internal rotation, whereas the latissimus dorsi muscle along with the posterior deltoid contribute mostly to extension and internal rotation.

1.2 Shoulder Kinematics

1.2.1 Shoulder Movements

Due to the unique make-up of the shoulder, including the osseous and soft tissue structures, the shoulder joint can achieve a wide range of motion, which enables people to move their arms freely in many directions[12]: flexion (forward), extension (backward), abduction (out), adduction (in), internal rotation (in or down), external rotation (out or up) and even circumduction (a combination of flexion, extension, abduction, and adduction) (Figure 1-7).

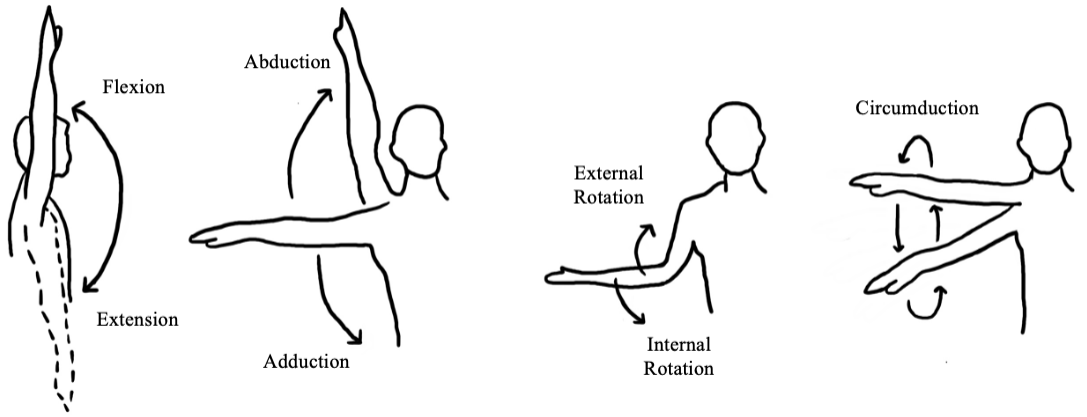

Figure 1-7: Basic Shoulder Movements

An illustration of all the basic shoulder movements that allow people to move their arms.

The humerus position relative to the scapula can be described by different sequences of motion including, planes of elevation, elevation angles and axial rotation angles (Figure 1-8). Planes of elevations refers to the various planes that occur when the shoulder is elevated. Looking at Figure 1-8, 0° shows flexion, 180° shows extension, and 90° shows abduction in the frontal plane. Elevation angles are various angles that occur when the arm moves away (abduction) or towards (adduction) the body. Axial rotation angles are how much the humeral head is rotated about its long axis, also referring to internal and external rotation.

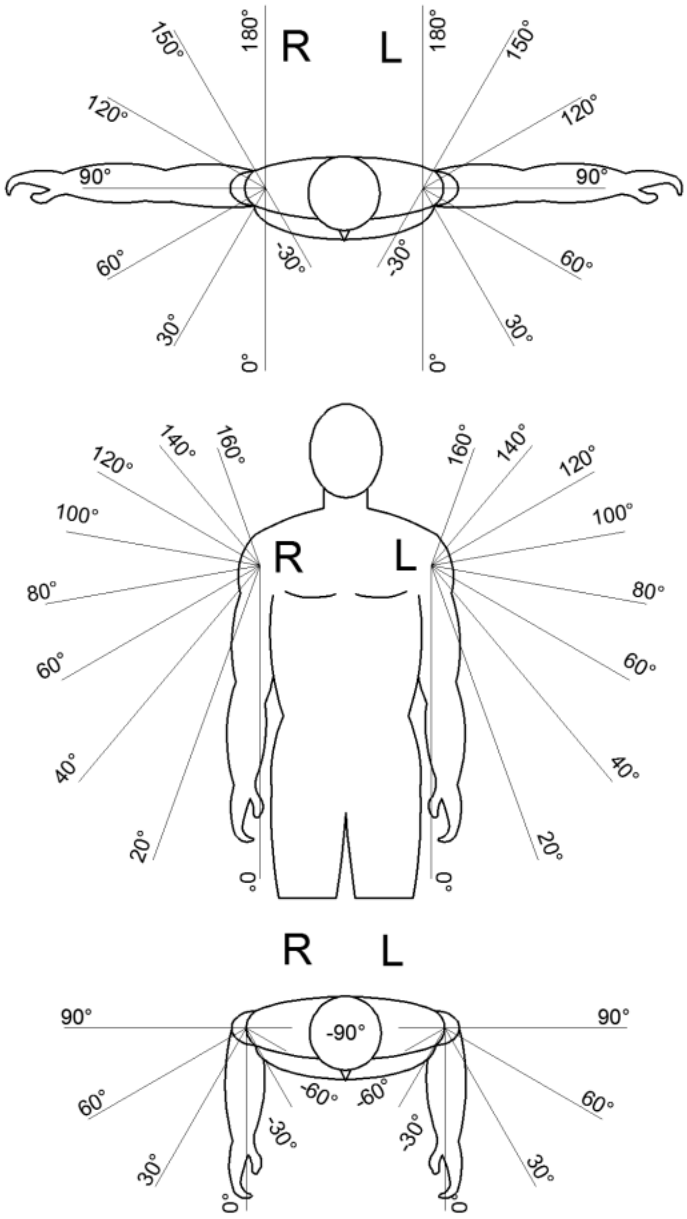

Figure 1-8: Shoulder Positions in Different Planes of Motion

The top illustrates the planes of elevation, the middle illustrates elevation angles (abduction and adduction), and the bottom illustrates axial rotation angles (internal and external humeral rotation).

1.2.2 Glenohumeral Rotation and Translation

Humeral head rotation and translation are crucial for providing the glenohumeral joint with its extensive range of motion and fluidity, facilitating smooth and coordinated shoulder movements. The articular surface of the humeral head is greater than that of the glenoid fossa, having a surface area ratio of around a 3:1, and giving the joint an appearance similar to a golf ball on a tee.[14] If the glenohumeral joint only allowed for rotation of the humeral head, it would run out of room to rotate quickly after starting abduction and the deltoid would pull the head of the humerus into the acromion causing impingement. However, the glenohumeral joint rotates along the glenoid, while also sliding inferiorly, so that it remains in contact with the glenoid throughout the entire motion. Another point to note is that complete abduction of the shoulder can only occur when the humeral head is laterally rotated.[15] When the humeral head is medially rotated, the greater tuberosity runs into the acromion process, inhibiting full range of motion. However, when the humeral head is laterally rotated, the greater tuberosity is being rotated from under the acromion process to allow for that full range of motion.[15] This showcases the complexity of glenohumeral joint motion and how translation and rotation are vital in allowing a person to achieve full range of motion of their shoulder.

Currently, it has not been well-established in literature how much translation is essential to providing a healthy range of motion in the shoulder, especially for specific populations of people. Previously, there has been research done to study glenohumeral translations, but there are several limitations within the research that currently exist. Many of the studies have been mainly focused on patients who have already acquired pathologies (i.e., osteoarthritis (OA) or instability) or who have already undergone shoulder surgeries,[16–21] not on healthy patients. The studies that have focused on healthy glenohumeral joint movement have primarily used cadaveric specimens,[19,22–24] however, the in vitro loading environment may not fully stimulate the in vivo physiological state.[25–27] As well, the majority of these studies have assessed the shoulder using static imaging modalities and have not yet been able to see dynamically what is happening at the joint. Additionally, the majority of these studies have used the centre of the humeral head to track translation within the shoulder, and not the actual joint surfaces. All of these limitations within this

area of research have led to a specific knowledge gap surrounding glenohumeral arthrokinematics (translation) during active motion for various ages of people. The second chapter of this thesis tackles this gap in knowledge by completing an in-depth analysis of the healthy glenohumeral joint during active motion for various age groups.

Understanding healthy glenohumeral translation is important because it establishes a benchmark for normal range of motion, enabling surgeons and clinicians to assess whether full functional and anatomical restoration of the joint has been achieved following reparative or reconstructive surgeries (arthroplasty). Arthroplasty is the surgical reconstruction or replacement of a joint. As discussed in more detail in Section 1.5, there are three main arthroplasty options for glenohumeral OA: anatomic total shoulder arthroplasty (TSA), reverse total shoulder arthroplasty (RTSA), and hemiarthroplasty. TSA is when the implant components match the normal anatomy of the shoulder,[28] RTSA is when the implant components of the glenohumeral joint are the opposite of human anatomy, and hemiarthroplasty is when the humeral articular surface of the native joint is replaced with a stemmed humeral component and the native glenoid is mainly left untouched. Following a TSA, some patients may experience unpredictable outcomes in regaining full range of motion in the shoulder. The variability in these outcomes may be related to incomplete restoration of translation at the glenohumeral joint. At present, glenohumeral implants account for translation in the glenohumeral joint by designing for a mismatch in radius of curvature between the glenoid and humeral head components.[29] Understanding the normal translation that occurs in the healthy shoulder may allow implant manufacturers to design implants with an idealized mismatch to allow for more normalized glenohumeral translations. Unlike the lower extremity gait cycle, movements in the upper extremity tend to be more variable and less cyclic, which has caused most past research to study the glenohumeral joint during more planar movements, such as abduction and adduction.[30] However, this simplification may not fully represent the complete range of functional shoulder movements. Internal rotation to the back, in particular, which is an extremely important movement in daily living, has unpredictable range of motion outcomes after total shoulder arthroplasty and has been under-researched within shoulder kinematics studies.[31] This indicates the importance of analyses of more complex activities of daily living.

Moreover, RTSAs limit translation at the glenohumeral joint and are known for inhibiting internal rotation.[32] Studying internal rotation to the back is important to understand more about why this occurs and how inhibiting this motion can also be prevented in anatomic total shoulder arthroplasties. Internal rotation to the back is also a movement that is highly relevant to routine activities of daily living, such as showering/bathing, dressing, and toileting.[33] Reaching overhead is another movement that is sometimes inhibited after receiving a TSA and is also important in routine activities of daily living such as brushing/combing hair, and placing/retrieving items from high cupboards or shelves. Due to the importance of these movements in activities of daily living, internal rotation to the back (IR) and forward elevation (FE) were chosen as the movements to be examined in this thesis.

1.2.2.1 Scapulohumeral Rhythm

An important concept to understand in shoulder range of motion is the fact the glenohumeral joint is not solely responsible for the motion of the humerus during movements such as abduction or flexion. There is a relationship that exists between the humerus and the scapula that allows the shoulder to hold such large upper extremity motion, and it is called scapulohumeral rhythm (Figure 1-9). It is best described by the movement coordination between the shoulder girdle and the glenohumeral joint. During the initial 30° of shoulder joint motion, movement is solely within the glenohumeral joint. Beyond this point, for every 2° of shoulder flexion or abduction, there is a corresponding 1° of upward rotation of the scapula. This proportional relationship maintains a 2:1 ratio (glenohumeral joint rotation : scapulothoracic joint rotation).[34]

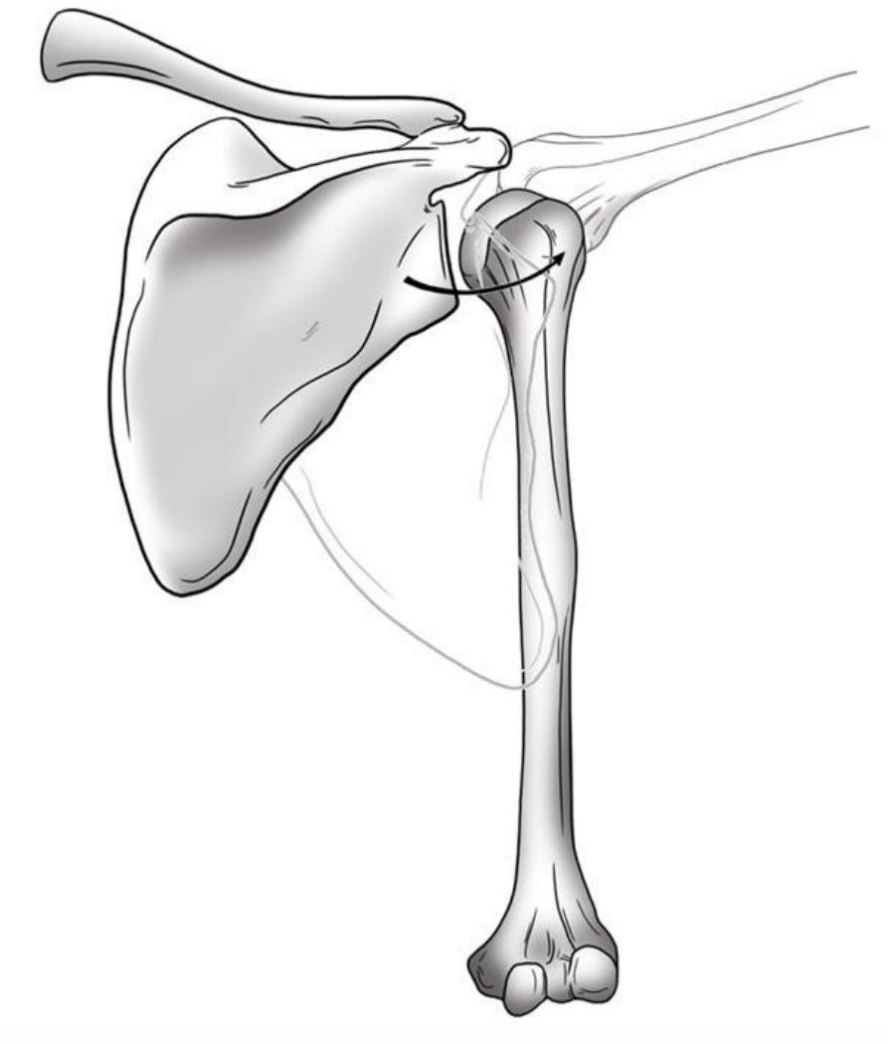

Figure 1-9: Scapulohumeral Rhythm

This image illustrates that the scapula and humerus rotate together as the arm elevates. Note that the dark shading indicates the arm by the side, and the light shade indicates the humerus (arm) elevated around 90°.

1.2.3 Glenohumeral Joint Proximity

Research on joint function typically encompasses the study of kinematics, which refers to the relative motion between two consecutive segments of the human body. For example, glenohumeral kinematics is the study of how the humerus is moving relative to the scapula. However, arthrokinematics, which is the study of the movement of joint surfaces, is equally as important because it provides detailed insights into how bones and cartilage engage with each other during motion. This level of detail is crucial for understanding joint stability, cartilage wear, and how implants affect the joint, which cannot be fully captured by examining kinematics alone. Historically, glenohumeral joint analysis has involved using the centre of the humeral head and locating how that moves relative to the glenoid, [8,18,19,35–41] however, this is not as ideal as taking into account exactly how the joint surfaces (humeral head articular surface and glenoid articular surface) are moving relative to one another. In Chapter 2 of this thesis, a true arthrokinematic analysis will be employed to study joint proximity during various movements, which will provide a much more accurate representation of what is happening at the joint surfaces. Joint proximity in this thesis refers to the spatial relationship between the articular surfaces of the glenohumeral joint, specifically how close or far apart the glenoid and the humeral head are from each other during movement. Tracking how the actual joint surfaces are moving relative to one another is more accurate than tracking the centre of the humeral head and how that moves with respect to the humeral head because it directly captures what is happening at the articulation, providing a true representation of joint behaviour and movement. This method also offers better insight into joint stability by reflecting how the joint surfaces maintain contact during motion. Assessing joint proximity of the shoulder joint is important because it influences movement patterns,[42] load distribution,[43,44] and joint stability,[45–47] which are important for joint health and performance. It can help clinicians identify potential risk factors and implement preventative measures accordingly. Abnormal joint proximity can predispose the glenohumeral joint to subluxation/dislocation,[48,49] and impingement syndromes.[50,51]

Most joint proximity analyses include a display of joint proximity maps, which are made so that it can be seen where on the glenoid the humeral head contacts the glenoid the

most (anterior, posterior, superior or inferior), and how that changes throughout a specific movement. Joint proximity maps can also be used in the study of erosion patterns of the shoulder, as well as aid in the testing of glenohumeral joint implants, since it will allow implant designers to confirm that the joint surface proximity is within a normal, healthy range.

1.3 Imaging Modalities Used to Track Joint Motion

Imaging, which is a representation or reproduction of an object's form, is a popular and powerful tool used to view the human body in order to diagnose, monitor or treat medical conditions.[52] There are various imaging modalities that exist, each with advantages and disadvantages of their own. For the use of shoulder biomechanic analysis (kinematics and arthrokinematics), the most widely used imaging modalities include, radiography (X-ray), fluoroscopy, computed tomography, and most recently, four-dimensional computed tomography (4DCT). The following section will highlight a brief history of each imaging modality including an explanation of how the imaging modality works and how it has been used in shoulder research.

1.3.1 Radiography (X-ray)

Radiography, otherwise known as X-ray, is an imaging modality which uses high energy photons that are capable of passing through most objects in the body.[53] Bones readily absorb X-rays (due to being dense and containing mostly calcium, which has a high atomic number), and produce high contrast on the X-ray detector, which make them appear mainly white on the image. X-rays travel more easily through fat, muscle, and lungs (due to being less dense), which make them appear as shadows (dark) on the radiograph.[54] X-ray imaging resulted in the birth of modern medical imaging in 1895 when the first image was acquired and it is essentially a 2D map of the path integral of the attenuation coefficient. It is often used as a first line investigation for most musculoskeletal diseases (e.g. trauma, fractures).[55] Some advantages include being cost-effective, easy to obtain, excellent contrast for bone/lung applications, and easily implemented in emergency situations. However, some disadvantages include, poor soft-tissue contrast (e.g., cartilage, muscle),

difficulty in interpreting areas of complex anatomy (overlying structures obscure detail), and increased risk of developing cancer from exposure to ionizing radiation. X-rays are mainly used for the shoulder to diagnose conditions like broken bones, arthritis, and dislocation.[56] Within research, X-rays have primarily been used to investigate the pathologic shoulder including, osteoarthritis, subluxation/dislocation, malalignment, and rotator cuff tears.

1.3.2 Fluoroscopy

Fluoroscopy is an imaging modality that displays a continuous X-ray image on a monitor, essentially like an X-ray video.[57] The X-rays continuously pass through the body, which allow for real time images of a body part, instrument, or contrast again (i.e., X-ray dye) to be seen on a monitor. Fluoroscopy is widely used in examinations and procedures to diagnose or treat patients.[58] Many past studies have employed this imaging modality to assess shoulder kinematics and arthrokinematics because it allows for a dynamic assessment to be made, instead of analyzing a joint purely statically.[8,9,17,59–64] However, this imaging technique has a limited field of view, which is a challenge for larger joints with a wide range of motion, such as the shoulder. It is also limited by only assessing joints in 2D. These limitations make it more difficult to assess complex musculoskeletal movements and pathologies.

1.3.3 Computed Tomography (CT)

Computed Tomography, otherwise known as CT or 3DCT, is a diagnostic imaging procedure that uses a combination of X-rays and computer technology to produce images of the inside of the body.[65] CT scans can essentially be described as 3D X-rays and were developed in the early 1970s, well after conventional X-rays were invented.[66] In contrast to conventional X-rays, which just pass X-rays straight through the body in one-direction, CT scans pass X-rays around the patient via a gantry (i.e., a giant ring that rotates).[67] This technique allows for new technology and software to turn these 2D slices into 3D images of inside the body. Being able to look internally at anatomy in 3D has revolutionized the medical imaging sector and advantages of CT scans include, 3D imaging and cross-sectional anatomy avoids complication of overlying structures, provides accurate

geometrical data, obtains better soft tissue anatomy than projection radiography, is fast, and can gather quantitative image data as scans include bone density. In research, computed tomography is the most used imaging technique. The majority of past studies that examine shoulder subluxation have used CT.[68] CT is also the main imaging used in preoperative planning for shoulder arthroplasty. However, some disadvantages include, significant risk due to ionizing radiation, soft tissue contrast is inferior to MRI, and CT is a static imaging technique and cannot dynamically assess joints.

1.3.4 Four-Dimensional Computed Tomography (4DCT)

The human body has been engineered for motion, yet most imaging techniques (e.g., X-rays, computed tomography, etc.) capture us at rest. However, a newer imaging modality, four-dimensional computed tomography (4DCT), otherwise known as dynamic CT or kinematic CT, consists of capturing volume sequences (3DCT) over time to create a dynamic volume set that depicts real-time motion.[69] Recent developments in acquisition technology, which have helped reduce the radiation dose, have led this imaging modality (that is able to capture real time joint motion) to be a more safe and feasible option. In the musculoskeletal field, although 4DCT has been primarily used to examine wrist motion, it has also been used more recently within other joints including the ankle, knee, hip, elbow, and shoulder. 4DCT has been used to assess shoulder joint kinematics, instability and impingement, but primarily for the sternoclavicular,[70] acromioclavicular,[71] and scapulothoracic joints[72]. In these studies, 4DCT was used to assess the sternoclavicular joint and acromioclavicular joint to measure range of motion and quantify translation during various movements for the pathologic shoulder.[70] Clinicians have used 4DCT to investigate snapping scapula syndrome in the scapulothoracic joint, allowing clinicians to pin-point the precise point of impingement and ensure the pathologic joint is addressed correctly.[72] Another previous study has used 4DCT to visualize movement patterns of the acromioclavicular (AC) joint during abduction, discovering that posterior and superior translation are the main movements of the AC joint.[73] Since this imaging modality has been gaining more recognition, a recent 2022 study has used 4DCT to analyze glenohumeral contact area, centre of glenohumeral contact area, and centre of humeral head during simulated pitching motion in collegiate baseball pitchers.[10]

Although 4DCT has allowed for a more complete analysis of joints throughout movement, this imaging modality does not come without its shortcomings. One limitation of using 4DCT is that the movements performed while using the 4DCT must fit within the gantry of the scanner, which limits the range of motion that is able to be performed during the scan.[74] Another limitation of using 4DCT is that the patient is not able to stand up while performing the motion. This can introduce error into the analysis due to the fact that gravity, weight, and other forces would be acting in a different direction than normal.[74] However, an upright 4DCT scanner has recently been developed to mitigate this limitation and has been showing comparable results to conventional 4DCT scanners.[75]

1.4 Shoulder Pathologies

The shoulder's extensive range of motion (ROM) inherently compromises its stability, contributing to a higher incidence of shoulder pathologies, often resulting in the need for shoulder replacements.

1.4.1 Osteoarthritis (OA)

Osteoarthritis (OA) is not only the most common form of arthritis, but is also the most common joint disease.[76] As of 2021, it affects approximately 4 million Canadians (1 in 7 adults), which is roughly 15% of people over the age of 20 years old.[77] It is known to most people as degenerative joint disease, or simply, “wear and tear” arthritis.[76] Osteoarthritis causes symptoms like pain, aching, stiffness, swelling and limited range of motion. This is due to cartilage degeneration, bone deformation, osteophyte growth and inflammation within the joint capsule. There are many risk factors for OA including, joint injury/trauma or overuse, joint malalignment, obesity, genetics, age, sex, and race.[76] Although the prevalence of OA increases with age, it is important to note that it is not an “old person disease”, as more than half of adults who live with OA are under the age of 65 years old and one third of those people are diagnosed before age 45.[77] OA most commonly affects load/weight bearing joints in the hands, knees, hips and spine. Although studied most often in these joints, OA can damage any joint in the body, including the shoulder.[78]

1.4.1.1 Shoulder Osteoarthritis

Shoulder osteoarthritis (OA), although not as prevalent as hip and knee OA, is said to be equally as debilitating,[79] and comparable to some chronic medical conditions including, diabetes, acute myocardial infraction, and congestive heart failure.[80] Focusing in on glenohumeral OA more specifically, loss of cartilage and other joint tissues begin around the humeral head and glenoid, taking away the ability for the two bones to glide smoothly over one another. This increased friction between the two bone surfaces causes pain to increase, thereby inhibiting movement, which further develops into stiffness in the joint. Due to this severe pain and stiffness in the joint, people start to experience difficulty in performing simple activities of daily living. Shoulder OA can be classified into two categories: primary OA or secondary OA.[81] Primary OA is diagnosed when there is no specific cause, but can be due to age, sex, race, or genetics. Secondary OA, however, is diagnosed when there is a known cause including, traumatic shoulder injury, dislocation/instability, surgery, or massive rotator cuff tears.[82,83]

1.4.1.2 Glenohumeral Osteoarthritis

Shoulder OA can occur in the acromioclavicular joint and/or the glenohumeral joint,[84] but for the purpose of this thesis, only glenohumeral OA will be highlighted. The number one cause of total shoulder replacements is glenohumeral OA. During the progression of glenohumeral OA, various changes to the joint occur: degenerative changes of the rotator cuff, joint cartilage, or long biceps tendon, which results in abnormal load distribution, adaptive changes to the subchondral bone (bony sclerosis), joint space narrowing, as well as osteophyte formation.[85,86] In addition, humeral flattening and glenoid erosion are common changes that end up limiting shoulder range of motion. The posterior glenoid and central aspect of the humeral head are the first two areas to be affected.[87]

1.4.2 Glenohumeral OA Classification: Morphological Features

Glenohumeral OA does not develop the same way in everyone. Neer stated in 1982 that posterior humeral head subluxation and posterior glenoid wear commonly occurs in primary glenohumeral OA, but there was no distinct classification system that described the various morphological features that appear.[88] In 1999, Walch et al. developed a

classification system for primary glenohumeral OA to describe various glenohumeral interactions.[89] This was made to aid in preop planning for surgeons, and glenoid reaming during the surgery.[90] Walch classifications are made based on 2D axial cuts of CT scans and are split into 3 main groups, Type A, Type B and Type C, with various sub-groups (Figure 1-10). These groups are based on three parameters: the presence and location of glenoid erosion, the degree of glenoid retroversion, and the amount of subluxation of the humeral head in relation to the glenoid fossa.[68]

Type A, which accounts for 52% of all cases, is described best by a centred humeral head and a balanced distribution of load against the glenoid fossa with symmetric erosion due to the absence of subluxation.[89] Type A1 is described as minor wear of the glenoid, versus Type A2, which is severe or major central erosion of the glenoid.[90] Type B, which accounts for 32% of all cases, can be noted by the apparent posterior subluxation, which occurs due to the asymmetric loads against the glenoid fossa.[89] Type B1 displays posterior humeral head subluxation with joint space narrowing and retroversion, versus Type B2, which shows posterior glenoid erosion due to the posterior humeral head subluxation with a biconcave appearance.[91] Type B2 has worse outcomes with shoulder arthroplasties (reoccurrence of instability and early glenoid loosening). For Type B2 cases, it is recommended to place an augmented glenoid component or if very severe to suggest a reverse total shoulder arthroplasty.[92] Type C, which accounts for the remaining 16% of all cases, is described as a dysplastic glenoid with retroversion > 25°.[89]

Preoperative characterization of these morphological features of the glenoid can impact implant selection. It can also have an influence on shoulder implant survivorship/lifetime, as well as poor patient reported outcomes. Due to the severity of the asymmetric loading on the posterior part of the glenoid in Type B cases, it is possible that the patient may experience glenoid loosening through the rocking horse effect if the augmented implant is not put in properly.[68,93] It is imperative for surgeons to carefully examine preop glenohumeral morphology to determine the correct implant and to ensure that glenohumeral subluxation is eliminated completely after surgery.

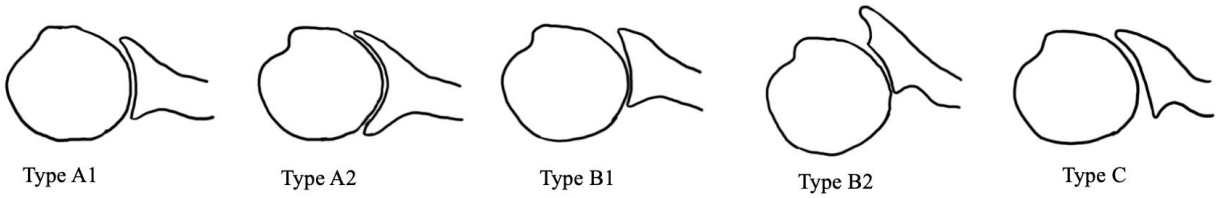

Figure 1-10: Walch Classification Types for the Osteoarthritic Glenohumeral Joint

The five distinct types of osteoarthritic glenohumeral morphology types: Type A1-centred humeral head with minor central wear of glenoid; Type A2-centred humeral head with severe or major central wear of glenoid; Type B1-posterior humeral head subluxation with joint space narrowing and retroversion; Type B2-posterior humeral head subluxation with major posterior glenoid erosion and a biconcave appearance; and Type C-glenoid retroversion >25° with no glenoid erosion.

1.4.3 Age-Related Differences in the Shoulder Joint

Currently, there is a limited amount of knowledge regarding how glenohumeral joint motion changes with age. When people age, there are many physiological changes that occur that can alter the musculoskeletal system, which can ultimately affect muscle mass and strength,[94] joint mechanics,[95] and range of motion.[94]

One of the most common conditions that affects the glenohumeral joint as people age is osteoarthritis (OA), which leads to a breakdown in cartilage causing pain, stiffness and decreased range of motion.[86] An in-depth description of OA and how it leads to many individuals needing shoulder arthroplasties is described in Section 1.4.1. In addition to OA, tendons of the shoulder (especially the rotator cuff tendons) undergo degenerative changes and can potentially tear, which can affect the movement, function, and stability of the shoulder. One recent study that looked at shoulder instability in an aging population found that acute high-grade or full-thickness rotator cuff tears are seen with higher frequency in older populations after anterior glenohumeral dislocation, which showcases that changes in tendons are occurring in older populations.[96] As well, another study found that no participants younger than 60 years old had macroscopic degeneration of the rotator cuff, joint cartilages or long biceps tendon. However, after the age of 60 years old, degenerative changes of these structures became more common.[85]

Additionally, reduced muscle mass and strength can also come with age and can affect shoulder stability, movement and function.[94] As people get older, a loss of muscle mass can occur (sarcopenia), which can decrease the muscle strength of important shoulder stabilizers such as the deltoid and rotator cuff muscles. One study found that shoulder strength significantly decreased with age (older individuals had significantly less shoulder strength than younger individuals), with abduction and external rotation showing the strongest negative correlations.[94] As well, although age did not have a significant effect on range of motion, abduction, forward elevation and internal rotation were all still found to decrease over time. Since muscles like the deltoid and rotator cuffs are so crucial in achieving proper function of the shoulder, glenohumeral joint range of motion can be severely affected. In a study that looked at individuals over the age of 60 years old, 36% of all individuals reported having difficulty in performing daily tasks.[97] This was attributed mainly to a decrease in internal rotation of the shoulder, which had negative effects on quality of life. Internal rotation is one of the main movements studied in this thesis.

Other changes to the glenohumeral joint that can occur with age are that the joint capsule can become tighter and less flexible and the ligaments and other connective tissues can lose elasticity.[98] This can lead to more stiffness within the joint, which can increase joint proximity and decrease joint translation, which can both alter healthy joint mechanics. Most past studies have looked at the aging shoulder in terms of degenerative changes and how that affects overall range of motion,[94,95,99] flexibility and function of the shoulder,[100,101] but not many have looked at the healthy shoulder and how age affects joint surface contact (joint proximity) and joint surface movement (arthrokinematics). This is an extremely important area of research to study, which has not yet been well-established within literature. However, it is important to note that recruiting participants with healthy shoulders over 45 years old is challenging due to the increased prevalence of prior shoulder injuries and pathologies.[102,103] Consequently, the age of 45 has been used in studies to represent the older population.

1.4.4 Subluxation

One fundamental aspect of a functional shoulder is its stability, which is partly characterized by the humeral head maintaining its position centred within the glenoid.[104,105] When the shoulder joint loses its centred position, the joint can experience subluxation, which is partial separation/displacement (dislocation) of the bones within the joint. In the extreme case, if the bones fully separate/displace from one another, complete dislocation can occur. Shoulder instability (e.g., posterior subluxation) can occur due to a variety of reasons, including trauma, repetitive overhead movement, laxity of the shoulder ligaments, degenerative joint disease (e.g., Osteoarthritis), muscle weakness/imbalance, anatomical factors, or underlying conditions like connective tissue disorders.[104] For the purpose of this work, glenohumeral subluxation due to degenerative joint disease (e.g., Osteoarthritis) will be the focus. When the humeral head shifts off-centre (subluxates), this causes an increase in mechanical stress on the joint surfaces. When the humeral head subluxates posteriorly out of its centred position within the glenoid fossa, it can cause asymmetric loading on the posterior part of the glenoid, which can cause posterior glenoid wear.[106] This is also classified as an osteoarthritic shoulder with a Walch Type B2 glenoid. According to the Walch classification of glenoid morphology, a subluxation between 45% and 55% represents a centred humeral head.[89] A subluxation of more than 55% represents posterior subluxation with 100% being posterior dislocation, and less than 45% represents anterior subluxation with 0% being anterior dislocation. In the past, posterior subluxation was always measured using 2D measurements, but these have been shown to be less accurate and statistically different than 3D measurements due to positional errors,[107–110] which is why in this thesis 3D measurements were made to determine subluxation.

Currently there is no cure for osteoarthritis, and end stage treatment is total shoulder arthroplasty (TSA), which has long-term survival and satisfaction rates up to 95%.[111] To correct subluxation with a TSA, posterior augmented glenoid (PAG) implants are used to improve posterior subluxation of the humeral head in B2 glenoids.[112] However, if the humeral head is not well aligned with the glenoid following a TSA, the continued subluxation can cause asymmetric loading on the posterior part of the glenoid component, which can then cause glenoid loosening (a common complication of a TSA occurring in

6% of all patients) through the rocking horse effect.[93] With glenoid loosening accounting for nearly 32% of all complications,[113] it is imperative to determine if subluxation can be corrected and maintained throughout movement to avoid this increasing burden of revision surgeries. Additionally, most studies on the B2 glenoid, whether preoperative or post TSA, assess subluxation statically. It is presently unknown if subluxation recurs after a TSA with a PAG or if it varies dynamically throughout active motion.

In the past, subluxation was first described as the displacement of the humeral head in relation to the glenoid articular surface, however, more recently subluxation has been referred to as the displacement of the humeral head with respect to the plane of the scapula.[68] When the glenoid is severely eroded it can be misaligned with the scapula and muscle action lines, which is why Walch more recently proposed using the scapula as a reference to measure subluxation.[110,114] Overall, it is apparent that surgically reducing the subluxation of the humeral head on the glenoid does improve postoperative shoulder function and lowers the risk of glenoid component failure attributed to eccentric loading.[68] Thus, having the capability to assess the positioning of the humeral head in relation to the glenoid/scapula makes it possible for surgeons to evaluate the effectiveness of shoulder arthroplasties that they perform.

1.5 Shoulder Replacements

Osteoarthritis of the glenohumeral joint can progress at different rates into different severities, at which point various treatments for glenohumeral OA would need to be considered. The first option for treating glenohumeral OA would be nonoperative treatment: physical therapy, activity modification, anti-inflammatory drugs (NSAIDs), and intra-articular injections.[115] If none of these are successful, the next step is to consider the various surgical treatments of glenohumeral OA: arthroscopic treatment or arthroplasty treatment.[116] The most effective treatment for severe OA is arthroplasty treatment. Arthroplasty is the surgical reconstruction or replacement of a joint, in this case the glenohumeral joint. It includes either restoration/resurfacing of the bones or replacing the damaged/worn-out bone and cartilage with an artificial joint (i.e., prosthetic implant), typically made out of metal, plastic, or ceramic. Currently, there are three main arthroplasty

options for glenohumeral OA: anatomic total shoulder arthroplasty (TSA), reverse total shoulder arthroplasty (RTSA), and hemiarthroplasty (Figure 1-11). For the purpose of the work in this thesis, anatomic total shoulder arthroplasty will be the main focus.

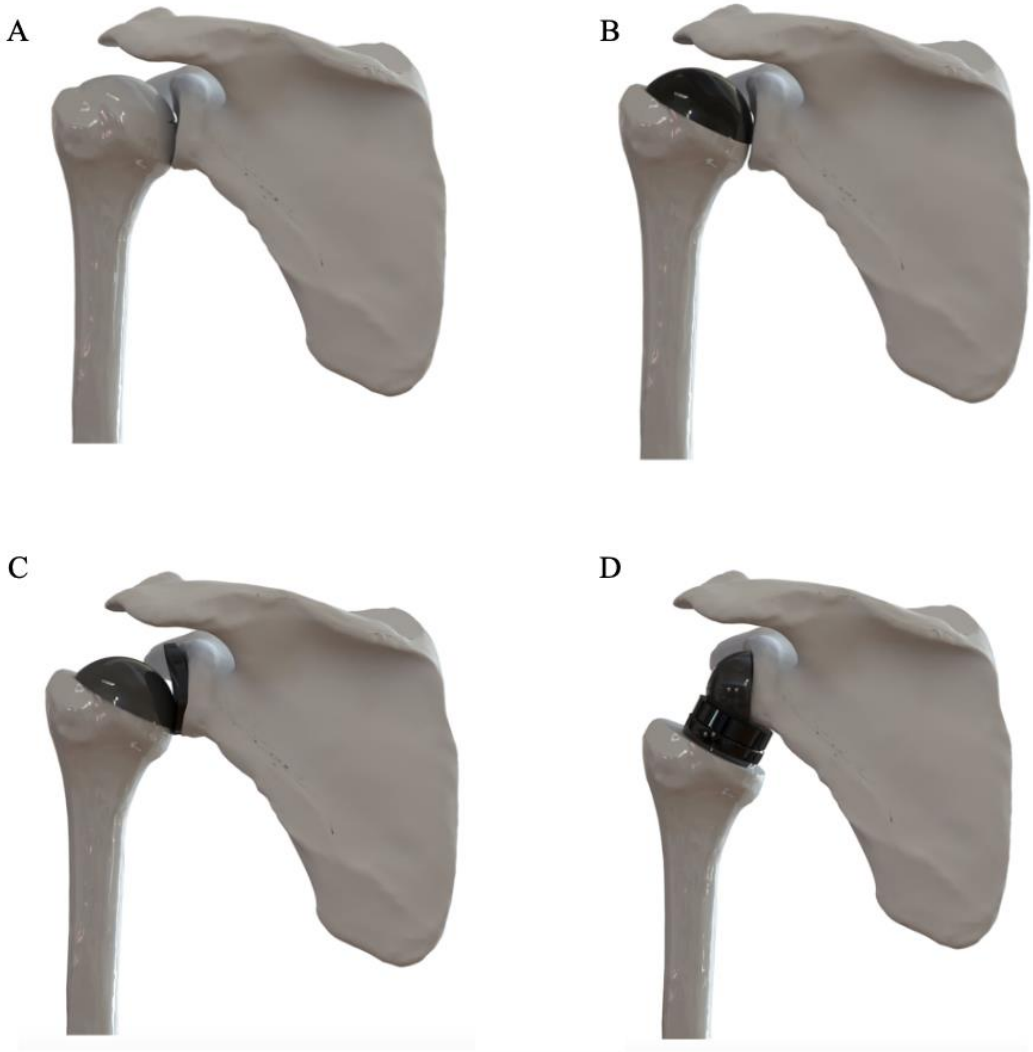

Figure 1-11: Various Shoulder Arthroplasties Compared to the Native Joint

(A) Native Glenohumeral Joint (B) Hemiarthroplasty (C) Anatomic Total Shoulder Arthroplasty (D) Reverse Total Shoulder Arthroplasty

1.5.1 Anatomic Shoulder Arthroplasty (TSA)

Anatomic total shoulder arthroplasty (TSA), is when the implant components match the normal anatomy of the shoulder.[28] The native humeral head is replaced with a metal humeral head component and the native glenoid is replaced with a shallow polyethylene glenoid component.[117] TSA is the gold standard shoulder arthroplasty for patients with an intact rotator cuff and sufficient glenoid bone because it offers reliable pain relief, high patient satisfaction, improved quality of life, predictable improvement to shoulder range of motion, excellent implant longevity, and a low incidence of complications.[99,118] In comparison to other options including hemiarthroplasty, which is when the humeral articular surface of the native joint is replaced with a humeral component and the native glenoid is left untouched, TSA has better functional results, and significantly greater pain relief and range of motion.[80,116,119] As well, long-term survival and satisfaction rates are up to 95% for people who receive a TSA.[120]

The primary reason to consider receiving a TSA for glenohumeral osteoarthritis is if a significant amount of pain and discomfort still exists, even after nonsurgical measures are pursued. The secondary indication for TSA is typically to regain shoulder function and range of motion to be able to get back to everyday activities. Restoration of shoulder range of motion following surgery is less predictably achieved than pain relief.[121] However, if a TSA is successful, normal or near normal restoration of function, in addition to complete pain relief, can be achieved.[122]

Although pain is the primary reason for obtaining a TSA, it is expected that by receiving a TSA, better range of motion will be restored to the shoulder, which is the main focus in this thesis.[121] There have been many studies that have analyzed range of motion before and after TSA, all of which have reported improvement. One recent study that analyzed 34 OA shoulders before and after TSA, found a 47° increase in active elevation and 34° increase in external rotation.[123] In another study, it was found that range of motion significantly improved with a TSA after 6 months: flexion 104° to 147° (43° improvement), abduction 86° to 145° (59° improvement), internal rotation 43° to 54° (11° improvement) and external rotation 25° to 50° (25° improvement).[124] Another study showed similar improvement after TSA: flexion, 98° to 142° (44° improvement), abduction 69° to 101° (32° improvement),

internal rotation (40% improvement), external rotation 18° to 50° (32° improvement).[99] This study also found that preoperative range of motion was the most predictive of postop range of motion in patients. Barrett et al. (1987) found that the average range of active forward elevation in all of the shoulders improved from 71° to 100°, with both external and internal rotation improving as well.[125] This study also found improvement from 14% to 78% in a patient's ability to perform five specific activities of daily living. A more long-term study (12-year follow up) reported satisfactory pain relief in 83% of shoulders, with a 40% improvement in active abduction.[123] It is clear from all of these previous studies that a TSA is successful in restoring ROM to patients.

However, the benefits of TSA do not come without its associated risks. Some common risks of TSA include infection, glenoid and humeral component loosening, rotator cuff tear, periprosthetic fracture, and neurologic injury.[126] Glenoid loosening is the most common complication of TSA due to posterior instability (subluxation), and occurs in 6% of all patients.[93] Some of the most common factors that contribute to glenoid loosening are rotator cuff deficiency, glenoid morphology, and osteolysis.[126] Glenoid loosening is also greater when glenoid reaming occurs due to the fact that it weakens the glenoid surface, losing the support from the subchondral bone and then exposes the components to excessive compressive forces.[127] Mechanically, all of these factors contribute to eccentric forces/loading, which eventually can lead to the rocking horse effect mentioned in Section 1.4.2. Management of glenoid loosening includes either placement of a new glenoid component or removal of the glenoid component and bone grafting, with 91% and 78% success rates at 5 years, respectively.[128] Overall, it is important to note that a TSA has shown to improve pain and range of motion effectively, but complications such as glenoid loosening are still prevalent.

1.5.2 Reverse Total Shoulder Arthroplasty (RTSA)

Reverse Total Shoulder Arthroplasty (RTSA) is when the implant components of the glenohumeral joint are the opposite of human anatomy. Possible reasons for getting RTSA include, rotator cuff arthropathy, failed TSA, massive irreparable rotator cuff tears, and proximal humerus fractures.[117] During RTSA, the glenoid is replaced with a metal (i.e., cobalt chromium or titanium) sphere, and the humeral head is replaced with a polyethylene

cup.[32] The metal sphere and polyethylene cup create a true ball and socket joint. This new ball and socket joint changes the joint centre of rotation and constrains the joint so that minimal translation is allowed, only rotation. In the native joint, the centre of rotation is the centre of the humeral head, but by reversing the anatomy and having the centre of rotation now as the centre of the metal sphere, it shifts the joint centre medially. This increases the length of the deltoid moment arm, which decreases the force required by the deltoid to raise the arm.[117] Overall, this allows the shoulder joint to maintain stability and movement even without a fully intact rotator cuff. However, due to the reversal of glenohumeral components, a major problem in RTSA is the loss of internal rotation movement. This inhibits people from performing many activities of daily living.[33] Many researchers are currently studying specific factors that influence the loss of this internal rotation movement,[129] but research suggests that the restriction from translation within the glenohumeral joint is one of the main reasons for the loss of this movement.[32]

1.5.3 Hemiarthroplasty

Hemiarthroplasty, as mentioned above in Section 1.5.1, is when the humeral articular surface of the native joint is replaced with a humeral component and the native glenoid is left untouched. It is a commonly performed procedure for shoulder disorders, including glenohumeral arthritis, avascular necrosis, capsulorrhaphy arthropathy, and proximal humeral fractures.[130] Originally, the aim of the hemiarthroplasty was to keep the native joint intact as much as possible, but has now been known to have a high rate of patient dissatisfaction and revision surgeries, especially in younger individuals.[131,132] To avoid revision surgeries, the condition of the glenoid is critical in whether hemiarthroplasty will be successful. In particular, patients with concentric glenoid wear and primary OA seem to have better outcomes than those with eccentric glenoid wear and secondary OA.[133] Additional reasons for revision surgery after hemiarthroplasty include, pain and stiffness, rotator cuff or tuberosity failure, weakness, component loosening, instability, or erosion of the bony glenoid surface. Due to all of these reasons, it is important to take a complete assessment of the shoulder to ensure hemiarthroplasty will be successful in restoring comfort and function to the shoulder.

1.6 Thesis Rationale/Motivation

The shoulder is the most mobile joint in the human body, allowing people to move their arms in a wide range of motion.[1] However, after undergoing total shoulder arthroplasty, some individuals still experience inhibited range of motion during various movements.[126] This restriction in mobility can be attributed to various factors, including the complexity of the joint, postoperative complications, and limitations in the design and functionality of current implants. The failure to restore all degrees of freedom in rotation, and particularly translation, is believed to inhibit specific shoulder movements, such as internal rotation to the back, which is an important movement in everyday activities such as showering/bathing, dressing (e.g., tucking in shirts and/or putting on a bra), or even managing toileting.[33] Notably, research and advancements surrounding shoulder joint implants are well behind those for other weight bearing joints such as the hip and knee. This disparity has led to significant knowledge gaps regarding shoulder implants, highlighting the need for enhanced research efforts to improve outcomes for individuals undergoing total shoulder arthroplasty.

To advance shoulder implant research, it is essential first to understand the functionality of the healthy glenohumeral joint, in vivo and throughout active motion, to establish a benchmark for the joint's normal range of motion. It is hypothesized that the limitation of translation within the glenohumeral joint constrains the shoulder's full range of motion. Using 4DCT, we will quantify the translation occurring at the glenohumeral joint during various movements, enabling implant designers, such as Stryker, to ensure these implants accurately mimic the native healthy joint and test them under more realistic conditions. Historically, the centre of the humeral head has been used to track glenohumeral joint arthrokinematics.[8,18,19,35–41] However, this method is less accurate than using the exact contact point between joint surfaces, which will be employed in this study. Furthermore, determining the proximity of the glenohumeral joint surfaces will allow us to identify when the joint surfaces are in closer contact (i.e., experience higher contact pressure), facilitating future studies on erosion patterns. Additionally, examining age-related differences will help determine if age affects translation. Overall, understanding glenohumeral joint

proximity and translation will enhance our knowledge of global shoulder motion, aiding in the development of in vitro experiments, simulators, and shoulder implants.

In patients with osteoarthritis (OA), anatomic total shoulder arthroplasty (TSA) is considered the gold standard for shoulder replacement. However, some OA patients, specifically those classified as Type B2, experience posterior humeral head subluxation and posterior glenoid erosion. This can lead to glenoid loosening, and in severe cases, implant failure and the need for revision surgery post-TSA.[91] Glenoid loosening occurs when subluxation is not fully corrected, resulting in an imbalance of forces acting on the glenoid implant component.[93] Notably, glenoid loosening accounts for 32% of all TSA complications.[113] Given the prevalence of this complication, it is crucial to determine if subluxation is adequately corrected during TSA and if this correction is maintained throughout movement to reduce the need for revision surgeries. The implications of uncorrected subluxation on shoulder range of motion remain uncertain, although it is suspected that loss of internal rotation may occur due to the subluxation hindering joint translation. To date, subluxation has not been dynamically assessed during active motion. However, with the arrival of 4DCT technology, it is now possible to observe how subluxation changes throughout active motion, providing critical insights into improving TSA outcomes.

Overall, the aim of this thesis is to advance research in shoulder biomechanics with special interest in motion at the articulation, by utilizing 4DCT technology to investigate healthy glenohumeral arthrokinematics and anatomic implant subluxation during active motion.

1.7 Objectives and Hypotheses

The objectives of this thesis were distributed across two studies and are outlined in Chapter 2 and Chapter 3.

Chapter 2

Primary Objective: To measure and quantify glenohumeral joint proximity and glenohumeral joint surface tracking (translation) in healthy participants throughout forward elevation and internal rotation using 4DCT.

Secondary Objective: To determine if there were age (young versus old), position (beginning versus middle versus end of movement), or direction (superior/inferior versus anterior/posterior) related differences in the healthy glenohumeral joint throughout forward elevation and internal rotation.

Secondary Hypothesis: Glenohumeral joint proximity will increase with age, and glenohumeral joint surface tracking (translation) will decrease with age due to the closer joint proximity.

Chapter 3

Primary Objective: To determine if Walch type B2 patients managed with a TSA and a PAG implant would maintain correction of subluxation when examined statically and when stressed with active motion.

Primary Hypothesis: Subluxation will be corrected postoperatively and will maintain a centred joint alignment throughout active movement.

Secondary Objective: To analyze if a patient's range of motion (good or limited), magnitude of B2, or PAG implant size (15° or 25°) affect postoperative correction of subluxation.

Secondary Hypothesis: There will be no difference in subluxation postoperatively between various PAG implants sizes and magnitudes of B2 erosions, and patients with better postoperative range of motion will have greater subluxation postoperatively.

1.8 Thesis Overview

Chapter 2 describes glenohumeral joint proximity and glenohumeral joint surface tracking (translation) in healthy patients throughout forward elevation and internal rotation. This chapter also investigates if there are any age, position, or direction related differences in the healthy glenohumeral joint.

Chapter 3 examines subluxation of the glenohumeral joint before and after an anatomic total shoulder arthroplasty (TSA). Subluxation throughout active motion has never been studied before, so this chapter aims to assess subluxation postoperatively throughout active motion. An additional analysis includes evaluating if a patient's range of motion (good or limited), magnitude of B2 erosion, or PAG implant size (15° or 25°) affect subluxation.

Chapter 4 includes a summary and discusses the strengths and limitations of the work presented in this thesis. Possible future work is also outlined.

1.9 References

1. Patel RM, Gelber JD, Schickendantz MS. The Weight-Bearing Shoulder. *J Am Acad Orthop Surg*. 2018;26(1):3-13. doi:10.5435/JAAOS-D-15-00598

2. lefevre-colau marie martine, Nguyen C, Palazzo C, et al. Recent advances in kinematics of the shoulder complex in healthy people. *Ann Phys Rehabil Med*. 2017;61. doi:10.1016/j.rehab.2017.09.001

3. Terry GC, Chopp TM. Functional Anatomy of the Shoulder. *J Athl Train*. 2000;35(3):248-255.

4. Miniato MA, Anand P, Varacallo M. Anatomy, Shoulder and Upper Limb, Shoulder. In: *StatPearls*. StatPearls Publishing; 2024. Accessed July 8, 2024. http://www.ncbi.nlm.nih.gov/books/NBK536933/

5. Netter F. *Netter Atlas of Human Anatomy: Classic Regional Approach*. Eighth. Elsevier Inc.; 2023.

6. Bakhsh W, Nicandri G. Anatomy and Physical Examination of the Shoulder. *Sports Med Arthrosc Rev*. 2018;26(3):e10-e22. doi:10.1097/JSA.0000000000000202

7. Mamatha T, Pai S, Bv M, Kalthur S, Pai M, Kumar B. Morphometry of Glenoid Cavity. *Online J Health Allied Sci*. 2011;10.

8. Massimini DF, Boyer PJ, Papannagari R, Gill TJ, Warner JP, Li G. In-vivo glenohumeral translation and ligament elongation during abduction and abduction with internal and external rotation. *J Orthop Surg*. 2012;7:29. doi:10.1186/1749-799X-7-29

9. Matsuki K, Matsuki KO, Yamaguchi S, et al. Dynamic In Vivo Glenohumeral Kinematics During Scapular Plane Abduction in Healthy Shoulders. *J Orthop Sports Phys Ther*. 2012;42(2):96-104. doi:10.2519/jospt.2012.3584

10. Momma D, Espinoza Orías AA, Irie T, et al. Four-dimensional computed tomography evaluation of shoulder joint motion in collegiate baseball pitchers. *Sci Rep*. 2022;12:3231. doi:10.1038/s41598-022-06464-5

11. Hess SA. Functional stability of the glenohumeral joint. *Man Ther*. 2000;5(2):63-71. doi:10.1054/math.2000.0241

12. Chang LR, Anand P, Varacallo M. Anatomy, Shoulder and Upper Limb, Glenohumeral Joint. In: *StatPearls*. StatPearls Publishing; 2023. Accessed June 13, 2023. http://www.ncbi.nlm.nih.gov/books/NBK537018/

13. Peat M. Functional anatomy of the shoulder complex. *Phys Ther*. 1986;66(12):1855-1865. doi:10.1093/ptj/66.12.1855

14. Panjaitan T. Anatomy and Biomechanic of the Shoulder. *Orthop J Sports Med*. 2019;7(11_suppl6):2325967119S00466. doi:10.1177/2325967119S00466

15. Lippert LS. *Clinical Kinesiology and Anatomy*. F. A. Davis Company; 2011. Accessed April 23, 2024. http://ebookcentral.proquest.com/lib/west/detail.action?docID=2038738

16. Bey MJ, Kline SK, Zauel R, Kolowich PA, Lock TR. In Vivo Measurement of Glenohumeral Joint Contact Patterns. *EURASIP J Adv Signal Process*. 2009;2010(1):1-6. doi:10.1155/2010/162136

17. Bey MJ, Kline SK, Zauel R, Lock TR, Kolowich PA. Measuring dynamic in-vivo glenohumeral joint kinematics: Technique and preliminary results. *J Biomech*. 2008;41(3):711-714. doi:10.1016/j.jbiomech.2007.09.029

18. Friedman RJ. Glenohumeral translation after total shoulder arthroplasty. *J Shoulder Elbow Surg*. 1992;1(6):312-316. doi:10.1016/S1058-2746(09)80058-X

19. Karduna AR, Williams GR, Williams JL, Iannotti JP. Glenohumeral Joint Translations before and after Total Shoulder Arthroplasty. A Study in Cadavera*. *JBJS*. 1997;79(8):1166.

20. Muench LN, Murphey M, Oei B, et al. Elliptical and spherical heads show similar obligate glenohumeral translation during axial rotation in total shoulder arthroplasty. *BMC Musculoskelet Disord*. 2023;24(1):171. doi:10.1186/s12891-023-06273-5

21. Poppen NK, Walker PS. Normal and abnormal motion of the shoulder. *J Bone Joint Surg Am*. 1976;58(2):195-201.

22. Harryman DT, Sidles JA, Clark JM, McQuade KJ, Gibb TD, Matsen FA. Translation of the humeral head on the glenoid with passive glenohumeral motion. *J Bone Joint Surg Am*. 1990;72(9):1334-1343.

23. Warner JJP, Bowen K, Hannafin JA, Arnoczky P, Warren RF. Articular contact patterns of the normal glenohumeral joint. *J Shoulder Elb Surg*. 1998;7(4).

24. Wuelker N, Schmotzer H, Thren K, Korell M. Translation of the glenohumeral joint with simulated active elevation. *Clin Orthop*. 1994;309:193-200.

25. Greis PE, Scuderi MG, Mohr A, Bachus KN, Burks RT. Glenohumeral articular contact areas and pressures following labral and osseous injury to the anteroinferior quadrant of the glenoid. *J Shoulder Elbow Surg*. 2002;11(5):442-451. doi:10.1067/mse.2002.124526

26. Gupta R, Lee TQ. Positional-dependent changes in glenohumeral joint contact pressure and force: Possible biomechanical etiology of posterior glenoid wear. *J Shoulder Elbow Surg*. 2005;14(1, Supplement):S105-S110. doi:10.1016/j.jse.2004.10.005

27. Yu J, McGarry MH, Lee YS, Duong LV, Lee TQ. Biomechanical effects of supraspinatus repair on the glenohumeral joint. *J Shoulder Elbow Surg*. 2005;14(1):S65-S71. doi:10.1016/j.jse.2004.09.019

28. Halperin SJ, Dhodapkar MM, Kim L, et al. Anatomic vs. reverse total shoulder arthroplasty: usage trends and perioperative outcomes. *Semin Arthroplasty JSES*. 2024;34(1):91-96. doi:10.1053/j.sart.2023.08.014

29. Schoch B, Abboud J, Namdari S, Lazarus M. Glenohumeral Mismatch in Anatomic Total Shoulder Arthroplasty. *JBJS Rev*. 2017;5(9):e1-e1. doi:10.2106/JBJS.RVW.17.00014

30. Rau G, Disselhorst-Klug C, Schmidt R. Movement biomechanics goes upwards: from the leg to the arm. *J Biomech*. 2000;33(10):1207-1216. doi:10.1016/S0021-9290(00)00062-2

31. Daher B, Hunter J, Athwal GS, Lalone EA. How does computed tomography inform our understanding of shoulder kinematics? A structured review. *Med Biol Eng Comput*. 2023;61(5):967-989. doi:10.1007/s11517-022-02755-1

32. Roche CP. Reverse Shoulder Arthroplasty Biomechanics. *J Funct Morphol Kinesiol*. 2022;7(1):13. doi:10.3390/jfmk7010013

33. Kim MS, Jeong HY, Kim JD, Ro KH, Rhee SM, Rhee YG. Difficulty in performing activities of daily living associated with internal rotation after reverse total shoulder arthroplasty. *J Shoulder Elbow Surg*. 2020;29(1):86-94. doi:10.1016/j.jse.2019.05.031

34. Scibek JS, Carcia CR. Assessment of scapulohumeral rhythm for scapular plane shoulder elevation using a modified digital inclinometer. *World J Orthop*. 2012;3(6):87-94. doi:10.5312/wjo.v3.i6.87

35. von Eisenhart-Rothe RMO, Jäger A, Englmeier KH, Vogl TJ, Graichen H. Relevance of Arm Position and Muscle Activity on Three-Dimensional Glenohumeral Translation in Patients with Traumatic and Atraumatic Shoulder Instability. *Am J Sports Med*. 2002;30(4):514-522. doi:10.1177/03635465020300041101

36. Graichen H, Stammberger T, Bonel H, Karl-Hans Englmeier, Reiser M, Eckstein F. Glenohumeral translation during active and passive elevation of the shoulder — a 3D open-MRI study. *J Biomech*. 2000;33(5):609-613. doi:10.1016/S0021-9290(99)00209-2

37. Harryman D, Sidles J, Clark J, McQuade K, Gibb T, Matsen F. Translation of the humeral head on the glenoid with passive glenohumeral motion. *J Bone Joint Surg Am*. 1990;72:1334-1343. doi:10.2106/00004623-199072090-00009

38. Howell SM, Galinat BJ, Renzi AJ, Marone PJ. Normal and abnormal mechanics of the glenohumeral joint in the horizontal plane. *J Bone Joint Surg Am*. 1988;70(2):227-232.

39. Karduna AR, Williams GR, Iannotti JP, Williams JL. Kinematics of the glenohumeral joint: Influences of muscle forces, ligamentous constraints, and articular geometry. *J Orthop Res*. 1996;14(6):986-993. doi:10.1002/jor.1100140620

40. Kozono N, Okada T, Takeuchi N, et al. In vivo kinematic analysis of the glenohumeral joint during dynamic full axial rotation and scapular plane full abduction in healthy shoulders. *Knee Surg Sports Traumatol Arthrosc*. 2017;25(7):2032-2040. doi:10.1007/s00167-016-4263-2

41. Matsumura N, Oki S, Fukasawa N, et al. Glenohumeral translation during active external rotation with the shoulder abducted in cases with glenohumeral instability: a 4-dimensional computed tomography analysis. *J Shoulder Elbow Surg*. 2019;28(10):1903-1910. doi:10.1016/j.jse.2019.03.008

42. Massimini DF, Warner JJP, Li G. Glenohumeral joint cartilage contact in the healthy adult during scapular plane elevation depression with external humeral rotation. *J Biomech*. 2014;47(12):3100-3106. doi:10.1016/j.jbiomech.2014.06.034

43. Kennedy DJ, Mattie R, Nguyen Q, Hamilton S, Conrad B. Glenohumeral Joint Pain Referral Patterns: A Descriptive Study. *Pain Med*. 2015;16(8):1603-1609. doi:10.1111/pme.12797

44. Yang Z, Xu G, Yang J, Li Z. Effect of different loads on the shoulder in abduction postures: a finite element analysis. *Sci Rep*. 2023;13(1):9490. doi:10.1038/s41598-023-36049-9

45. Di Giacomo G, Piscitelli L, Pugliese M. The role of bone in glenohumeral stability. *EFORT Open Rev*. 2018;3(12):632-640. doi:10.1302/2058-5241.3.180028

46. Gasbarro G, Bondow B, Debski R. Clinical anatomy and stabilizers of the glenohumeral joint. *Ann Jt*. 2017;2(10). doi:10.21037/aoj.2017.10.03

47. Massimini DF. *Technique and Application for Quantifying Dynamic Shoulder Joint Kinematics and Glenohumeral Joint Contact Patterns*. Thesis. Massachusetts Institute of Technology; 2014. Accessed August 24, 2023. https://dspace.mit.edu/handle/1721.1/87979

48. Olds M, Ellis R, Donaldson K, Parmar P, Kersten P. Risk factors which predispose first-time traumatic anterior shoulder dislocations to recurrent instability in adults: a systematic review and meta-analysis. *Br J Sports Med*. 2015;49(14):913-922. doi:10.1136/bjsports-2014-094342

49. Porcellini G, Campi F, Pegreffi F, Castagna A, Paladini P. Predisposing Factors for Recurrent Shoulder Dislocation After Arthroscopic Treatment. *JBJS*. 2009;91(11):2537. doi:10.2106/JBJS.H.01126

50. Creech JA, Silver S. Shoulder Impingement Syndrome. In: *StatPearls*. StatPearls Publishing; 2024. Accessed April 22, 2024. http://www.ncbi.nlm.nih.gov/books/NBK554518/

51. Garving C, Jakob S, Bauer I, Nadjar R, H. Brunner U. Impingement Syndrome of the Shoulder. *Dtsch Ärztebl Int*. 2017;114(45):765-776. doi:10.3238/arztebl.2017.0765

52. Health C for D and R. Medical X-ray Imaging. FDA. August 15, 2023. Accessed April 18, 2024. https://www.fda.gov/radiation-emitting-products/medical-imaging/medical-x-ray-imaging

53. X-Ray (Radiology) | LHSC. Accessed July 8, 2024. https://www.lhsc.on.ca/medical-imaging/x-ray-radiology

54. X-rays. National Institute of Biomedical Imaging and Bioengineering. Accessed June 10, 2024. https://www.nibib.nih.gov/science-education/science-topics/x-rays

55. Tubiana M. [Wilhelm Conrad Röntgen and the discovery of X-rays]. *Bull Acad Natl Med*. 1996;180(1):97-108.

56. Shoulder X Ray: Anatomy, Procedure & What to Expect. Cleveland Clinic. Accessed June 10, 2024. https://my.clevelandclinic.org/health/diagnostics/22531-shoulder-x-ray

57. Fluoroscopy Procedure. May 20, 2024. Accessed July 8, 2024. https://www.hopkinsmedicine.org/health/treatment-tests-and-therapies/fluoroscopy-procedure

58. Health C for D and R. Fluoroscopy. *FDA*. Published online August 15, 2023. Accessed June 10, 2024. https://www.fda.gov/radiation-emitting-products/medical-x-ray-imaging/fluoroscopy

59. Mozingo JD, Akbari-Shandiz M, Van Straaten MG, et al. Comparison of glenohumeral joint kinematics between manual wheelchair tasks and implications on the subacromial space: A biplane fluoroscopy study. *J Electromyogr Kinesiol Off J Int Soc Electrophysiol Kinesiol*. 2022;62:102350. doi:10.1016/j.jelekin.2019.08.004

60. Nishinaka N, Tsutsui H, Mihara K, et al. Determination of in vivo glenohumeral translation using fluoroscopy and shape-matching techniques. *J Shoulder Elbow Surg*. 2008;17(2):319-322. doi:10.1016/j.jse.2007.05.018

61. Bey MJ, Zauel R, Brock SK, Tashman S. Validation of a New Model-Based Tracking Technique for Measuring Three-Dimensional, In Vivo Glenohumeral Joint Kinematics. *J Biomech Eng*. 2006;128(4):604-609. doi:10.1115/1.2206199

62. Dal Maso F, Blache Y, Raison M, Lundberg A, Begon M. Glenohumeral joint kinematics measured by intracortical pins, reflective markers, and computed tomography: A novel technique to assess acromiohumeral distance. *J Electromyogr Kinesiol*. 2016;29:4-11. doi:10.1016/j.jelekin.2015.07.008

63. Matsuki K, Matsuki KO, Mu S, et al. In vivo 3-dimensional analysis of scapular kinematics: comparison of dominant and nondominant shoulders. *J Shoulder Elbow Surg*. 2011;20(4):659-665. doi:10.1016/j.jse.2010.09.012

64. Baumer TG, Giles JW, Drake A, Zauel R, Bey MJ. Measuring Three-Dimensional Thorax Motion Via Biplane Radiographic Imaging: Technique and Preliminary Results. *J Biomech Eng*. 2016;138(1):014504. doi:10.1115/1.4032058

65. Buzug TM. Computed Tomography. In: Kramme R, Hoffmann KP, Pozos RS, eds. *Springer Handbook of Medical Technology*. Springer Berlin Heidelberg; 2011:311-342. doi:10.1007/978-3-540-74658-4_16

66. Cierniak R. Some Words About the History of Computed Tomography. In: Cierniak R, ed. *X-Ray Computed Tomography in Biomedical Engineering*. Springer; 2011:7-19. doi:10.1007/978-0-85729-027-4_2

67. Seeram E. Computed Tomography: Physical Principles and Recent Technical Advances. *J Med Imaging Radiat Sci*. 2010;41(2):87-109. doi:10.1016/j.jmir.2010.04.001

68. Matsen FAI, Hsu JE. Subluxation in the Arthritic Shoulder. *JBJS Rev*. 2021;9(9):e21.00102. doi:10.2106/JBJS.RVW.21.00102

69. Wong MT, Wiens C, Kuczynski M, Manske S, Schneider PS. Four-dimensional computed tomography: musculoskeletal applications. *Can J Surg*. 2022;65(3):E388-E393. doi:10.1503/cjs.023420

70. Hislop-Jambrich JL, Troupis JM, Moaveni AK. The Use of a Dynamic 4-Dimensional Computed Tomography Scan in the Diagnosis of Atraumatic Posterior Sternoclavicular Joint Instability. *J Comput Assist Tomogr*. 2016;40(4):576-577. doi:10.1097/RCT.0000000000000410

71. Dyer DR, Troupis JM, Kamali Moaveni A. Wide field of view CT and acromioclavicular joint instability: A technical innovation. *J Med Imaging Radiat Oncol*. 2015;59(3):326-330. doi:10.1111/1754-9485.12283

72. Bell SN, Troupis JM, Miller D, Alta TD, Coghlan JA, Wijeratna MD. Four-dimensional computed tomography scans facilitate preoperative planning in

snapping scapula syndrome. *J Shoulder Elbow Surg*. 2015;24(4):e83-e90. doi:10.1016/j.jse.2014.09.020

73. Alta TD, Bell SN, Troupis JM, Coghlan JA, Miller D. The New 4-Dimensional Computed Tomographic Scanner Allows Dynamic Visualization and Measurement of Normal Acromioclavicular Joint Motion in an Unloaded and Loaded Condition: *J Comput Assist Tomogr*. 2012;36(6):749-754. doi:10.1097/RCT.0b013e31826dbc50

74. Kwong Y, Mel AO, Wheeler G, Troupis JM. Four-dimensional computed tomography (4DCT): A review of the current status and applications. *J Med Imaging Radiat Oncol*. 2015;59(5):545-554. doi:10.1111/1754-9485.12326

75. Jinzaki M, Yamada Y, Nagura T, et al. Development of Upright Computed Tomography With Area Detector for Whole-Body Scans: Phantom Study, Efficacy on Workflow, Effect of Gravity on Human Body, and Potential Clinical Impact. *Invest Radiol*. 2020;55(2):73. doi:10.1097/RLI.0000000000000603

76. Osteoarthritis | CDC. June 13, 2023. Accessed April 24, 2024. https://www.cdc.gov/arthritis/types/osteoarthritis.htm

77. Badley EM Wilfong JM, Zahid S, AV P. Burden of Osteoarthritis in Canada. Published online 2021.

78. Casagrande D, Stains JP, Murthi AM. Identification of shoulder osteoarthritis biomarkers: comparison between shoulders with and without osteoarthritis. *J Shoulder Elbow Surg*. 2015;24(3):382-390. doi:10.1016/j.jse.2014.11.039

79. Lo IKY, Litchfield RB, Griffin S, Faber K, Patterson SD, Kirkley A. Quality-of-life outcome following hemiarthroplasty or total shoulder arthroplasty in patients with osteoarthritis. A prospective, randomized trial. *J Bone Joint Surg Am*. 2005;87(10):2178-2185. doi:10.2106/JBJS.D.02198

80. Gartsman GM, Roddey TS, Hammerman SM. Shoulder arthroplasty with or without resurfacing of the glenoid in patients who have osteoarthritis. *J Bone Joint Surg Am*. 2000;82(1):26-34. doi:10.2106/00004623-200001000-00004

81. Osteoarthritis. March 31, 2022. Accessed July 8, 2024. https://www.hopkinsmedicine.org/health/conditions-and-diseases/arthritis/osteoarthritis

82. Boselli KJ, Ahmad CS, Levine WN. Treatment of Glenohumeral Arthrosis. *Am J Sports Med*. 2010;38(12):2558-2572. doi:10.1177/0363546510369250

83. Cole BJ, Yanke A, Provencher MT. Nonarthroplasty alternatives for the treatment of glenohumeral arthritis. *J Shoulder Elbow Surg*. 2007;16(5, Supplement):S231-S240. doi:10.1016/j.jse.2007.03.011

84. Osteoarthritis of the Shoulder. Accessed July 8, 2024. https://www.arthritis.org/diseases/more-about/osteoarthritis-of-the-shoulder

85. Petersson CJ. Degeneration of the Gleno-Humeral Joint: An Anatomical Study. *Acta Orthop Scand*. 1983;54(2):277-283. doi:10.3109/17453678308996570

86. Kerr R, Resnick D, Pineda C, Haghighi P. Osteoarthritis of the glenohumeral joint: a radiologic-pathologic study. *Am J Roentgenol*. 1985;144(5):967-972. doi:10.2214/ajr.144.5.967

87. Menge TJ, Boykin RE, Byram IR, Bushnell BD. A comprehensive approach to glenohumeral arthritis. *South Med J*. 2014;107(9):567-573. doi:10.14423/SMJ.0000000000000166

88. Neer CS, Watson KC, Stanton FJ. Recent experience in total shoulder replacement. *J Bone Joint Surg Am*. 1982;64(3):319-337.

89. Walch G, Badet R, Boulahia A, Khoury A. Morphologic study of the Glenoid in primary glenohumeral osteoarthritis. *J Arthroplasty*. 1999;14(6):756-760. doi:10.1016/S0883-5403(99)90232-2

90. Vo KV, Hackett DJ, Gee AO, Hsu JE. Classifications in Brief: Walch Classification of Primary Glenohumeral Osteoarthritis. *Clin Orthop*. 2017;475(9):2335-2340. doi:10.1007/s11999-017-5317-6

91. Denard PJ, Walch G. Current concepts in the surgical management of primary glenohumeral arthritis with a biconcave glenoid. *J Shoulder Elbow Surg*. 2013;22(11):1589-1598. doi:10.1016/j.jse.2013.06.017

92. Favorito PJ, Freed RJ, Passanise AM, Brown MJ. Total shoulder arthroplasty for glenohumeral arthritis associated with posterior glenoid bone loss: results of an all-polyethylene, posteriorly augmented glenoid component. *J Shoulder Elbow Surg*. 2016;25(10):1681-1689. doi:10.1016/j.jse.2016.02.020

93. Walch G, Boulahia A, Boileau P, Kempf JF. Primary glenohumeral osteoarthritis: clinical and radiographic classification. The Aequalis Group. *Acta Orthop Belg*. 1998;64 Suppl 2:46-52.

94. Pike JM, Singh SK, Barfield WR, Schoch B, Friedman RJ, Eichinger JK. Impact of age on shoulder range of motion and strength. *JSES Int*. 2022;6(6):1029-1033. doi:10.1016/j.jseint.2022.08.016

95. Kolz CW, Sulkar HJ, Aliaj K, et al. Age-related differences in humerothoracic, scapulothoracic, and glenohumeral kinematics during elevation and rotation motions. *J Biomech*. 2021;117:110266. doi:10.1016/j.jbiomech.2021.110266

96. Abballe VD, Walter WR, Lin DJ, Alaia MJ, Alaia EF. Anterior Shoulder Instability in the Aging Population: MRI Injury Pattern and Management. *Am J Roentgenol*. 2021;216(5):1300-1307. doi:10.2214/AJR.20.24011

97. Burner T, Abbott D, Huber K, et al. Shoulder Symptoms and Function in Geriatric Patients. *J Geriatr Phys Ther 2001*. 2014;37(4):154-158. doi:10.1519/JPT.0b013e3182abe7d6

98. St Angelo JM, Taqi M, Fabiano SE. Adhesive Capsulitis. In: *StatPearls*. StatPearls Publishing; 2024. Accessed July 8, 2024. http://www.ncbi.nlm.nih.gov/books/NBK532955/

99. Levy JC, Ashukem MT, Formaini NT. Factors predicting postoperative range of motion for anatomic total shoulder arthroplasty. *J Shoulder Elbow Surg*. 2016;25(1):55-60. doi:10.1016/j.jse.2015.06.026

100. Stathokostas L, McDonald MW, Little RMD, Paterson DH. Flexibility of Older Adults Aged 55–86 Years and the Influence of Physical Activity. *J Aging Res*. 2013;2013:743843. doi:10.1155/2013/743843

101. Kinnucan E, Molcjan MT, Wright DM, Switzer JA. A Prospective Look at the Link Between Frailty and Shoulder Function in Asymptomatic Elderly Individuals. *Geriatr Orthop Surg Rehabil*. 2018;9:2151459318777583. doi:10.1177/2151459318777583

102. Tempelhof S, Rupp S, Seil R. Age-related prevalence of rotator cuff tears in asymptomatic shoulders. *J Shoulder Elbow Surg*. 1999;8(4):296-299. doi:10.1016/S1058-2746(99)90148-9

103. Thomas M, Bidwai A, Rangan A, et al. Glenohumeral osteoarthritis. *Shoulder Elb*. 2016;8(3):203-214. doi:10.1177/1758573216644183

104. Tannenbaum E, Sekiya JK. Evaluation and Management of Posterior Shoulder Instability. *Sports Health*. 2011;3(3):253-263. doi:10.1177/1941738111400562

105. Doehrmann R, Frush TJ. Posterior Shoulder Instability. In: *StatPearls*. StatPearls Publishing; 2024. Accessed May 14, 2024. http://www.ncbi.nlm.nih.gov/books/NBK557648/

106. Gerber C, Costouros JG, Sukthankar A, Fucentese SF. Static posterior humeral head subluxation and total shoulder arthroplasty. *J Shoulder Elbow Surg*. 2009;18(4):505-510. doi:10.1016/j.jse.2009.03.003

107. Choi CH, Kim HC, Kang D, Kim JY. Comparative study of glenoid version and inclination using two-dimensional images from computed tomography and three-dimensional reconstructed bone models. *Clin Shoulder Elb*. 2020;23(3):119-124. doi:10.5397/cise.2020.00220

108. Jacxsens M, Van Tongel A, Willemot LB, Mueller AM, Valderrabano V, De Wilde L. Accuracy of the glenohumeral subluxation index in nonpathologic shoulders. *J Shoulder Elbow Surg*. 2015;24(4):541-546. doi:10.1016/j.jse.2014.07.021

109. Matache BA, Alnusif N, Chaoui J, Walch G, Athwal GS. Humeral head subluxation in Walch type B shoulders varies across imaging modalities. *JSES Int*. 2021;5(1):98-101. doi:10.1016/j.jseint.2020.08.016

110. Terrier A, Ston J, Farron A. Importance of a three-dimensional measure of humeral head subluxation in osteoarthritic shoulders. *J Shoulder Elbow Surg*. 2015;24(2):295-301. doi:10.1016/j.jse.2014.05.027

111. Raniga S, Arenas-Miquelez A, Bokor DJ. Anatomic total shoulder arthroplasty in patients under 50 and over 80 years of age. Part 1. *Obere Extrem*. 2022;17(4):259-266. doi:10.1007/s11678-022-00708-6

112. Ho JC, Amini MH, Entezari V, et al. Clinical and Radiographic Outcomes of a Posteriorly Augmented Glenoid Component in Anatomic Total Shoulder Arthroplasty for Primary Osteoarthritis with Posterior Glenoid Bone Loss. *JBJS*. 2018;100(22):1934. doi:10.2106/JBJS.17.01282

113. Sheth M, Sholder D, Abboud J, Lazarus M, Williams G, Namdari S. Revision of Anatomic Total Shoulder Arthroplasty to Hemiarthroplasty: Does it work? *Arch Bone Jt Surg*. 2020;8(2):147-1153. doi:10.22038/abjs.2019.34244.1897

114. Terrier A, Ston J, Larrea X, Farron A. Measurements of three-dimensional glenoid erosion when planning the prosthetic replacement of osteoarthritic shoulders. *Bone Jt J*. 2014;96-B(4):513-518. doi:10.1302/0301-620X.96B4.32641

115. Magni A, Agostoni P, Bonezzi C, et al. Management of Osteoarthritis: Expert Opinion on NSAIDs. *Pain Ther*. 2021;10(2):783-808. doi:10.1007/s40122-021-00260-1

116. Parsons IM, Weldon EJ, Titelman RM, Smith KL. Glenohumeral arthritis and its management. *Phys Med Rehabil Clin N Am*. 2004;15(2):447-474. doi:10.1016/j.pmr.2003.12.001

117. Pandya J, Johnson T, Low AK. Shoulder replacement for osteoarthritis: A review of surgical management. *Maturitas*. 2018;108:71-76. doi:10.1016/j.maturitas.2017.11.013

118. Kennedy JS, Garrigues GE, Pozzi F, et al. The American Society of Shoulder and Elbow Therapists' consensus statement on rehabilitation for anatomic total shoulder arthroplasty. *J Shoulder Elbow Surg*. 2020;29(10):2149-2162. doi:10.1016/j.jse.2020.05.019

119. Collins DN, Harryman DT, Wirth MA. Shoulder arthroplasty for the treatment of inflammatory arthritis. *J Bone Joint Surg Am*. 2004;86(11):2489-2496. doi:10.2106/00004623-200411000-00020

120. Westermann R, Pugely A, Martin CT, Gao Y, Wolf B, Hettrich C. Reverse Shoulder Arthroplasty in the United States: A Comparison of National Volume, Patient Demographics, Complications, and Surgical Indications. *Iowa Orthop J*. Published online 2015. Accessed July 1, 2024. https://www.semanticscholar.org/paper/Reverse-Shoulder-Arthroplasty-in-the-United-States%3A-Westermann-Pugely/81abb85b2a2c713892beb7d9ad3ab3d9f96589b6

121. Chillemi C, Franceschini V. Shoulder Osteoarthritis. *Arthritis*. 2013;2013:370231. doi:10.1155/2013/370231

122. Millett PJ, Gobezie R, Boykin RE. Shoulder Osteoarthritis: Diagnosis and Management. *Am Fam Physician*. 2008;78(5):605-611.

123. Torchia ME, Cofield RH, Settergren CR. Total shoulder arthroplasty with the neer prosthesis: Long-term results. *J Shoulder Elbow Surg*. 1997;6(6):495-505. doi:10.1016/S1058-2746(97)90081-1

124. Sperling JW, Kaufman KR, Schleck CD, Cofield RH. A biomechanical analysis of strength and motion following total shoulder arthroplasty. *Int J Shoulder Surg*. 2008;2(1):1-3. doi:10.4103/0973-6042.39579

125. Barrett WP, Franklin JL, Jackins SE, Wyss CR, Matsen FA. Total shoulder arthroplasty. *J Bone Joint Surg Am*. 1987;69(6):865-872.

126. Eichinger JK, Galvin JW. Management of complications after total shoulder arthroplasty. *Curr Rev Musculoskelet Med*. 2015;8(1):83-91. doi:10.1007/s12178-014-9251-x

127. Walch G, Young AA, Boileau P, Loew M, Gazielly D, Molé D. Patterns of loosening of polyethylene keeled glenoid components after shoulder arthroplasty for primary osteoarthritis: results of a multicenter study with more than five years of follow-up. *J Bone Joint Surg Am*. 2012;94(2):145-150. doi:10.2106/JBJS.J.00699

128. Cheung EV, Sperling JW, Cofield RH. Revision shoulder arthroplasty for glenoid component loosening. *J Shoulder Elbow Surg*. 2008;17(3):371-375. doi:10.1016/j.jse.2007.09.003

129. Kim SC, Lee JE, Lee SM, Yoo JC. Factors affecting internal rotation after reverse shoulder arthroplasty. *J Orthop Sci*. 2022;27(1):131-138. doi:10.1016/j.jos.2020.11.012

130. Hackett DJ, Hsu JE, Matsen FA. Primary Shoulder Hemiarthroplasty: What Can Be Learned From 359 Cases That Were Surgically Revised? *Clin Orthop*. 2018;476(5):1031-1040. doi:10.1007/s11999.0000000000000167

131. Rispoli DM, Sperling JW, Athwal GS, Schleck CD, Cofield RH. Humeral head replacement for the treatment of osteoarthritis. *J Bone Joint Surg Am*. 2006;88(12):2637-2644. doi:10.2106/JBJS.E.01383

132. Sperling JW, Cofield RH, Rowland CM. Minimum fifteen-year follow-up of Neer hemiarthroplasty and total shoulder arthroplasty in patients aged fifty years or younger. *J Shoulder Elbow Surg*. 2004;13(6):604-613. doi:10.1016/S1058274604001296

133. Levine WN, Fischer CR, Nguyen D, Flatow EL, Ahmad CS, Bigliani LU. Long-term follow-up of shoulder hemiarthroplasty for glenohumeral osteoarthritis. *J Bone Joint Surg Am*. 2012;94(22):e164. doi:10.2106/JBJS.K.00603

Chapter 2

2 Healthy Glenohumeral Arthrokinematics Using Four-Dimensional Computed Tomography Throughout Internal Rotation and Forward Elevation

Glenohumeral arthrokinematics studies that have used a diseased or healthy cadaveric shoulder, may not fully characterize the in vivo physiological state. Currently, glenohumeral joint translation throughout active motion is not well-established in literature, especially for more complex motions of daily living including, internal rotation to the back. Historically, glenohumeral joint tracking employed the humeral head centre instead of the actual contact point between the two surfaces, which is more accurate as it considers exactly how the joint surfaces are moving relative to one another. This chapter explores glenohumeral arthrokinematics, including glenohumeral joint proximity and joint translation, for more complex motions of daily living by using 4DCT to accurately track the glenohumeral surfaces within an in vivo environment. Additionally, this chapter analyzes differences in age, position of movement, and direction of translation for the glenohumeral joint.

A version of this work has been accepted to be published in the Journal of Shoulder and Elbow Surgery (JSES) International.

2.1 Introduction

As discussed in Chapter 1, the shoulder is the most mobile joint in the human body, enabling people to move their arms freely in many directions.[1] Due to the relatively large size of the humeral head in comparison to the glenoid, which is very shallow in nature (3:1 surface area ratio), there is a high incidence of instability at the glenohumeral (GH) joint.[2] It is unknown how the healthy humeral head tracks relative to the glenoid, and how that changes over time as people age. Previous research has focused on patients who have already acquired pathologies (i.e., OA or instability) or who have already undergone shoulder surgeries,[3–8] not on healthy people. The studies that have focused on healthy GH joint movement have primarily used cadaveric specimens,[6,9–11] however, the in vitro loading environment may not fully simulate the in vivo physiological state.[12–14]

In recent years, imaging techniques have been used to measure shoulder motion. These have included, magnetic resonance imaging (MRI),[15,16] X-ray/radiography,[8,17,18] and fluoroscopy.[19] Some advantages for MRI and X-ray/radiography include that MRI emits no ionizing radiation[20] and X-rays/radiographs are cost-effective.[21] However, one disadvantage is that X-ray/radiography does not have the capability to assess active motion.[22] On the other hand, fluoroscopy is capable of dynamic imaging, but has a limited field of view and is 2D in nature,[3,4,23] which is especially challenging for the analysis of larger joints, such as the shoulder. Four-dimensional computed tomography (4DCT) is a newer imaging modality that consists of capturing volume sequences (3DCT) over time to create a dynamic volume set, allowing for a more complete analysis of the shoulder joint over an entire movement.[24] 4DCT has been previously used to assess the shoulder, but primarily for the sternoclavicular,[25] acromioclavicular,[26] and scapulothoracic joints.[27] In these studies, 4DCT was used to assess joint instability and detect and locate pathologic motion, but has not yet been used to assess normal GH motion, particularly parameters such as joint proximity and joint surface tracking (translation).

Assessing joint proximity of the shoulder joint is important because it influences movement patterns,[28] load distribution,[29,30] and joint stability,[31–33] which are important for joint health and performance. Abnormal joint proximity can predispose the glenohumeral joint to subluxation/dislocation,[34,35] and impingement syndromes.[36,37] In respect to joint surface

tracking (translation), many previous studies have used the centre of the humeral head to track the translation at the glenohumeral joint,[5,6,9,15,17,18,38–41] but this study will use the actual contact point between humeral head and the glenoid, which will provide a more insightful and accurate representation of what is happening at the joint surfaces because it directly captures what is happening at the articulation and provides a truer representation of joint behavior, stability and movement. It is important to characterize how the healthy GH joint moves. Currently, there is a limited amount of knowledge regarding how much the humeral head rotates and translates on the glenoid during various movements for individuals of various ages. As people age, there are many physiological changes that occur that can alter the musculoskeletal system, which can ultimately affect muscle mass and strength,[42] joint mechanics,[43] and range of motion.[42] Understanding not only how much rotation, but how much translation is happening in healthy glenohumeral joints is important so that implant designers can capture the true sense of surface motion (i.e., rotation and translation) in shoulder implants accurately. Overall, determining the amount of GH joint translation and rotation, while also analyzing the variances in different ages, will allow for a better understanding of global shoulder motion to assist with in vitro experiments, simulator and shoulder implant development.

Although previous studies have evaluated GH joint movement in various ways, none have done it specifically for healthy people using dynamic imaging (4DCT) for simple movements such as forward elevation (FE) and more complex movements such as internal rotation to the back (IR). IR is a movement that is typically restricted after reverse total shoulder arthroplasties (RTSAs). One reason this is the case is due to the inversion of the anatomical concavities, which creates a fixed fulcrum that can only rotate.[44] This is a major issue due to IR being important in activities of daily living such as, showering/bathing, dressing (e.g., tucking in shirts and/or putting on a bra), or even managing toileting.[45] FE (i.e., reaching overhead) is another movement that is sometimes inhibited after receiving a total shoulder arthroplasty and is also important in routine activities of daily living such as brushing/combing hair and placing/retrieving items from high cupboards or shelves. To allow people to regain this important range of motion, it is vital to determine the amount of translation that is occurring in the healthy joint, so that it can be implemented into the testing and the design of shoulder implants.

The primary objective of this study was to measure and quantify GH joint proximity and GH joint surface tracking (translation) in healthy participants throughout FE and IR using 4DCT. The secondary objective of the study was to determine if there were age (young versus old), position (beginning versus middle versus end of movement), or direction (superior/inferior (S/I) versus anterior/posterior (A/P)) related differences in the healthy GH joint throughout FE and IR. It was hypothesized that the GH joint proximity will increase with age, and that the GH surface tracking (translation) will decrease with age due to the closer joint proximity.

2.2 Materials and Methods

2.2.1 Study Protocol

2.2.1.1 Participants

Thirty-one (31) participants (between 18 and 86 years old with an average age of 45 years old) were recruited for this study and were split into two cohorts depending on age: young (≤ 37 years old) and old (≥45 years old). These age groups were based on a previous study used to assess age-related differences in shoulder kinematics.[43] Recruitment of participants with healthy shoulders over the age of 45 years old is challenging due to increased occurrence of prior shoulder injuries and pathologies.[46,47] Therefore, numerous studies have utilized healthy control groups under the age of 37 for comparison with clinical populations over 45 years old.[48,49] Inclusion criteria included males over the age of 18 with no previous history of any major shoulder injury. Due to higher breast tissue sensitivity and risk of cancer in females compared to males, females were excluded from this study as per Investigational Research Board recommendations. The 4DCT scans of the participants were reviewed by an orthopaedic surgeon to ensure no erosion or pathologies were present. After obtaining consent, participants were assessed to ensure they could reach their dominant hand over their head and behind their back in order to complete the two movements (e.g., IR and FE) that would be performed during the scan. Please note, STROBE guidelines were used to inform the reporting of this observational study.[50]

2.2.1.2 Scanning

A total of three scans (one static and two dynamic) were taken of each participant's dominant shoulder using a CT scanner (Revolution CT Scanner, GE Healthcare, Waukesha, Wisconsin, USA). Prior to the static and dynamic scans, a localizer scan was taken to frame the correct field of view of the participant's shoulder. For the static scan, the participant was placed on their back (i.e., in the supine position) with their arm by their side to ensure that a completely neutral position was obtained. The participant was instructed to remain still during the static scan so that it was clear, accurate and free of any artifact that would affect the bone model making process. The static scan followed a standard static imaging protocol (120kV, 211mA, 1.0s rotation time, 512x512 matrix, axial) and produced 192 1.25mm thick slices for a volume of size 250x250x240mm^3. For the first dynamic scan, the participant was placed on their back, with their elbow at 90° and their hand resting over their abdomen. The participant was then asked to perform FE, which required the participant to lift their hand from their belly up until it was stretched past their head as far as they could go comfortably and then back down to the starting position. The first half of this FE movement is shown in Figure 2-1. For the second dynamic scan, the participant was placed on their non-dominant side, with their dominant shoulder up. The participant was asked to perform IR, which started with the participant pressing the palm of their hand into their belly for a few seconds, then reaching their hand around their side, behind their back as far up the back as possible, and then back to the starting position. The first half of this IR movement is shown in Figure 2-2. For each dynamic scan, the participant was instructed by a technologist on how to perform the entire movement within the scan time and practised it until they were comfortable to perform it by themselves. During the actual scan, verbal cues were provided to guide the participant through the motion to ensure consistency of motion within the allotted time of 18-21 seconds.

The dynamic scans followed a standard dynamic imaging protocol (80kV, 130mA, 0.35s rotation time, 512x512 matrix, axial) producing 64 2.50mm thick slices with each volume of size 450x450x160mm^3. The IR scan lasted for 21 seconds, generating 60 volumes and the FE scan lasted for 18 seconds, generating 50 volumes. As per radiation dose of the entire process, each localizer scan had a dose-length product (DLP) of 8 mGy*cm, the

static scan had a DLP of 281 mGy*cm, the IR dynamic scan had a DLP of 428 mGy*cm, and the FE dynamic scan had a DLP of 357 mGy*cm. Therefore, using the effective dose conversion factor for a typical chest CT (0.014 $mSv*mGy^{-1}*cm^{-1}$),[51] the effective dose of the entire procedure was estimated at 15.3mSv.

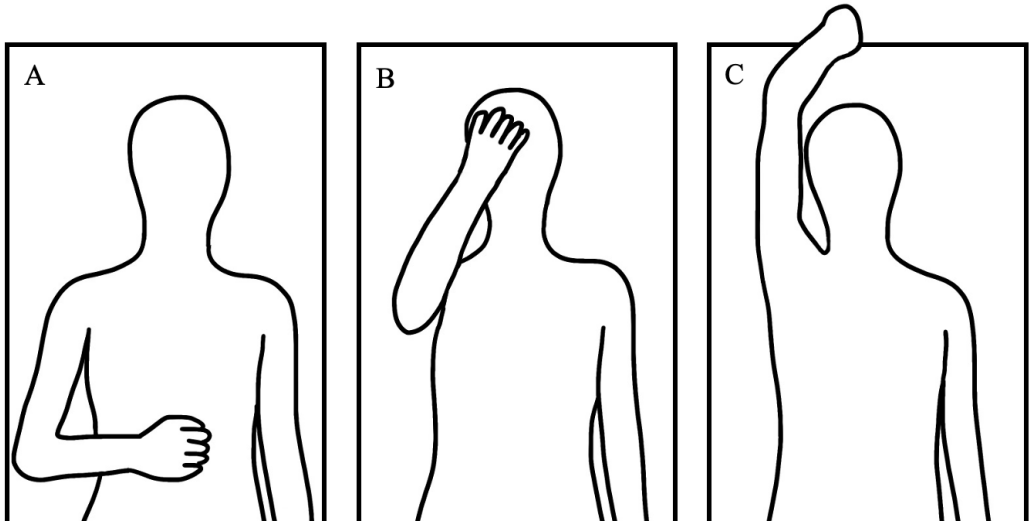

Figure 2-1: Participant lying with back flat against the scanner bed performing FE. (A) Beginning (B) Middle and (C) End of the first half of the movement (anterior view)

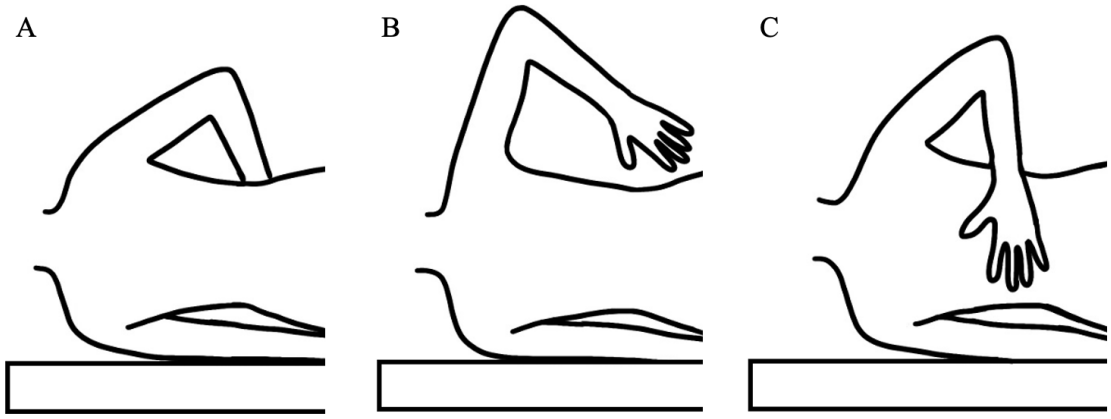

Figure 2-2: Participant lying on side with dominant shoulder facing up performing IR. (A) Beginning (B) Middle and (C) End of the first half of the movement (posterior view)

2.2.2 Image Analysis & Registration

The completed scans for each participant were then uploaded to 3D Slicer, an open-source segmentation, modelling, and registration software (www.slicer.org, Version 4.11). A semi-automated reconstruction process was used to build exact patient-specific bone models of the humerus and scapula (Figure 2-3). Features, including, threshold, scissors, paint, erase, and smoothing were used to obtain high quality bone models. After segmentation and modelling, one static model and numerus dynamic models of the scapula and humerus were completed for each subject.

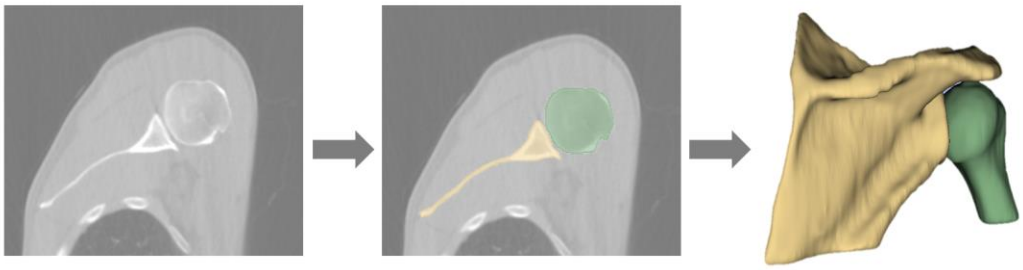

Figure 2-3: 4DCT scan (left) used for segmentation of shoulder bones (middle) to make models of humerus and scapula (right)

Next, using an iterative closest point (ICP) algorithm[52] in 3D Slicer and the CMFregistration extension (cmf.slicer.org), the static model was registered to the position of the dynamic models for each participant in both movements (Figure 2-4). This allowed a transformation matrix to be obtained describing the position of the static model in each dynamic frame.

Figure 2-4: Static model (blue) being registered to the dynamic model (red) through ICP in 3D Slicer

2.2.3 Glenohumeral Arthrokinematics

2.2.3.1 Joint Proximity

Proximity maps of the GH joint, displaying the distance between the glenoid and the humeral head projected on the glenoid fossa, were created. This process involved using the transformed models from registration and then employing a previously developed inter-bone distance algorithm.[53] This algorithm displayed the bones in Paraview version 4.4.0 (Kitware, Inc., New York, New York, www.paraview.org). The proximity maps for each participant and for both movements (IR and FE) were used to visualize GH joint proximity changes throughout the motions assessed.

The reliability of the patient-specific bone models was tested by remaking 3D bone models of the humerus and scapula for one participant in 3D Slicer. These models were then inputted into a previously developed inter-bone distance algorithm[53] to determine the distances between the surfaces for both trials. By averaging the inter-bone distances between surfaces for both trials, the error was discovered to be 0.06mm for the humerus and 0.26mm for the glenoid.[54]

The same transformed models that were used to establish the proximity maps were then used to determine the joint proximity of the GH joint. The following steps were completed for every other frame of movement, for each participant and for both movements. First, using the 'Integrate Variables' feature on Paraview, a threshold of 0mm to 4mm was applied to the model, which displayed the area of the glenoid that was within 4mm of the humeral head (mm^2). A threshold of 4mm was chosen based on mean articular cartilage thickness of the humeral head and glenoid cavity.[55] From this threshold data, the centroids of all points within 4mm were then averaged to determine the overall centroid point that was later used to determine the GH translation. The full glenoid surface area (mm^2) was calculated using SolidWorks via Mesh Prep Wizard, by reducing the mesh to ~40,000 and using 'Spline on Surface' to sketch/trace the glenoid area. Finally, the overall GH joint proximity was found by dividing the area of the glenoid within 4mm of the humeral head (mm^2) by the full glenoid surface area (mm^2), which was then expressed as a percentage. This GH joint proximity (%) was then used to look at differences in age over the entire

movements, as well as more closely during different time points throughout the movements (i.e., beginning, middle, and end).[56] The beginning of the movement is comprised of two frames: the starting position frame and the one just after the participant begins moving their arm out of the starting position. The middle of the movement is when the participant is halfway through the movement (50% of the motion time). The end of the movement also is comprised of two frames: the terminal position frame and the one just before the participant begins moving their arm into the terminal position.

2.2.3.2 Joint Surface Tracking (Translation)

From the data obtained through the initial joint proximity analysis, the GH joint surface tracking (translation) was determined by utilizing coordinate systems to track the centroids in space using the previously validated single vertebra image based (SVIB) technique.[57] Specific landmarks on the glenoid and humeral head from the static scans were chosen and used to a create a local coordinate system. A transformation was then used to describe the overall centroid points for each frame of movement (found from Paraview) in the newly defined local coordinate system. Note: This local coordinate system is different for each frame of movement. From this, the translation at the GH joint was found by taking the difference between the maximum and the minimum values in both the S/I and A/P direction. For example, translation in the S/I direction was the difference between the max and min y-plane values, and the translation in the A/P direction was the difference between the max and min z-plane values.

To test the reliability of the joint surface tracking (translation), a statistical analysis for intra-observer reliability was performed using SPSS and an intraclass correlation coefficient (ICC) (two-way random model with consistency) was used to measure intra-observer reliability of the arthrokinematics for one participant between two trials. The ICC value of the two trials was 0.0951 (95% coefficient, 0.877-0.981), which reported excellent agreement (>0.9) between the two trials for measuring translation.[54]

2.2.4 Statistical Analysis

All statistical analyses were completed using SPSS (SPSS Statistics v26; IBM, 350, Armonk, NJ). A two-way ANOVA was used to assess the effect of age (young and old) and position of movement (beginning, middle, and end) on the joint proximity in the GH joint. Similarly, a two-way ANOVA was used to assess the effect of age (young and old) and direction (S/I and A/P) on translation in the GH joint. A Bonferroni correction was used to correct for the multiple statistical analyses performed, with the significance value set as $p<0.05$.

2.3 Results

2.3.1 Participants

The participant data for each age group is summarized in Table 1. One participant was excluded from the IR motion and six were excluded from the FE motion due to either motion blurring or bones moving out of the field of view.

Table 2-1: Participant Data

	Internal Rotation (IR)	**Forward Elevation (FE)**
Young (≤37 years old)	n = 15 26 ± 6 (18-37)	n = 12 26 ± 6 (18-37)
Old (≥45 years old)	n = 15 63 ± 12 (45-86)	n = 13 62 ± 12 (45-84)

2.3.2 Joint Proximity

Proximity maps, which are visual representations of the GH joint proximity, are shown for FE (Figure 2-5) and IR (Figure 2-6), for one representative participant. The proximity maps for all participants throughout FE and IR can be found in Appendix A. The proximity maps visually show how the GH joint proximity varies throughout each movement, starting from the beginning of the motion (Frame 0) and displaying every other frame until the end of the motion. Note: The end frame for each participant varied depending on timing of the participant's motion. A scale from 0mm to 6mm was chosen for these joint proximity maps

because it provided the most effective visual representation of joint proximity within the glenohumeral joint. A full data set of all proximity maps can be found in the supplementary data.

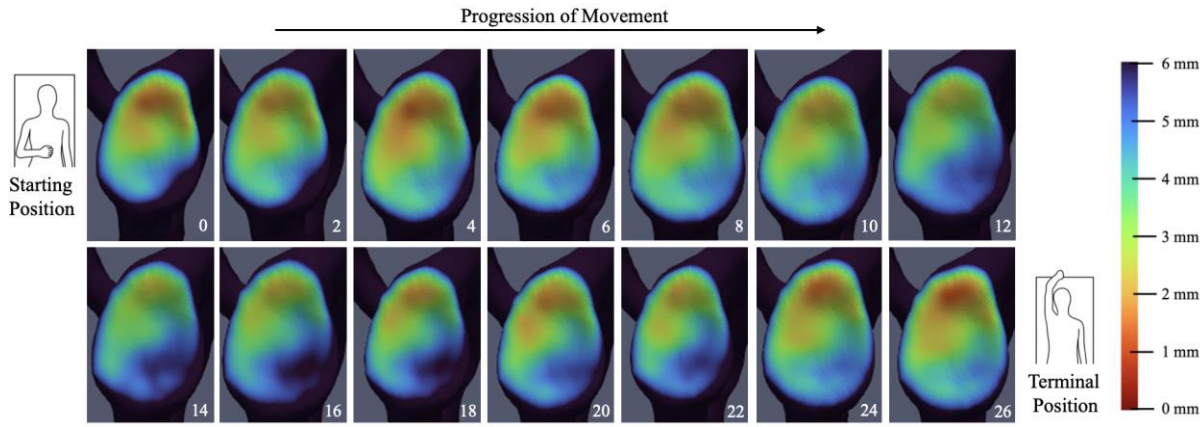

Figure 2-5: Proximity map for a representative participant throughout FE at different reference frames. Starting position shown in top left (Frame 0) and movement progresses to the right ending with terminal position shown in bottom right (Frame 26)

Note: 0mm (red) shows close proximity and 6mm (dark blue) shows far proximity.

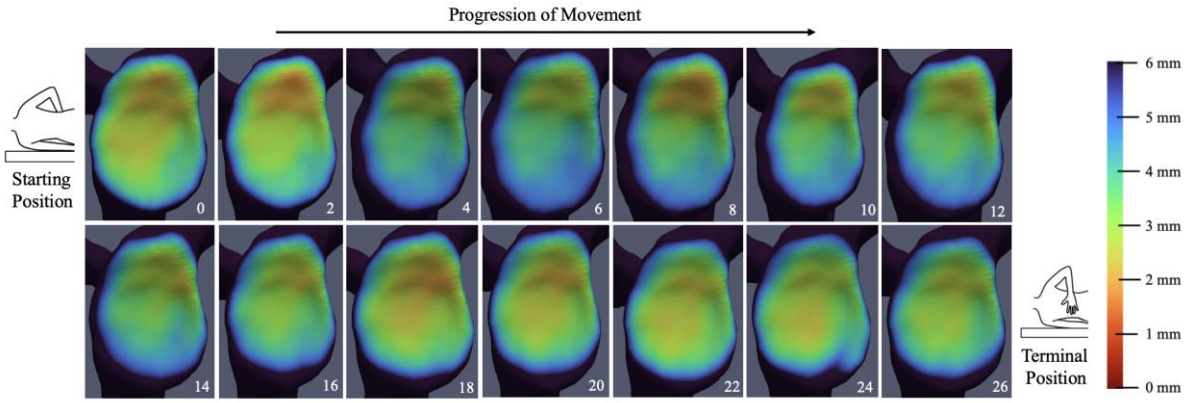

Figure 2-6: Proximity map for a representative participant throughout IR at different reference frames. Starting position shown in top left (Frame 0) and movement progresses to the right ending with terminal position shown in bottom right (Frame 26)

Note: 0mm (red) shows close proximity and 6mm (dark blue) shows far proximity.

2.3.2.1 Forward Elevation

The average GH joint proximity for FE at the beginning, middle, and end of the movement is shown in Figure 2-7. A higher joint proximity value corresponds to a closer GH joint proximity, whereas a lower joint proximity value indicates further GH joint proximity. There were no significant differences in joint proximity for any of the three different stages of the movement for the younger group when compared to the older group.

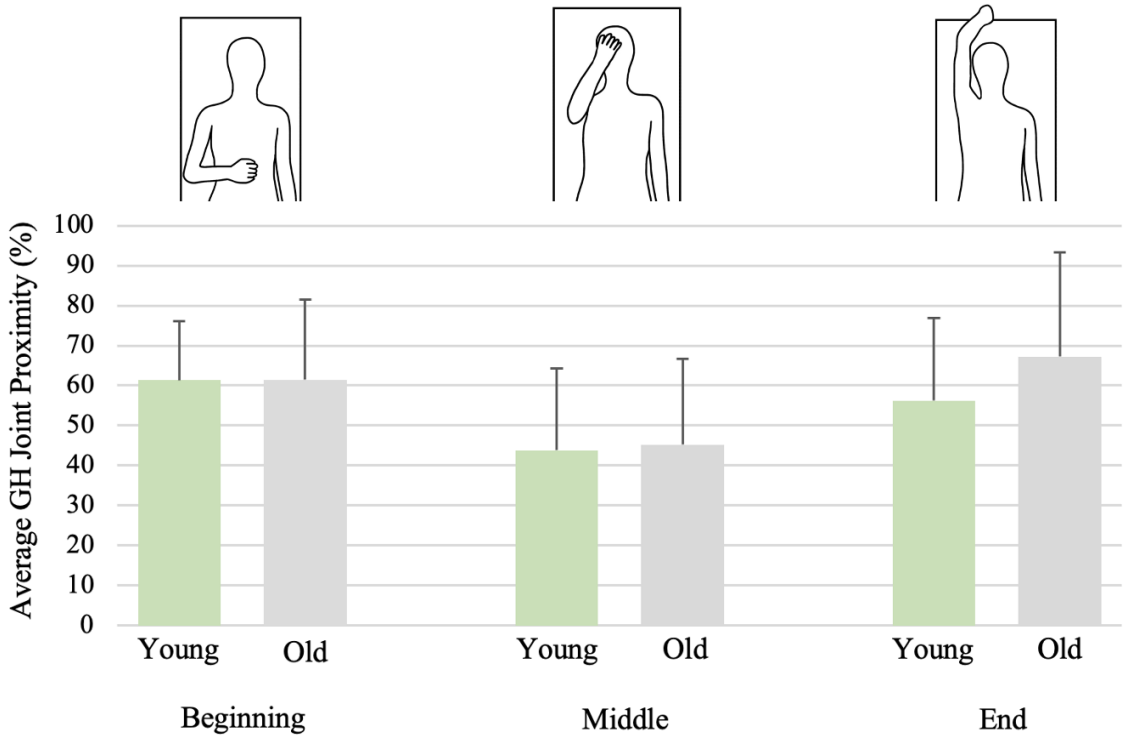

Figure 2-7: FE average GH joint proximity for the younger and older cohorts at the beginning, middle, and end of the movement

2.3.2.2 Internal Rotation

For IR, the average GH joint proximity for IR at the beginning, middle, and end of the movement is shown in Figure 2-8. The older cohort experienced higher joint proximity (63% of glenoid surface was within 4mm of humeral head) during the middle of the movement than the younger cohort (52% of glenoid surface within 4mm of humeral head) (p=0.039, 11.0% difference). No other significant differences were found when comparing age-based cohorts (young versus old) and different stages of movement (beginning versus middle versus end).

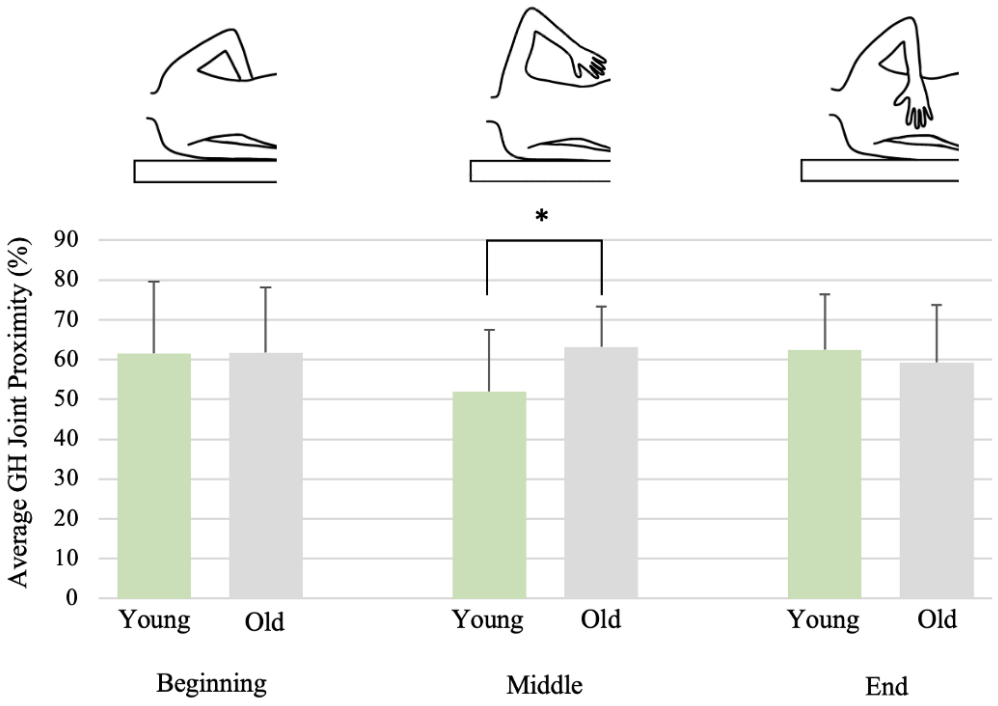

Figure 2-8: IR average GH joint proximity for the younger and older cohorts at the beginning, middle, and end of the movement

2.3.3 Joint Surface Tracking (Translation)

Glenohumeral translations were determined for both S/I and A/P directions (Figure 2-9).

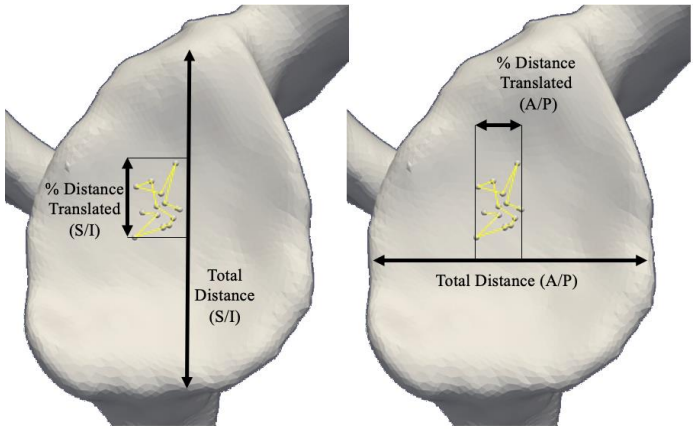

Figure 2-9: The glenohumeral representation of the distance the humeral head translated (%) in the superior/inferior direction (left) and anterior/posterior direction (right) used for the analysis of FE and IR joint surface tracking (translation)

Each yellow point represents the centroid of the joint surface contact for each frame of movement for one representative participant. This showcases where the humeral head translates on the glenoid throughout an entire movement.

2.3.3.1 Forward Elevation

Throughout FE for all individuals 6 ± 2mm (15 ± 6%) of translation occurred in the S/I direction and 5 ± 3mm (16 ± 8%) of translation occurred in the A/P direction (Figure 2-10A and Figure 2-10C. Overall, there were no age or direction significant differences between the younger and older cohorts.

2.3.3.2 Internal Rotation

Throughout IR for all individuals, 6 ± 3mm (15 ± 6%) of translation occurred in the S/I direction and 3 ± 2mm (11 ± 5%) of translation occurred in the A/P direction (Figure 2-10B and Figure 2-10D). There were no age-related significant differences between the S/I and A/P directions during this movement. However, there were direction-related differences in translation for IR, most notably the younger cohort experienced more translation in the S/I

direction than A/P direction over the entire movement when compared to the older cohort (6% difference, p=0.016).

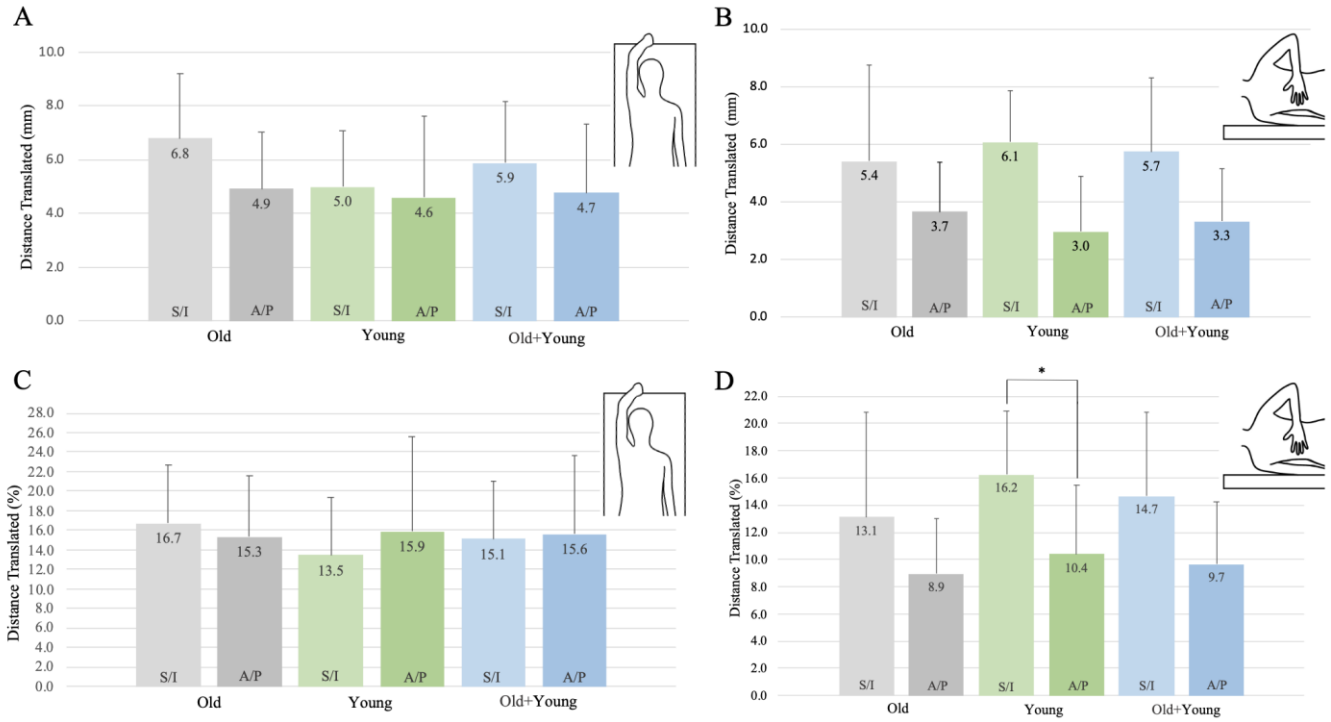

Figure 2-10: Total translation of GH joint for the younger and older cohorts for FE and IR (A) FE (mm); (B) IR (mm); (C) FE (%); (D) IR (%)

2.4 Discussion

Quantifying healthy GH joint proximity and joint surface tracking (translation) is important in understanding how the joint functions, how it may become pathologic, and how it can be replicated with an in vitro simulator for use of more accurate joint movement in cadaver testing.

Understanding joint arthrokinematics enables designers to create implants that closely replicate normal joint movements. Additionally, documenting surface tracking patterns in healthy individuals establishes a benchmark for normal ROM, helping clinicians assess arthrokinematic restoration after reparative or reconstructive surgeries. Overall, for the entire study, no significant results were found for FE, but there were some significant results found for the more complex movement, IR. It was found that older participants had

closer joint proximity during the middle of the IR movement, and that younger participants had more translation in the S/I direction than A/P direction, also for IR. Additionally, it was found that the younger cohort had more translation in the S/I direction than the A/P direction for IR.

The complexity of the shoulder has made it a difficult joint to study over the years. Most previous studies on GH joint mechanics have examined simple planar movements, such as abduction.[8,15–19,33,40,41] In this study, the use of 4DCT allowed the assessment of complex movements, such as IR, which are important in routine activities of daily living, such as showering/bathing, dressing, and toileting.

In total, there were two statistically significant results in the analysis of GH joint proximity and joint tracking (translation). Firstly, when examining GH joint proximity, older participants displayed closer joint proximity during the middle of the movement compared to the younger participants (11.0% difference, $p=0.039$) for IR. Secondly, also for IR, the translation that occurred in the GH joint differed between the S/I and A/P directions. The younger participants had more translation in the S/I direction (16%) compared to the A/P direction (10%) in IR (6% difference total, $p=0.016$). Over the entire study, for FE, no significant differences were found when examining the effects of age and position on joint proximity and age and direction on translation. Overall, despite some of the small differences seen in translation between different ages, positions, and directions, it was apparent that translation in the GH joint was important when performing these different movements, since translation ranged from 9% to 16% in the A/P direction (width of glenoid) and from 13% to 16% in the S/I direction (height of glenoid).

The GH joint proximity maps visually showed which areas (i.e., superior, inferior, posterior or anterior) of the glenoid were in the closest proximity and which were in the farthest proximity to the humeral head. These maps also showed where in the movement the joint proximity decreased and where it increased through each movement. This made it possible to explicitly note where within these movements there was close joint proximity, which could possibly lead to high points of stress and contact in the joint. In agreement with Bey et al. (2009), these maps allow for a visualization and a measure of joint function that is

not fully captured in normal GH kinematic analyses, and it is important in restoring GH joint articular mechanics that may be altered in many shoulder pathologies.

Investigating GH joint proximity (%) allowed joint articular contact patterns to be mapped throughout the various movements examined. It was hypothesized that joint proximity would increase with age, therefore having closer humeral head to glenoid proximity in older individuals. For IR, this hypothesis held true during the middle of the movement, due to the fact that the older cohort experienced 11% closer joint proximity than the younger cohort ($p=0.039$). This proximity could be due to the slight loss of articular cartilage in the older cohort, or due to overall increased age-related joint stiffness that did not allow the GH joint to open up fully when individuals moved their arms around their torsos and in terminal positions. For FE, very similar joint proximity was seen between the younger and older cohorts during the beginning, middle, and end of the movements, making all differences statistically non-significant and disagreeing with the original hypothesis for this movement specifically.

In terms of GH joint surface tracking (translation), the hypothesis was that the older cohort would have less translation due to joint space narrowing, causing less movement and more stiffness in the joint. The results of this study disagreed with the hypothesis due to the fact that there were no significant differences found in glenohumeral translation between the younger and older cohorts, meaning that despite age, a similar amount of translation occurred in all participants throughout both movements. However, one result that was significant was that the younger cohort had more translation in the S/I direction than the A/P direction (6% difference, $p=0.016$). Bey et al. (2009) studied GH joint mechanics in coronal-plane abduction for repaired (rotator cuff) and contralateral shoulders. In the Bey et al. study, it was found that joint contact centre position translated mainly in the S/I direction (8mm) compared to the A/P direction (4mm) during shoulder abduction in both the repaired and contralateral shoulders. Similarly to Bey et al. (2009), Massimini (2014) studied GH joint mechanics, but with scapular plane abduction-adduction motion with external humeral rotation. It was also found in the Massimini study that the majority of translation happened in the S/I direction (18.3mm) compared to the A/P direction (4.5mm). Furthermore, a more recent study from Matsumura et al. (2019) studied GH translation

during active external rotation with the shoulder abducted. This study used 4DCT technology and found that the humeral head translated more in the A/P direction (3.4mm) compared to the S/I (1.7mm) direction. These papers all studied different shoulder movements, and all had slightly varying results when comparing S/I and A/P translations for individuals of all ages. Comparing these previous studies to the current study shows how the GH joint surface tracking can vary with the imaging technique, sample size, sample age, and shoulder movements studied. Despite these slight differences in translation direction, these studies demonstrate that translational movement at the GH joint are important in achieving full healthy ROM.

Humeral head translation on the glenoid seems to be important for obtaining maximal ROM. This natural design feature of the glenohumeral joint may also apply to anatomic shoulder arthroplasty implants. At present, several implant manufacturers have a radius of curvature mismatch between the humeral head replacement and the glenoid polyethylene. Understanding the normal translation that occurs in the healthy shoulder may allow implant manufacturers to design implants with an idealized mismatch to allow for more normalized glenohumeral translations.

2.5 Conclusion

This study utilized 4DCT to quantify GH joint proximity and GH joint translation throughout various shoulder motions in healthy participants to determine if there were any age, position, or direction related differences. It was found that there were only significant differences in the more complex IR motion. Quantifying the total translation in the healthy GH joint showed just how important translational movement is in completing these different shoulder motions, which will aid implant manufacturers in designing implants that will allow for more normalized glenohumeral translations. In the future, it is hoped that the same analysis will be conducted on unhealthy/diseased and implanted shoulders, enabling a comparative study to determine the differences in glenohumeral translation between different patient groups. In conclusion, it is anticipated that these findings will allow biomedical technology companies to implement the information regarding GH joint proximity and translation into implant design and testing to ultimately optimize shoulder implants in the future.

2.6 References

1. Patel RM, Gelber JD, Schickendantz MS. The Weight-Bearing Shoulder. *J Am Acad Orthop Surg*. 2018;26(1):3-13. doi:10.5435/JAAOS-D-15-00598

2. Chang LR, Anand P, Varacallo M. Anatomy, Shoulder and Upper Limb, Glenohumeral Joint. In: *StatPearls*. StatPearls Publishing; 2023. Accessed June 13, 2023. http://www.ncbi.nlm.nih.gov/books/NBK537018/

3. Bey MJ, Kline SK, Zauel R, Kolowich PA, Lock TR. In Vivo Measurement of Glenohumeral Joint Contact Patterns. *EURASIP J Adv Signal Process*. 2009;2010(1):1-6. doi:10.1155/2010/162136

4. Bey MJ, Kline SK, Zauel R, Lock TR, Kolowich PA. Measuring dynamic in-vivo glenohumeral joint kinematics: Technique and preliminary results. *J Biomech*. 2008;41(3):711-714. doi:10.1016/j.jbiomech.2007.09.029

5. Friedman RJ. Glenohumeral translation after total shoulder arthroplasty. *J Shoulder Elbow Surg*. 1992;1(6):312-316. doi:10.1016/S1058-2746(09)80058-X

6. Karduna AR, Williams GR, Williams JL, Iannotti JP. Glenohumeral Joint Translations before and after Total Shoulder Arthroplasty. A Study in Cadavera*. *JBJS*. 1997;79(8):1166.

7. Muench LN, Murphey M, Oei B, et al. Elliptical and spherical heads show similar obligate glenohumeral translation during axial rotation in total shoulder arthroplasty. *BMC Musculoskelet Disord*. 2023;24(1):171. doi:10.1186/s12891-023-06273-5

8. Poppen NK, Walker PS. Normal and abnormal motion of the shoulder. *J Bone Joint Surg Am*. 1976;58(2):195-201.

9. Harryman D, Sidles J, Clark J, McQuade K, Gibb T, Matsen F. Translation of the humeral head on the glenoid with passive glenohumeral motion. *J Bone Joint Surg Am*. 1990;72:1334-1343. doi:10.2106/00004623-199072090-00009

10. Warner JJP, Bowen K, Hannafin JA, Arnoczky P, Warren RF. Articular contact patterns of the normal glenohumeral joint. *J Shoulder Elb Surg*. 1998;7(4).

11. Wuelker N, Schmotzer H, Thren K, Korell M. Translation of the glenohumeral joint with simulated active elevation. *Clin Orthop*. 1994;309:193-200.

12. Greis PE, Scuderi MG, Mohr A, Bachus KN, Burks RT. Glenohumeral articular contact areas and pressures following labral and osseous injury to the anteroinferior quadrant of the glenoid. *J Shoulder Elbow Surg*. 2002;11(5):442-451. doi:10.1067/mse.2002.124526

13. Gupta R, Lee TQ. Positional-dependent changes in glenohumeral joint contact pressure and force: Possible biomechanical etiology of posterior glenoid wear. *J*

Shoulder Elbow Surg. 2005;14(1, Supplement):S105-S110. doi:10.1016/j.jse.2004.10.005

14. Yu J, McGarry MH, Lee YS, Duong LV, Lee TQ. Biomechanical effects of supraspinatus repair on the glenohumeral joint. *J Shoulder Elbow Surg*. 2005;14(1):S65-S71. doi:10.1016/j.jse.2004.09.019

15. Graichen H, Stammberger T, Bonel H, Karl-Hans Englmeier, Reiser M, Eckstein F. Glenohumeral translation during active and passive elevation of the shoulder — a 3D open-MRI study. *J Biomech*. 2000;33(5):609-613. doi:10.1016/S0021-9290(99)00209-2

16. Matsui K, Tachibana T, Nobuhara K, Uchiyama Y. Translational movement within the glenohumeral joint at different rotation velocities as seen by cine MRI. *J Exp Orthop*. 2018;5:7. doi:10.1186/s40634-018-0124-x

17. Howell SM, Galinat BJ, Renzi AJ, Marone PJ. Normal and abnormal mechanics of the glenohumeral joint in the horizontal plane. *J Bone Joint Surg Am*. 1988;70(2):227-232.

18. Kozono N, Okada T, Takeuchi N, et al. In vivo kinematic analysis of the glenohumeral joint during dynamic full axial rotation and scapular plane full abduction in healthy shoulders. *Knee Surg Sports Traumatol Arthrosc*. 2017;25(7):2032-2040. doi:10.1007/s00167-016-4263-2

19. Matsuki K, Kenmoku T, Ochiai N, Sugaya H, Banks SA. Differences in glenohumeral translations calculated with three methods: Comparison of relative positions and contact point. *J Biomech*. 2016;49(9):1944-1947. doi:10.1016/j.jbiomech.2016.03.042

20. Jadvar H, Colletti PM. Competitive advantage of PET/MRI. *Eur J Radiol*. 2014;83(1):84-94. doi:10.1016/j.ejrad.2013.05.028

21. Sailer AM, van Zwam WH, Wildberger JE, Grutters JPC. Cost-effectiveness modelling in diagnostic imaging: a stepwise approach. *Eur Radiol*. 2015;25(12):3629-3637. doi:10.1007/s00330-015-3770-8

22. Weishaupt D, Köchli V, Marincek B. *How Does MRI Work?* Springer; 2006. doi:10.1007/978-3-540-37845-7

23. Guan S, Gray H, Keynejad F, Pandy M. Mobile Biplane X-Ray Imaging System for Measuring 3D Dynamic Joint Motion During Overground Gait. *IEEE Trans Med Imaging*. 2015;35. doi:10.1109/TMI.2015.2473168

24. Kwong Y, Mel AO, Wheeler G, Troupis JM. Four-dimensional computed tomography (4DCT): A review of the current status and applications. *J Med Imaging Radiat Oncol*. 2015;59(5):545-554. doi:10.1111/1754-9485.12326

25. Hislop-Jambrich JL, Troupis JM, Moaveni AK. The Use of a Dynamic 4-Dimensional Computed Tomography Scan in the Diagnosis of Atraumatic Posterior Sternoclavicular Joint Instability. *J Comput Assist Tomogr*. 2016;40(4):576-577. doi:10.1097/RCT.0000000000000410

26. Dyer DR, Troupis JM, Kamali Moaveni A. Wide field of view CT and acromioclavicular joint instability: A technical innovation. *J Med Imaging Radiat Oncol*. 2015;59(3):326-330. doi:10.1111/1754-9485.12283

27. Bell SN, Troupis JM, Miller D, Alta TD, Coghlan JA, Wijeratna MD. Four-dimensional computed tomography scans facilitate preoperative planning in snapping scapula syndrome. *J Shoulder Elbow Surg*. 2015;24(4):e83-e90. doi:10.1016/j.jse.2014.09.020

28. Massimini DF, Warner JJP, Li G. Glenohumeral joint cartilage contact in the healthy adult during scapular plane elevation depression with external humeral rotation. *J Biomech*. 2014;47(12):3100-3106. doi:10.1016/j.jbiomech.2014.06.034

29. Kennedy DJ, Mattie R, Nguyen Q, Hamilton S, Conrad B. Glenohumeral Joint Pain Referral Patterns: A Descriptive Study. *Pain Med*. 2015;16(8):1603-1609. doi:10.1111/pme.12797

30. Yang Z, Xu G, Yang J, Li Z. Effect of different loads on the shoulder in abduction postures: a finite element analysis. *Sci Rep*. 2023;13(1):9490. doi:10.1038/s41598-023-36049-9

31. Di Giacomo G, Piscitelli L, Pugliese M. The role of bone in glenohumeral stability. *EFORT Open Rev*. 2018;3(12):632-640. doi:10.1302/2058-5241.3.180028

32. Gasbarro G, Bondow B, Debski R. Clinical anatomy and stabilizers of the glenohumeral joint. *Ann Jt*. 2017;2(10). doi:10.21037/aoj.2017.10.03

33. Massimini DF. *Technique and Application for Quantifying Dynamic Shoulder Joint Kinematics and Glenohumeral Joint Contact Patterns*. Thesis. Massachusetts Institute of Technology; 2014. Accessed August 24, 2023. https://dspace.mit.edu/handle/1721.1/87979

34. Olds M, Ellis R, Donaldson K, Parmar P, Kersten P. Risk factors which predispose first-time traumatic anterior shoulder dislocations to recurrent instability in adults: a systematic review and meta-analysis. *Br J Sports Med*. 2015;49(14):913-922. doi:10.1136/bjsports-2014-094342

35. Porcellini G, Campi F, Pegreffi F, Castagna A, Paladini P. Predisposing Factors for Recurrent Shoulder Dislocation After Arthroscopic Treatment. *JBJS*. 2009;91(11):2537. doi:10.2106/JBJS.H.01126

36. Creech JA, Silver S. Shoulder Impingement Syndrome. In: *StatPearls*. StatPearls Publishing; 2024. Accessed April 22, 2024. http://www.ncbi.nlm.nih.gov/books/NBK554518/

37. Garving C, Jakob S, Bauer I, Nadjar R, H. Brunner U. Impingement Syndrome of the Shoulder. *Dtsch Ärztebl Int*. 2017;114(45):765-776. doi:10.3238/arztebl.2017.0765

38. von Eisenhart-Rothe RMO, Jäger A, Englmeier KH, Vogl TJ, Graichen H. Relevance of Arm Position and Muscle Activity on Three-Dimensional Glenohumeral Translation in Patients with Traumatic and Atraumatic Shoulder Instability. *Am J Sports Med*. 2002;30(4):514-522. doi:10.1177/03635465020300041101

39. Karduna AR, Williams GR, Iannotti JP, Williams JL. Kinematics of the glenohumeral joint: Influences of muscle forces, ligamentous constraints, and articular geometry. *J Orthop Res*. 1996;14(6):986-993. doi:10.1002/jor.1100140620

40. Massimini DF, Boyer PJ, Papannagari R, Gill TJ, Warner JP, Li G. In-vivo glenohumeral translation and ligament elongation during abduction and abduction with internal and external rotation. *J Orthop Surg*. 2012;7:29. doi:10.1186/1749-799X-7-29

41. Matsumura N, Oki S, Fukasawa N, et al. Glenohumeral translation during active external rotation with the shoulder abducted in cases with glenohumeral instability: a 4-dimensional computed tomography analysis. *J Shoulder Elbow Surg*. 2019;28(10):1903-1910. doi:10.1016/j.jse.2019.03.008

42. Pike JM, Singh SK, Barfield WR, Schoch B, Friedman RJ, Eichinger JK. Impact of age on shoulder range of motion and strength. *JSES Int*. 2022;6(6):1029-1033. doi:10.1016/j.jseint.2022.08.016

43. Kolz CW, Sulkar HJ, Aliaj K, et al. Age-related differences in humerothoracic, scapulothoracic, and glenohumeral kinematics during elevation and rotation motions. *J Biomech*. 2021;117:110266. doi:10.1016/j.jbiomech.2021.110266

44. Roche C. Kinematics and Biomechanics of Reverse Total Shoulder Arthroplasty. In: ; 2013:45-54.

45. Kim MS, Jeong HY, Kim JD, Ro KH, Rhee SM, Rhee YG. Difficulty in performing activities of daily living associated with internal rotation after reverse total shoulder arthroplasty. *J Shoulder Elbow Surg*. 2020;29(1):86-94. doi:10.1016/j.jse.2019.05.031

46. Tempelhof S, Rupp S, Seil R. Age-related prevalence of rotator cuff tears in asymptomatic shoulders. *J Shoulder Elbow Surg*. 1999;8(4):296-299. doi:10.1016/S1058-2746(99)90148-9

47. Thomas M, Bidwai A, Rangan A, et al. Glenohumeral osteoarthritis. *Shoulder Elb*. 2016;8(3):203-214. doi:10.1177/1758573216644183

48. Bey MJ, Peltz CD, Ciarelli K, et al. In Vivo Shoulder Function After Surgical Repair of a Torn Rotator Cuff. *Am J Sports Med*. 2011;39(10):2117-2129. doi:10.1177/0363546511412164

49. Hébert LJ, Moffet H, McFadyen BJ, Dionne CE. Scapular behavior in shoulder impingement syndrome. *Arch Phys Med Rehabil*. 2002;83(1):60-69. doi:10.1053/apmr.2002.27471

50. Cuschieri S. The STROBE guidelines. *Saudi J Anaesth*. 2019;13(Suppl 1):S31-S34. doi:10.4103/sja.SJA_543_18

51. McCollough C, Cody D, Edyvean S, et al. *The Measurement, Reporting, and Management of Radiation Dose in CT*. AAPM; 2008. doi:10.37206/97

52. Besl P, McKay HD. A method for registration of 3-D shapes. IEEE Trans Pattern Anal Mach Intell. *Pattern Anal Mach Intell IEEE Trans On*. 1992;14:239-256. doi:10.1109/34.121791

53. Lalone EA, McDonald CP, Ferreira LM, Peters TM, King GW, Johnson JA. Development of an image-based technique to examine joint congruency at the elbow. *Comput Methods Biomech Biomed Engin*. 2013;16(3):280-290. doi:10.1080/10255842.2011.617006

54. Daher B. The Use of CT to Assess Shoulder Kinematics and Measure Glenohumeral Arthrokinematics. *Electron Thesis Diss Repos*. Published online December 7, 2021. https://ir.lib.uwo.ca/etd/8295

55. Carlson CG, Chen A, Patterson K, Ablove RH. Glenohumeral Cartilage Thickness: Implications in Prosthetic Design and Osteochondral Allograft Transplantation. *Cartilage*. 2023;14(3):278-284. doi:10.1177/19476035231154504

56. Mologne TS, Zhao K, Hongo M, Romeo AA, An KN, Provencher MT. The Addition of Rotator Interval Closure After Arthroscopic Repair of Either Anterior or Posterior Shoulder Instability; Effect on Glenohumeral Translation and Range of Motion. *Am J Sports Med*. 2008;36(6):1123-1132. doi:10.1177/0363546508314391

57. Hunter J, Lee TY, Athwal GS, Lalone EA. Development of a single-vertebra image-based technique to quantify shoulder kinematics using four-dimensional computed tomography. *Comput Methods Biomech Biomed Eng Imaging Vis*. 2023;0(0):1-9. doi:10.1080/21681163.2023.2282074

Chapter 3

3 Posterior Augmented Polyethylene Glenoid Implants Correct Posterior Subluxation and Maintain Joint Reduction Throughout Active Motion

Anatomic total shoulder arthroplasty (TSA) with posterior augmented glenoid (PAG) implants is a common procedure for people with symptomatic glenohumeral osteoarthritis who have Walch Type B2 glenoids (posterior humeral head subluxation and posterior glenoid wear). However, there is a limited amount of literature surrounding the outcome and success of these implants and their ability to correct and maintain subluxation throughout active motion. This chapter aims to explore if PAG implants are successful at correcting and maintaining subluxation throughout active motion after TSA. This chapter also seeks to explore if a patient's range of motion (good or limited), magnitude of B2, or PAG implant size (15° or 25°) affect postoperative correction of subluxation.

A version of this work is in the process of being submitted to the Journal of Shoulder and Elbow Surgery (JSES).

3.1 Introduction

As discussed in Chapter 1, osteoarthritis (OA) is the most common joint disease in the world.[1] More specifically, glenohumeral OA is reported to be equally as debilitating as hip and knee arthritis,[2] and comparable to some chronic medical conditions including, diabetes, acute myocardial infarction, and congestive heart failure.[3] Glenohumeral OA can cause pain, stiffness, dysfunction, and bony erosion.[4,5] Anatomic total shoulder arthroplasty (TSA) is one treatment option for patients with symptomatic glenohumeral OA and has long-term survival and satisfaction rates up to 95%.[6] However, TSA is known for having worse outcomes (e.g., higher complication and failure rates due to reoccurrence of instability and early glenoid aseptic loosening)[7] if the preoperative glenohumeral joint exhibits posterior humeral head subluxation and posterior glenoid wear.[8] If the humeral head is not well aligned with the glenoid following a TSA, the continued subluxation can cause asymmetric loading on the posterior part of the glenoid component, which can then cause glenoid loosening through the rocking horse effect.[8] With glenoid loosening accounting for nearly 32% of all complications,[9] it is imperative to determine if subluxation can be corrected and maintained throughout movement to reduce the burden of revision surgeries.

To address subluxation in Walch type B2 glenoids, posterior augmented glenoid (PAG) implants have been developed to realign the glenohumeral joint, to maintain the humeral head centred within the glenoid.[10] However, there is limited literature on the outcomes of PAG implants, and their ability to restore glenohumeral alignment. Additionally, glenohumeral subluxation after TSA has only been assessed statically with axillary radiographs or axial CT images. Furthermore, it is established that the glenohumeral joint undergoes translations and rotations, and that subluxation can occur statically and dynamically.[10–12] Four-dimensional computed tomography (4DCT) is a recent development, which captures three-dimensional (3D) images and allows a dynamic assessment of the glenohumeral joint throughout active motion. Additionally, 4DCT allows for 3D measurements to be used to determine subluxation, which have been shown to be more accurate than previously used two-dimensional (2D) measurements.[13–16]

The primary objective of this study was to determine if Walch type B2 patients managed with a TSA and a PAG implant would maintain correction of subluxation when examined statically and when stressed with active motion. This was accomplished by comparing preoperative glenohumeral joint subluxation to postoperative subluxation using 4DCT during an active motion protocol. The secondary objective was to analyze if a patient's range of motion (good or limited), magnitude of B2, or PAG implant size (15° or 25°) affect postoperative correction of subluxation. It was hypothesized that subluxation would be corrected postoperatively and would maintain a centred joint alignment throughout active movement. It was also hypothesized that there would be no difference in subluxation postoperatively between various PAG implant sizes and magnitudes of B2 erosions, and that patients with better postoperative range of motion would have greater subluxation postoperatively.

3.2 Materials and Methods

3.2.1 Study Protocol

3.2.1.1 Participants (Patients)

Participants (patients) from a single fellowship-trained shoulder surgeon at a tertiary orthopaedic centre were retrospectively identified for prospective enrolment in this imaging study. The inclusion criteria was comprised of participants who have undergone a stemless TSA for OA with a Walch type B2 glenoid, undergone 3D preoperative software planning with a planned retroversion correction to less than 5°, utilized a 15° or 25° half-wedge posteriorly augmented cemented glenoid implant (Perform Plus, Stryker, USA), and had a minimum follow-up period of at least two years. Preoperatively, it is the surgeon's routine protocol to conduct preoperative planning utilizing software (Blueprint, Stryker, Bloomington, MN, USA). If software planning allowed correction of retroversion to 5° with either a 15° or 25° half-wedge implant, the participant was considered to have met the inclusion criteria of this study.

Once consent was obtained, a participant's range of motion was assessed by completing the following movement: reaching the implanted arm behind the back and as far up as possible. This specific movement was chosen to assess the participant's active range of motion in

internal rotation (IR). Internal rotation was chosen for two reasons: First, activation of the subscapularis has been shown to increase posterior humeral head translation,[17] which would be an active provocative test to assess for active or dynamic posterior subluxation. Second, active IR is a motion that can be conducted within the gantry of a 4DCT scan. Additionally, each participant's IR was documented to the highest vertebral level.[18] Based on the participant's active range of motion throughout IR, each participant was grouped into two cohorts: good ROM and limited ROM. The good ROM patients included those who had ROM in the T1-T12 range. The limited ROM patients included those that had ROM in the Greater Trochanter-L1 range (Figure 3-1).

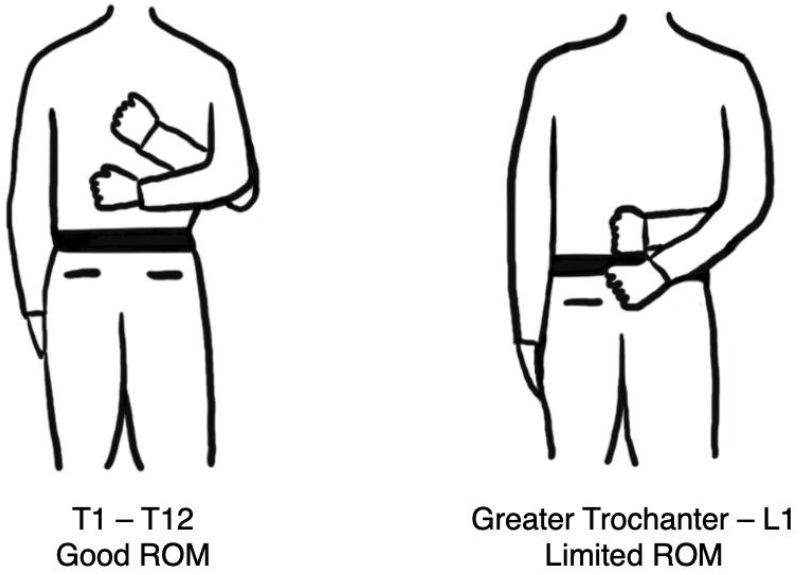

Figure 3-1: Internal Rotation Range of Motion Group

3.2.1.2 Patient Reported Outcomes

Each patient completed the American Shoulder and Elbow Surgeons (ASES) Score. The ASES score is a 100-point scale that evaluates two dimensions of shoulder function: Pain (50 points), and performance in activities of daily living (ADL) (50 points). Patients also completed a pain visual analog scale (VAS) that is represented within the pain score. A score of 0 indicates the worse pain and function loss, and a score of 50 indicates no pain and excellent function.[19]

3.2.1.3 Scanning

Two CT scans (one static preoperative and one dynamic postoperative) were taken of each patient's affected shoulder. The static preoperative scan was captured as a part of the patient's standard of care for use in the preoperative surgical planning software program. The dynamic postoperative CT scan (Revolution CT Scanner, GE Healthcare, Waukesha, Wisconsin, USA) was taken of the patient's implanted shoulder as a part of this study. As well, prior to the dynamic scan, a localizer scan was taken to frame the correct field of view of the patient's shoulder. For the dynamic scan, patients performed active IR, which required the patients to lie on their non-implanted side in the CT scanner, with their implanted shoulder up. The active motion started with the patient's hand resting on their abdomen (Figure 3-2A). Next, the patient lifted their hand and forearm off their abdomen, around their side (Figure 3-2B), as far up the back as possible (Figure 3-2C), and then back to the starting position. The first half of this IR movement is shown in Figure 3-2. For the dynamic scan, the patient was instructed by a technologist on how to perform the entire movement within the scan time and practised it until they were comfortable to perform it by themselves. During the actual scan, verbal cues were provided to guide the patient through the motion to ensure consistency of motion within the allotted time. For the radiation dose of the procedure, the localizer scan and the dynamic scan had a total dose-length product (DLP) of 1050.07mGy*cm. Therefore, using the effective dose conversion factor for a typical chest CT ($0.014 mSv*mGy^{-1}*cm^{-1}$),[20] the dose of the entire process was estimated at 14.70mSv.

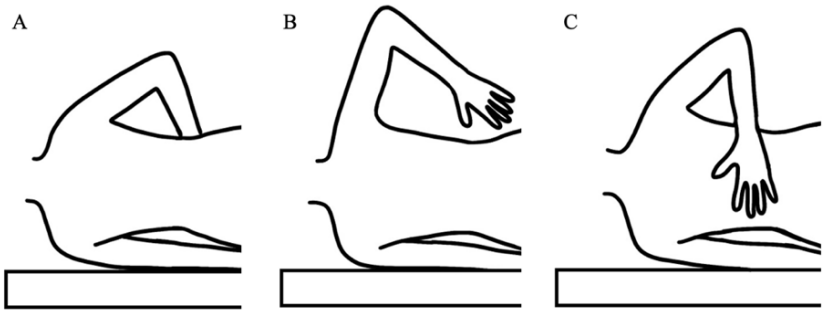

Figure 3-2: Patient lying on their side with the TSA shoulder facing up, performing active internal rotation. (A) Beginning (B) Middle and (C) End of the first half of the movement (posterior view)

3.2.2 Image Analysis

The static preoperative and dynamic postoperative scans were used for image analysis within 3D Slicer, an open-source segmentation, modelling, and registration software (www.slicer.org, Version 4.11). After uploading the scans, a semi-automated reconstruction process was used to build exact patient-specific bone/implant models of the humerus and scapula. Features including, threshold, scissors, islands, paint, erase, and smoothing were used to obtain high quality bone and implant models. The dynamic humerus models that were created used a threshold of 226HU to capture the humeral head implant component, in addition to humeral bone (Figure 3-3). After segmentation, thresholding, and modelling, one static and numerous dynamic models of the scapula and humerus at every other frame of the movement were created for each patient. Using an iterative closest point (ICP) algorithm[21] in 3D Slicer and the CMFregistration extension (cmf.slicer.org), the preoperative static models were registered to the dynamic models.

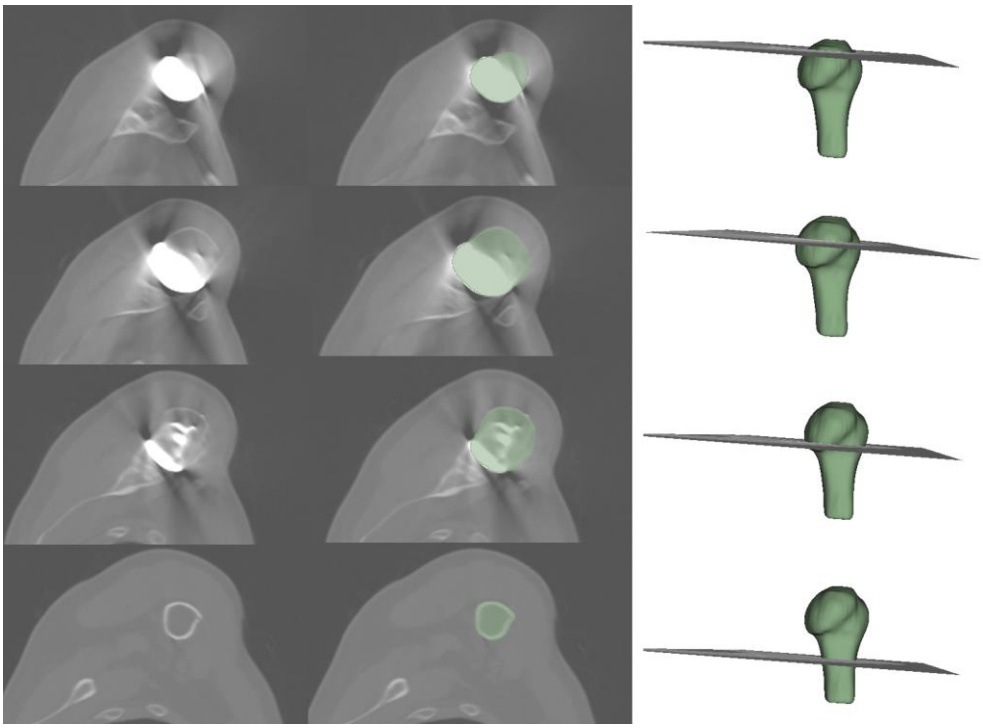

Figure 3-3: 3D Slicer segmentation of humeral head implant component and humerus bone using 4DCT scan

4DCT scan (left), segmentation of humeral head implant component and humerus bone (middle), and patient-specific model showing each associated slicing plane (right)

3.2.3 Landmark Selection and Coordinate System Creation

3.2.3.1 Scapular Coordinate System

Terrier et al. (2014) described a method to define a scapular coordinate system based on bony landmarks located away from the eroded zones of an osteoarthritic shoulder.[22] This newly defined way to develop a scapular coordinate system was built by using five landmarks along the supraspinatus fossa, five landmarks along the axillary border, and one point at the spinoglenoid notch (Figure 3-4). The landmarks along the supraspinatus fossa and axillary border were used to define the scapular plane (Figure 3-5). The spinoglenoid notch landmark was used to mark the origin of the scapular coordinate system (Figure 3-6). The z-axis was aligned with the plane of the scapula (+lateral), the x-axis was perpendicular to the scapular plane (+anterior), and the y-axis was perpendicular to the x-z plane (+superior).

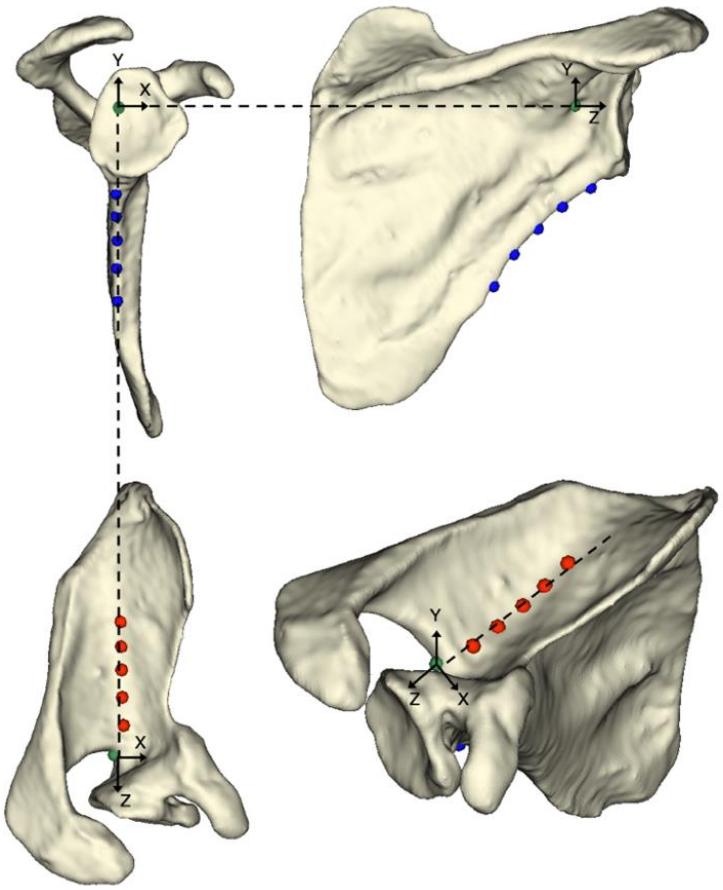

Figure 3-4: Scapular Landmark Selection

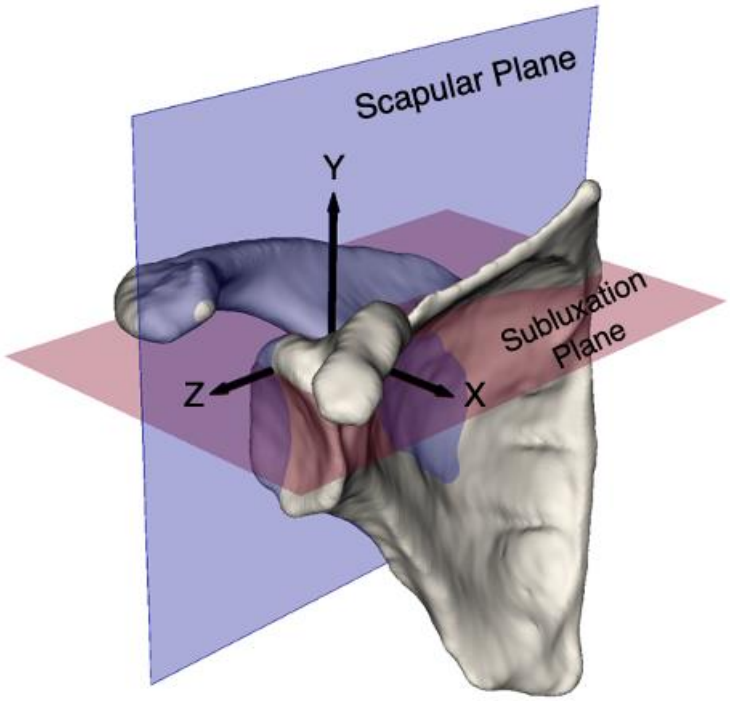

Figure 3-5: Scapular Plane (Blue) and Subluxation Plane (Red)

3.2.3.2 Humeral Coordinate System

The humeral coordinate system was based on using a sphere of best fit, which was derived from selected points on the articular surface of the humeral head. The centroid of the sphere of best fit was the origin of the coordinate system (Figure 3-6). The humerus used a modified International Society of Biomechanics (ISB) coordinate system, where the axes are mathematically aligned to the scapular coordinate system: z-axis (+lateral), x-axis (+anterior), and y-axis (+superior).[23]

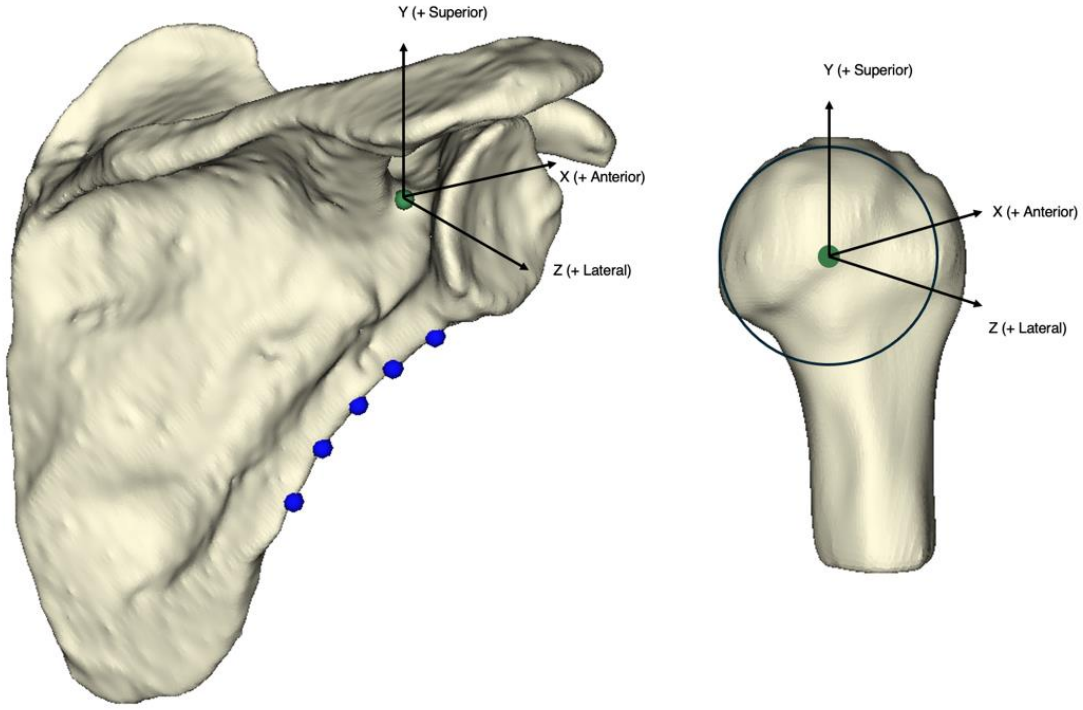

Figure 3-6: Scapular and Humeral Coordinate Systems

3.2.4 Subluxation

A custom MATLAB code was used to calculate the subluxation of each patient preoperatively (static), and postoperatively (throughout the active IR movement). The custom MATLAB code determined subluxation (mm) of the patients by finding the distance (mm) from the origin of the humeral coordinate system to the origin of the scapular coordinate system along the x-axis (anterior/posterior). Positive values note movement of the humeral head in the anterior direction and negative values note movement of the humeral head in the posterior direction (Figure 3-5). For the preoperative scans, the diameter of the preoperative humeral head (mm) in the A/P direction was measured using Blueprint and for the postoperative scans, the diameter of the humeral head metal implant (mm) was documented based on humeral head implant measurements. The overall subluxation (%) was found by taking the radius of the humeral head (HH), minus the subluxation (mm) found along the x-axis, divided by the diameter of the humeral head.

Below is an example displaying how the overall subluxation (%) was calculated for one frame of movement postoperatively of a patient with a 50mm humeral head implant.

$$\text{Overall Subluxation (\%)} = \frac{\text{Radius of HH (mm)-Subluxation along x-axis (mm)}}{\text{Diameter of the HH}}$$

$$\text{Overall Subluxation (\%)} = \frac{\left(\frac{50}{2}\right)\text{-(-0.4774)}}{50} = 0.5095*100 = 51\%$$

According to the Walch classification of glenoid morphology, a subluxation between 45% and 55% represents a centred humeral head.[24] A subluxation of more than 55% represents posterior subluxation with 100% being posterior dislocation, and less than 45% represents anterior subluxation with 0% being anterior dislocation. The subluxation example above shows a patient with a centred humeral head postoperatively.

3.2.5 Statistical Analysis

All statistical analyses were completed using SPSS (SPSS Statistics v26; IBM, 350, Armonk, NJ). A paired t-test was used to compare preoperative subluxation versus postoperative subluxation. Additionally, a two-way ANOVA was used to compare the mean differences between preoperative and postoperative subluxation for various cohorts of range of motion (good and limited) and glenoid augment (15° and 25°). A Bonferroni correction was used to correct for the multiple statistical analyses performed, with the significance value set as $p<0.05$.

3.3 Results

3.3.1 Patient Recruitment

Seventy-six (76) patients that had undergone a stemless TSA with a posteriorly augmented glenoid implant and had greater than 2 years follow-up were eligible to participate in this study. All female patients (22) were excluded from this study as per Investigational Research Board recommendations because of higher breast tissue sensitivity and risk of cancer in females when exposed to CT radiation. The remaining 54 patients were phone called and sent recruitment letters requesting participation in the study. Twenty-eight (28)

patients were excluded due to the following reasons: lived too far away (n=8), phone number not in service (n=6), left voicemail at least twice with no reply (n=4), did not show up at appointment (n=3), did not want to participate (n=6), and died (n=1). The remaining 26 patients were then recruited and scanned in the hospital. After completion of scanning, two more patients were excluded due to parts of the humerus and/or scapula moving out of the field of view during the scan, and four patients were excluded due to being reclassified as having type A1 glenoid morphology. The final 20 type B2 patients (mean age 68, range 54 to 83 years) were included in the study. A flowchart outlining patient recruitment and reasons for excluding specific patients from the study is shown in Figure 3-7.

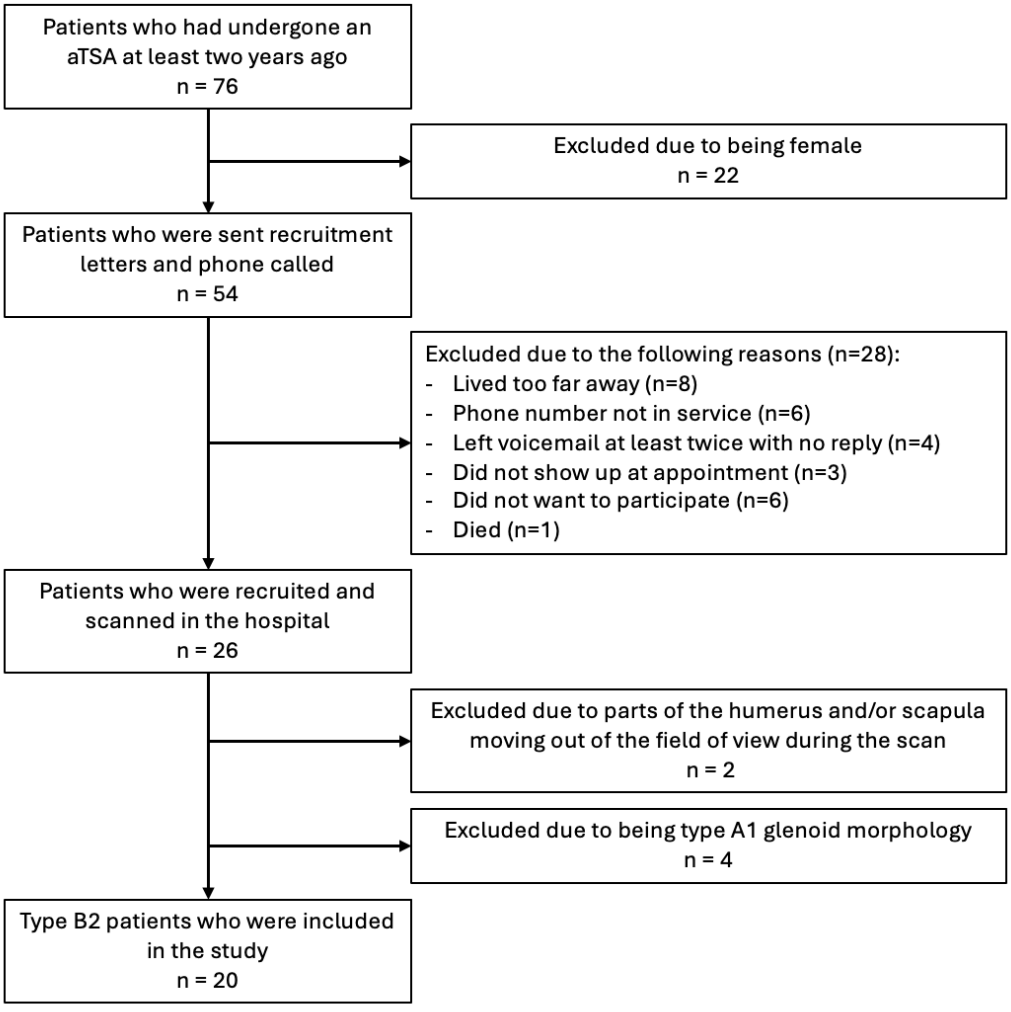

Figure 3-7: Patient Recruitment Flowchart

3.3.2 Patient Reported Outcomes

For this study, all 20 patients completed the ASES score. The mean postoperative ASES score for all the patients was 85 (range 53 to 100), with a mean pain score of 41 (range 20 to 50) and mean ADL score of 43 (range 27 to 50). The mean VAS score for all patients was 2 (range 0 to 6).

3.3.3 Subluxation Preoperative versus Postoperative

The mean subluxation postoperatively (54%) was a significant ($p<0.001$) improvement from the mean subluxation (66%) preoperatively (Figure 3-8 and Figure 3-9). Preoperatively, only three patients (15%) fell within the 45% to 55% definition of having a centred humeral head (patients 11, 17, and 18). However, postoperatively, nine patients had a centred humeral head (patients 1, 2, 5, 6, 7, 9, 11, 16, and 19), with 16 out of the 20 patients (80%) having subluxation between 40% and 60% (all but patients 2, 3, 12, and 15).

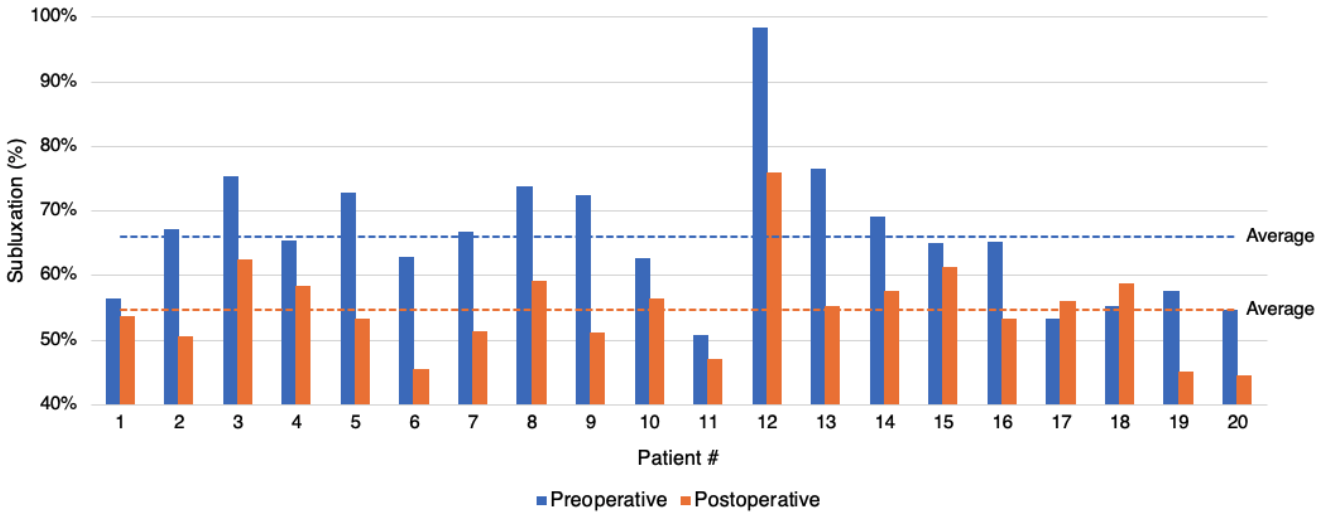

Figure 3-8: Subluxation (%) preoperatively (static) versus postoperatively (dynamic) per patient

The mean preoperative subluxation (66%) is indicated by the blue dashed line and mean postoperative subluxation (54%) is indicated by the orange dashed line.

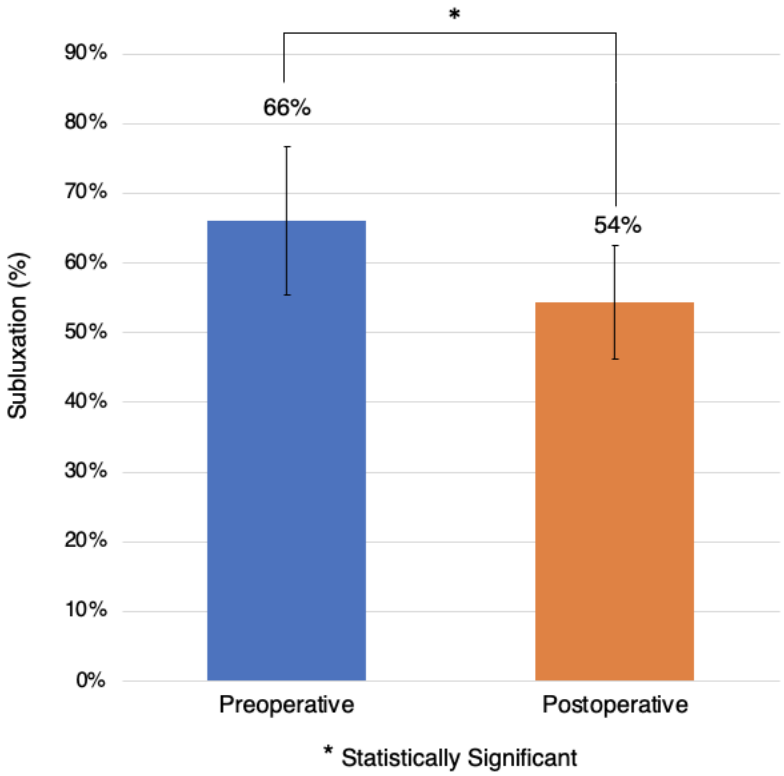

Figure 3-9: Mean subluxation (%) preoperatively (static) versus postoperatively (dynamic) for all patients

3.3.4 Subluxation During Active Internal Rotation Motion

On average for all patients postoperatively, subluxation ranged from 54% to 55% throughout active IR, indicating that a minimal change in subluxation was present throughout the entire movement (Figure 3-10).

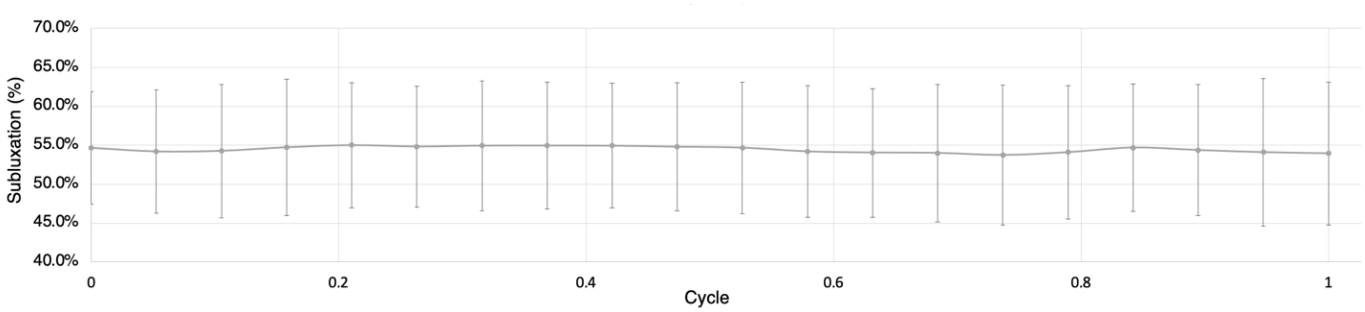

Figure 3-10: Subluxation During Active Internal Rotation

Standard deviations are shown by the lines at each time point throughout the cycle.

3.3.5 Subluxation for Range of Motion Groups

Based on the range of motion (ROM) that was documented for each patient when they performed IR during the postoperative scan, the patients were grouped into two cohorts, good ROM and limited ROM based on a previously established IR vertebral range (Figure 3-1).[18] The good ROM cohort included 12 patients (n=12), and the limited ROM cohort included eight patients (n=8). The mean ASES score was 86 for the good ROM cohort, and 82 for the limited ROM cohort (p=0.604). The subluxation preoperatively and postoperatively for patients in both the good ROM and limited ROM cohorts can be seen below in Figure 3-11. The good ROM cohort were subluxated 66% preoperatively, and 55% postoperatively (11% subluxation correction). The limited ROM cohort were subluxated 66% preoperatively, and 53% postoperatively (13% subluxation correction). Both cohorts were able to be corrected on average from being posteriorly subluxated (66%), to having centred humeral heads (55% for good ROM and 53% for limited ROM patients). The subluxation correction was found to be statistically significant ($p<0.001$), meaning that patients who received a TSA, with either good ROM or limited ROM, had corrected subluxation. Alternatively, there were no significant differences between preoperative subluxation for good ROM patients versus limited ROM patients, as well as no significant differences between postoperative subluxation for good ROM patients and limited ROM patients (p=0.632).

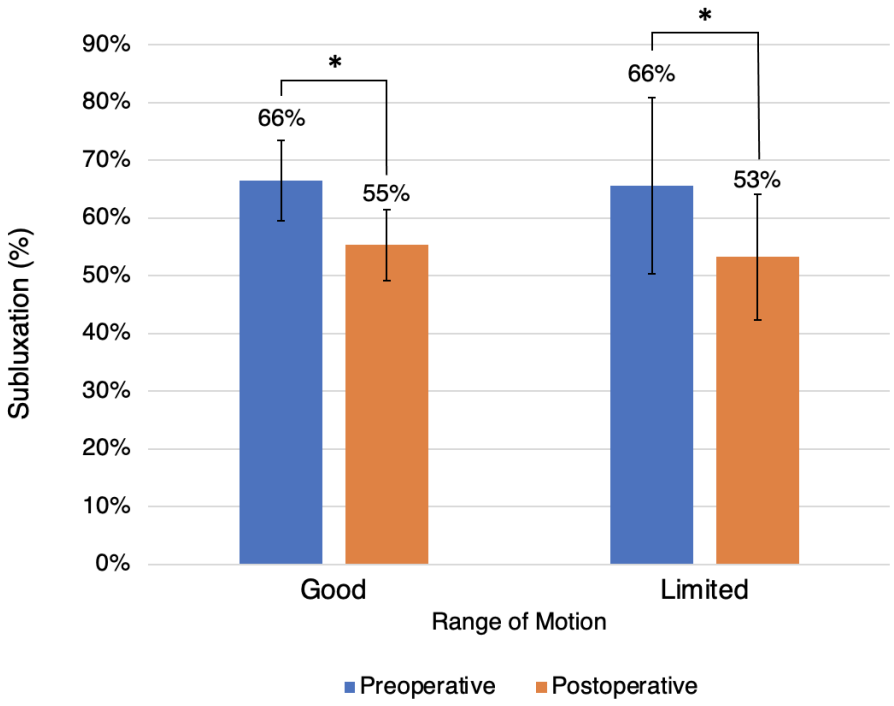

Figure 3-11: Subluxation for patients with good ROM (n=12) versus limited ROM (n=8)

3.3.6 Subluxation for 15° versus 25° Augments

Based on the size of the PAG implant utilized, patients were grouped into two cohorts: 15° augment and 25° augment. The 15° augment cohort included 10 patients (n=10), and the 25° augment cohort included 10 patients (n=10). The mean ASES score was 91 for the 15° cohort, and 79 for the 25° cohort (p=0.133). The subluxation preoperatively and postoperatively for patients in both the 15° augment and 25° augment cohorts are presented in Figure 3-12. Patients in the 15° augment cohort had a mean preoperative retroversion of 15°, and patients in the 25° augment cohort had a mean preoperative retroversion of 22°. The 15° augment cohort was subluxated 62% preoperatively, and 53% postoperatively (9% subluxation correction). The 25° augment cohort was subluxated 69% preoperatively, and 57% postoperatively (12% subluxation correction). Both the 15° and 25° augments significantly corrected subluxation from preoperative to postoperative (p=<0.001). Additionally, there were no significant differences between preoperative subluxation for 15° versus 25° augment patients, as well as no significant differences between postoperative subluxation for 15° versus 25° augment patients (p=0.070).

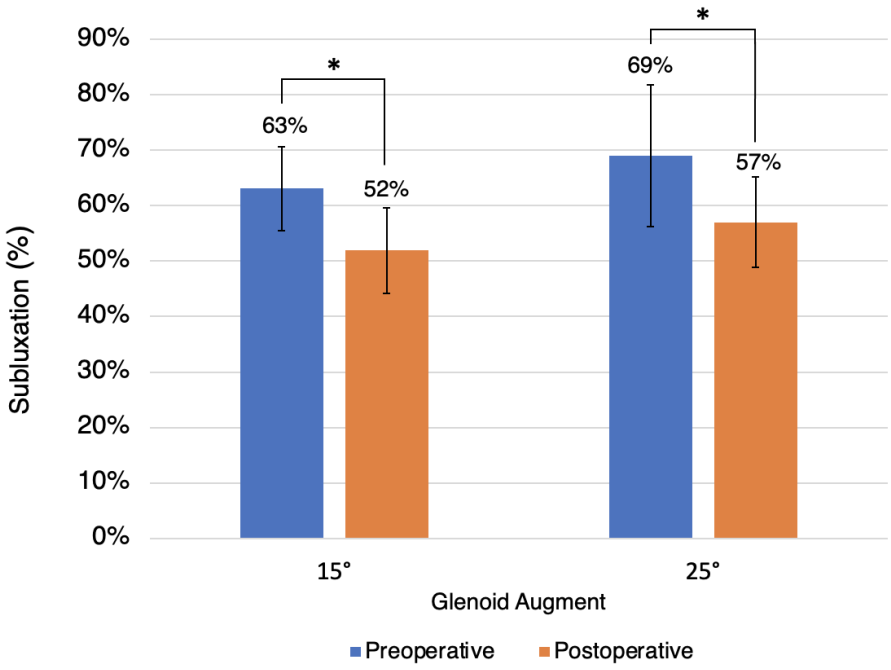

Figure 3-12: Subluxation for patients with 15° (n=10) versus 25° (n=10) glenoid augments

3.4 Discussion

Currently, it remains unclear whether TSAs with posterior augmented implants are successful in correcting subluxation in the long term, as well as maintaining a reduced glenohumeral joint during active motions. Additionally, it is unknown if a patient's range of motion, or the size of an augment has an effect on postoperative residual subluxation. Overall, the results of this study demonstrate that a TSA with a posterior augmented glenoid for a Walch type B2 glenoid was successful in correcting subluxation and maintaining subluxation throughout a provocative active internal rotation protocol. As well, there was no significant effect of patient postoperative range of motion (good or limited), or augment size used (15° or 25°) on postoperative subluxation. Both 15° and 25° augments were able to successfully correct subluxation in mild and moderate B2 deformities.

The primary objective of this study was to determine if Walch type B2 patients managed with a TSA and a PAG implant would maintain correction of subluxation when examined

statically and when stressed with active motion. The results agreed with this hypothesis as a statistically significant subluxation correction occurred ($p<0.001$), implying that the humeral head was centred postoperatively. It is conceivable that during static postoperative axillary radiographs the joint may be aligned, however, during active motion, the humeral head implant may subluxate posteriorly. The results of this active motion study demonstrated that the glenohumeral joint remains reduced throughout an active internal rotation motion, after retroversion correction with a posteriorly augmented implant. Interestingly, joint subluxation varied on average by 1% (range 54% to 55%) during active internal rotation. This is reassuring as large variations in posterior subluxation could cause asymmetric loading on the posterior part of the glenoid, which could lead to glenoid loosening and possible implant failure. Additionally, it has anecdotally been stated that in Walch type B2 patients after TSA, the humeral head may re-subluxate back to its preoperative location, as this has been its historic pathoanatomical position. The results of the study demonstrate that with correction of retroversion with a posteriorly augmented glenoid implant at a mean of 4 years, glenohumeral alignment is maintained and re-subluxation does not occur statically or actively

It was investigated whether various levels of range of motion would affect postoperative subluxation. Overall, whether patients had good or limited range of motion, significant subluxation correction ($p<0.001$) was seen for all patients and was not significantly different amongst cohorts ($p=0.632$). This means that subluxation was able to be corrected in patients despite having good ROM or limited ROM. Therefore, range of motion is independent of subluxation. This finding was contrary to the hypothesis as it was believed that patients with better/good ROM would have had greater glenohumeral translation and therefore, greater subluxation postoperatively. Additionally, the 15° and 25° augment patients were compared. In the 15° augment cohort, the mean preoperative retroversion was 15° and subluxation was 63%, and this cohort was described subjectively as a mild B2. The 25° implant group had a mean preoperative retroversion of 22° and subluxation of 69%, and this cohort was described subjectively as a moderate B2 deformity. Postoperatively, both groups had significant ($p<0.001$) improvements in subluxation, with no significant differences between groups ($p=0.070$). These results indicate that in the short term (mean 4 years postoperatively), both mild and moderate B2 deformities can be

managed successfully with posterior augmented implants, as subluxation did not recur. This agreed with the hypothesis that both 15° and 25° glenoid augments would successfully maintain joint reduction at follow-up.

Previous clinical studies have reported successful outcomes with a TSA and posteriorly augmented glenoid implants. Terrier et al. (2020) reported that posterior augments can successfully reduce subluxation in patients with B2 and B3 glenoid morphologies,[10] with Kohan et al. (2022) also confirming these findings.[25] Rice et al. (2008) and Garrigues et al. (2022) have also reported that posterior augmented implants can correct subluxation and also result in improved shoulder function.[26,27] Likewise, Ma et al. (2020) demonstrated that even with an augment >15°, there was no impact to clinical outcomes.[28] The results of this study are complementary to the available literature,[11,25–28] and add to it by assessing dynamic implant and joint alignment during active motion. To the authors' knowledge, dynamic 4DCT assessment of B2 patients managed with a TSA with a posteriorly augmented glenoid implant has not been reported. This new 4D motion capture technology provides definitive evidence that mild to moderate B2 patients managed with posterior augments maintain joint alignment without recurrent subluxation at a mean of 4 years postoperatively. Additionally, this technology allowed the assessment of subluxation throughout the full active motion of internal rotation and found minimal variability.

The present study used three-dimensional (3D) measurements to calculate subluxation instead of two-dimensional (2D) measurements, which have been used in past studies.[11,28] Two-dimensional measurements have been reported as less accurate due to positional errors.[13–16] As well, 2D and 3D subluxation have been shown to be statistically different and moderately correlated in arthritic shoulders,[16,29] with 2D subluxation being underestimated in 89% of cases[30] when compared to 3D subluxation for type B2 glenoids.[16,29]

3.5 Conclusion

At short-term follow-up (i.e., average 4 years postoperative), a TSA with an all-polyethylene posterior augmented glenoid implant to manage a Walch type B2 glenoid was successful at correcting posterior subluxation and maintaining glenohumeral alignment throughout a provocative active motion protocol. In patients with corrected retroversion with a half-wedge posteriorly augmented all-polyethylene cemented implant, subluxation did not recur statically or dynamically. Thus, TSA with a posteriorly augmented glenoid implant is an acceptable option for patients with mild or moderate B2 glenoids.

3.6 References

1. Chen B, Huang W, Liao J. Osteoarthritis: The Most Common Joint Disease and Outcome of Sports Injury. *J Clin Med*. 2023;12(15). doi:10.3390/jcm12155103

2. Lo IKY, Litchfield RB, Griffin S, Faber K, Patterson SD, Kirkley A. Quality-of-life outcome following hemiarthroplasty or total shoulder arthroplasty in patients with osteoarthritis. A prospective, randomized trial. *J Bone Joint Surg Am*. 2005;87(10):2178-2185. doi:10.2106/JBJS.D.02198

3. Gartsman GM, Brinker MR, Khan M, Karahan M. Self-assessment of general health status in patients with five common shoulder conditions. *J Shoulder Elbow Surg*. 1998;7(3):228-237. doi:10.1016/S1058-2746(98)90050-7

4. Kerr R, Resnick D, Pineda C, Haghighi P. Osteoarthritis of the glenohumeral joint: a radiologic-pathologic study. *Am J Roentgenol*. 1985;144(5):967-972. doi:10.2214/ajr.144.5.967

5. Petersson CJ. Degeneration of the Gleno-Humeral Joint: An Anatomical Study. *Acta Orthop Scand*. 1983;54(2):277-283. doi:10.3109/17453678308996570

6. Raniga S, Arenas-Miquelez A, Bokor DJ. Anatomic total shoulder arthroplasty in patients under 50 and over 80 years of age. Part 1. *Obere Extrem*. 2022;17(4):259-266. doi:10.1007/s11678-022-00708-6

7. Denard PJ, Walch G. Current concepts in the surgical management of primary glenohumeral arthritis with a biconcave glenoid. *J Shoulder Elbow Surg*. 2013;22(11):1589-1598. doi:10.1016/j.jse.2013.06.017

8. Walch G, Boulahia A, Boileau P, Kempf JF. Primary glenohumeral osteoarthritis: clinical and radiographic classification. The Aequalis Group. *Acta Orthop Belg*. 1998;64 Suppl 2:46-52.

9. Sheth M, Sholder D, Abboud J, Lazarus M, Williams G, Namdari S. Revision of Anatomic Total Shoulder Arthroplasty to Hemiarthroplasty: Does it work? *Arch Bone Jt Surg*. 2020;8(2):147-1153. doi:10.22038/abjs.2019.34244.1897

10. Terrier A, Goetti P, Becce F, Farron A. Reduction of scapulohumeral subluxation with posterior augmented glenoid implants in anatomic total shoulder arthroplasty: Short-term 3D comparison between pre- and post-operative CT. *Orthop Traumatol Surg Res*. 2020;106(4):681-686. doi:10.1016/j.otsr.2020.03.007

11. Gerber C, Costouros JG, Sukthankar A, Fucentese SF. Static posterior humeral head subluxation and total shoulder arthroplasty. *J Shoulder Elbow Surg*. 2009;18(4):505-510. doi:10.1016/j.jse.2009.03.003

12. Hoenecke HR, Tibor LM, D'Lima DD. Glenoid morphology rather than version predicts humeral subluxation: a different perspective on the glenoid in total shoulder

arthroplasty. *J Shoulder Elbow Surg*. 2012;21(9):1136-1141. doi:10.1016/j.jse.2011.08.044

13. Choi CH, Kim HC, Kang D, Kim JY. Comparative study of glenoid version and inclination using two-dimensional images from computed tomography and three-dimensional reconstructed bone models. *Clin Shoulder Elb*. 2020;23(3):119-124. doi:10.5397/cise.2020.00220

14. Jacxsens M, Van Tongel A, Willemot LB, Mueller AM, Valderrabano V, De Wilde L. Accuracy of the glenohumeral subluxation index in nonpathologic shoulders. *J Shoulder Elbow Surg*. 2015;24(4):541-546. doi:10.1016/j.jse.2014.07.021

15. Matache BA, Alnusif N, Chaoui J, Walch G, Athwal GS. Humeral head subluxation in Walch type B shoulders varies across imaging modalities. *JSES Int*. 2021;5(1):98-101. doi:10.1016/j.jseint.2020.08.016

16. Terrier A, Ston J, Farron A. Importance of a three-dimensional measure of humeral head subluxation in osteoarthritic shoulders. *J Shoulder Elbow Surg*. 2015;24(2):295-301. doi:10.1016/j.jse.2014.05.027

17. Nicolozakes CP, Coats-Thomas MS, Ludvig D, Seitz AL, Perreault EJ. Translations of the Humeral Head Elicit Reflexes in Rotator Cuff Muscles That Are Larger Than Those in the Primary Shoulder Movers. *Front Integr Neurosci*. 2022;15:796472. doi:10.3389/fnint.2021.796472

18. Triplet JJ, Everding NG, Levy JC, Moor MA. Functional internal rotation after shoulder arthroplasty: a comparison of anatomic and reverse shoulder arthroplasty. *J Shoulder Elbow Surg*. 2015;24(6):867-874. doi:10.1016/j.jse.2014.10.002

19. Agel J, Hebert-Davies J, Braman JP. American Shoulder and Elbow Surgeons score: what does it tell us about patients selecting operative treatment of a rotator cuff injury? *JSES Int*. 2023;7(5):751-755. doi:10.1016/j.jseint.2023.04.007

20. McCollough C, Cody D, Edyvean S, et al. *The Measurement, Reporting, and Management of Radiation Dose in CT*. AAPM; 2008. doi:10.37206/97

21. Besl P, McKay HD. A method for registration of 3-D shapes. IEEE Trans Pattern Anal Mach Intell. *Pattern Anal Mach Intell IEEE Trans On*. 1992;14:239-256. doi:10.1109/34.121791

22. Terrier A, Ston J, Larrea X, Farron A. Measurements of three-dimensional glenoid erosion when planning the prosthetic replacement of osteoarthritic shoulders. *Bone Jt J*. 2014;96-B(4):513-518. doi:10.1302/0301-620X.96B4.32641

23. Wu G, Van Der Helm FCT, (DirkJan) Veeger HEJ, et al. ISB recommendation on definitions of joint coordinate systems of various joints for the reporting of human joint motion—Part II: shoulder, elbow, wrist and hand. *J Biomech*. 2005;38(5):981-992. doi:10.1016/j.jbiomech.2004.05.042

24. Walch G, Badet R, Boulahia A, Khoury A. Morphologic study of the Glenoid in primary glenohumeral osteoarthritis. *J Arthroplasty*. 1999;14(6):756-760. doi:10.1016/S0883-5403(99)90232-2

25. Kohan EM, Hendy BA, Kowal LL, et al. Mid- to long-term outcomes of augmented and nonaugmented anatomic shoulder arthroplasty in Walch B3 glenoids. *J Shoulder Elbow Surg*. 2022;31(6, Supplement):S103-S109. doi:10.1016/j.jse.2021.12.016

26. Garrigues GE, Quigley RJ, Johnston PS, et al. Early clinical and radiographic outcomes of anatomic total shoulder arthroplasty with a biconvex posterior augmented glenoid for patients with posterior glenoid erosion: minimum 2-year follow-up. *J Shoulder Elbow Surg*. 2022;31(8):1729-1737. doi:10.1016/j.jse.2021.12.047

27. Rice RS, Sperling JW, Miletti J, Schleck C, Cofield RH. Augmented Glenoid Component for Bone Deficiency in Shoulder Arthroplasty. *Clin Orthop Relat Res*. 2008;466(3):579. doi:10.1007/s11999-007-0104-4

28. Ma CB, Xiao W, Salesky M, et al. Do glenoid retroversion and humeral subluxation affect outcomes following total shoulder arthroplasty? *JSES Int*. 2020;4(3):649-656. doi:10.1016/j.jseint.2020.04.009

29. Neyton L, Falk G, Simon R, Yoshihiro H. Walch B2 glenoids. 2D vs 3D comparison of humeral head subluxation and glenoid retroversion. *JSES Int*. 2022;6. doi:10.1016/j.jseint.2022.01.005

30. Jacxsens M, Karns MR, Henninger HB, Drew AJ, Van Tongel A, De Wilde L. Guidelines for humeral subluxation cutoff values: a comparative study between conventional, reoriented, and three-dimensional computed tomography scans of healthy shoulders. *J Shoulder Elbow Surg*. 2018;27(1):36-43. doi:10.1016/j.jse.2017.06.005

Chapter 4

4 General Discussion and Conclusions

This chapter summarizes the objectives and hypotheses of Chapters 2 and 3, as well as reviews the work done to achieve the outlined objectives. The strengths and limitations of the work completed in this thesis are also discussed. The chapter concludes with suggestions of future directions stemming from this research.

4.1 Summary

The shoulder is the most mobile joint in the human body, with the glenohumeral joint specifically allowing a wide range of motion and a high incidence of instability, due to its ability to translate, in addition to rotate in its socket.[1] However, the examination of how the humeral head tracks relative to the glenoid, and the extent of translation (subluxation) in a healthy glenohumeral joint and in a Walch type B2 glenoid (posterior glenoid subluxation and erosion) after receiving an anatomic total shoulder arthroplasty (TSA), has not yet been well-established in literature. Glenohumeral joint research so far has mainly focused on patients who have already acquired pathologies (i.e., OA or instability), who have already undergone shoulder surgeries [2–7], or who have used cadaveric specimens,[5,8–10] which may not fully simulate the in vivo physiological state.[11–13] For the osteoarthritic glenohumeral joint, when the joint becomes diseased, and subluxation and erosion start to occur, people classified with having Walch Type B2 glenoid often go through a TSA with a posterior augmented glenoid (PAG) implant.[14] After receiving a TSA with a PAG implant, it remains largely unknown if a joint that previously exhibited severe subluxation and erosion can be corrected to having a centralized humeral head that maintains its position throughout active motion.[15,16] Therefore, this thesis aimed to evaluate healthy glenohumeral arthrokinematics to benchmark normal joint proximity and translation, and to assess if a TSA with PAG implants can correct subluxation and maintain joint mechanics throughout active motion post-surgery.

In Chapter 2, our goal was to measure and quantify glenohumeral joint proximity and joint surface tracking (translation) in healthy participants during active motions, such as forward elevation (FE) and internal rotation to the back (IR), which are important in activities of daily living. This chapter sought to determine if there were any age (young versus old), position (beginning versus middle versus end), or direction (superior/inferior or anterior/posterior) related differences in the healthy glenohumeral joint throughout FE and IR. It was hypothesized that glenohumeral joint proximity will increase with age, and that glenohumeral joint surface tracking (translation) will decrease with age due to the closer joint proximity. To seek the answers to these objectives, 31 participants were recruited for this study and were divided into two cohorts depending on age: young ($\leq$ 37 years old) and old ($\geq$45 years old). Four-dimensional computed tomography (4DCT) scans were taken as these participants completed two movements of everyday life (e.g., FE and IR). 3D bone models of the humerus and scapula were created using 3D Slicer for all participants. Using these 3D bone models, an inter-bone distance algorithm[17] was used to determine glenohumeral joint proximity, and an iterative closest point (ICP) algorithm[18] was used to then determine glenohumeral joint surface tracking (translation). This study found that when examining healthy glenohumeral joint proximity, older participants displayed significantly closer joint proximity (63% of glenoid surface was within 4mm of humeral head) during the middle of the internal rotation to the back movement, compared to the younger participants (52% of glenoid surface within 4mm of humeral head). Also, for internal rotation to the back, when examining joint tracking (translation), younger participants had significantly more translation in the superior/inferior direction (16% of glenoid height) compared to the anterior/posterior direction (10% of glenoid width). Overall, this study demonstrated the significance of translational movements between the humeral head and the glenoid during different shoulder motions, which will aid implant manufacturers in designing implants that will allow for more normalized glenohumeral translations.

In Chapter 3, the goal was to determine if Walch type B2 patients managed with a total shoulder arthroplasty (TSA) and a posterior augmented glenoid (PAG) implant, could maintain correction of subluxation when examined statically and when stressed with active motion. It was hypothesized that subluxation would be corrected postoperatively and

would maintain a centred joint alignment throughout active movement. This chapter also analyzed if a patient's range of motion (good or limited), magnitude of B2, or PAG implant size (15° or 25°) affected postoperative correction of subluxation. It was hypothesized that there would be no difference in subluxation postoperatively between various PAG implant sizes and magnitudes of B2 erosions, and that patients with better postoperative range of motion would have greater subluxation postoperatively. To achieve these objectives, 20 Walch type B2 patients (mean age 68 years, range 54 to 83) underwent stemless TSA with a 15° or 25° PAG and were assessed at a minimum 2-year follow-up. All patients underwent dynamic 4DCT scanning to actively track glenohumeral implant alignment and subluxation during a provocative active internal rotation motion protocol. Bone and implant 3D models of the humerus and scapula for each 4DCT scan were created using 3D Slicer. Landmarks were selected on the models away from the osteoarthritic region of the shoulder[19] to create coordinate systems that were then used in conjunction with a custom program (MATLAB) to determine subluxation preoperatively (statically), and postoperatively (dynamically). It was found that posterior humeral head subluxation was significantly corrected ($p<0.001$) from an average of 66% (range 51%-98%) preoperatively to 54% (range 41%-77%) postoperatively. Concentric TSA joint alignment was maintained throughout an active motion protocol, as subluxation percentage only varied by 1% throughout IR movement (range 54% to 55%). Neither patient range of motion (good or limited) nor size of PAG (15° or 25°) had a significant effect ($p>0.05$) on subluxation postoperatively. In conclusion, at short-term follow-up, TSA with an all-polyethylene posterior augmented glenoid was successful at restoring and maintaining glenohumeral alignment with correction of subluxation throughout a provocative active motion protocol. As such, recurrence of subluxation does not occur statically or actively in patients who have undergone glenoid reconstruction with correction of posteroinferior erosion with a half-wedge posteriorly augmented all-polyethylene cemented implant. Thus, TSA with a posteriorly augmented glenoid implant is an acceptable option for patients with mild or moderate B2 glenoids.

Overall, this thesis showcased the importance of establishing glenohumeral joint translations within a healthy population for various ages, as well as for people that have undergone a TSA with PAG implants. Quantifying the amount of healthy glenohumeral

joint translation, while also analyzing the variances in different ages, allowed for a better understanding of global shoulder motion to assist in the future with in vitro experiments, simulator and shoulder implant development. Determining the amount of subluxation that occurs in patients post-TSA during active motion, established that PAG implants are successful in correcting glenohumeral subluxation, and they should be considered an acceptable option for patients with a mild or moderate B2 glenoid. This work also demonstrated that 4DCT can be used to assess glenohumeral translation and subluxation, for patients with and without total shoulder implants, during active motion, which to the authors' knowledge has not been previously reported.

4.2 Strengths and Limitations

The greatest strength of this study was the use of four-dimensional computed tomography (4DCT) to quantify glenohumeral arthrokinematics and kinematics. In Chapter 2, 4DCT provided a detailed view of the glenohumeral joint surfaces during activities of daily living, such as IR and FE, allowing for accurate quantification of joint proximity and translation at the glenohumeral joint. In Chapter 3, the use of 4DCT also permitted the quantification of subluxation postoperatively throughout active motion (IR). This is a major strength because subluxation has been mainly studied statically in past work, and it has been unknown if dynamic subluxation occurs during specific shoulder positions or motions.[14,15,20–29] Quantifying glenohumeral joint parameters dynamically in vivo also allowed the study of movements that are not as commonly found in literature. The majority of previous research has focused on examining basic arm movements, such as abduction.[7,30–36] However, the biomechanics of the glenohumeral joint during more complex multi-planar motions (IR), which is integral to numerous activities of daily living (e.g., showering/bathing, dressing, and toileting) remains inadequately understood. If simple movements, such as abduction, were the only movements analyzed, it would not have been possible to confidently quantify the actual glenohumeral joint mechanics, since some of the most important movements in everyday life are complex composite motions. Utilizing 4DCT to observe the glenohumeral joint during complex, daily movements provides an improved understanding of its mechanics and function. Employing 4DCT also offers us the ability to calculate parameters such as joint proximity, joint translation,

and subluxation in 3D space. In the past, measurement of these parameters was done using 2D measurements, but it has been confirmed in literature that 3D measurements are more accurate than the previously used 2D measuremnts.[4,11,16]

While this study offered the capability to execute and analyze work that has never been done before, it is important to acknowledge the limitations. One limitation was that only male participants were recruited for analyses within this thesis. This was because the research ethics committee only permitted males to participate due to the higher breast tissue sensitivity and risk of cancer in females from the ionizing radiation from the scans. As such, the results can only be applied to males. However, it is anticipated that in the near future optimization of a low dose 4DCT scan will enable the inclusion of females in subsequent analyses. Another limitation was that there was some variability in the movements performed amongst participants. Although instructed and guided verbally by a technologist, each participant moved along a slightly different path and at a slightly different rate. This unconstrained motion resulted in a higher inter-patient variability as they performed various movements. In addition, this made it difficult to analyze the data for each movement on a one-to-one frame basis to directly compare results, but this was counteracted by grouping and scaling various movements, which made it possible to compare patients' results. One challenge in this thesis was that the patient-specific bone models that were used in analyses were made manually through the use of the 4DCT scans in 3D Slicer. This is an extremely time-consuming process, especially when performing analyses throughout an entire movement. Due to the long hours it takes to model the humerus and scapula bones, only the forward half of the motion and every other frame was used within the analyses. One limitation specific to Chapter 3 is that only the active motion of internal rotation was assessed. It is conceivable that other motions such as forward flexion or abduction may also result in dynamic joint subluxation. Furthermore, the patient cohort only consisted of mild and moderate B2 patients with a mean retroversion of 19°, and therefore, these results cannot be applied to patients with severe B2 deformities managed with augmented implants. Moreover, it is the senior surgeon's (GSA) clinical practice to correct all B2 patients to <5° of residual retroversion with the use of a 15° or 25° PAG implant; in cases where this degree of correction cannot be attained, patients are converted to a reverse shoulder arthroplasty. As such, these results are only applicable

when a <5° retroversion correction is obtained with a PAG implant. The final limitation, also specific to the work completed in Chapter 3, was that a sphere of best fit was used on the preoperative humeral head to determine subluxation preoperatively. Due to these patients having OA, the articular surface of the humeral head in some patients was oddly shaped, and unevenly worn out, which may have given a less accurate preoperative subluxation measurement.

4.3 Future Directions

By reflecting upon the strengths and limitations of the work in this thesis, future directions that would further enhance this work were established.

As previously mentioned, female participants were excluded from this study due to the elevated radiation dose associated with increased breast tissue. Consequently, the study was conducted solely on male subjects, which constrained the scope of our conclusions. Given that females constitute 50% of the population and possess different genetic makeup and bone structure compared to males,[37] it is evident that analyzing this demographic is crucial. Future advancements in CT technology that reduce radiation dosage will enable similar analyses on female subjects. This would allow benchmarks to be established for the normal range of motion in healthy females and determine if there are differences in implant function/movement between sexes.

Additionally, due to concerns regarding radiation dosage, the study presented in Chapter 3 was limited to the analysis of a single active motion, specifically internal rotation. In the future, it is hoped to extend this subluxation analysis to include other daily activities, such as forward elevation, which is integral to tasks like brushing/combing hair and placing/retrieving items from high cupboards or shelves. This would allow other movements in daily living, which contribute to shoulder subluxation or dislocation post-TSA, to be determined.

Furthermore, the research conducted in Chapter 3 diverged from the original plan. The initial goal was to replicate the analysis performed in Chapter 2 on healthy patients, but with those who had undergone total shoulder arthroplasty (TSA). However, the artifacts

present in the 4DCT scans, caused by the metal humeral head component, obscured the glenoid surface, preventing the intended joint proximity analysis. It is hoped that in future studies a similar analysis on patients who have undergone reverse total shoulder arthroplasty (RTSA) will be conducted. Given that both sides of the RTSA contain metal, it will be possible to clearly segment the implanted components. This will allow for a thorough joint proximity analysis, as well as quantification of post-RTSA retroversion, inclination, and subluxation, leading to more robust conclusions.

Due to the extensive time required to construct the bone models for this analysis, only the forward half of each motion and every other frame were utilized, resulting in some remaining data available for further analyses. It is anticipated that in the future, the utilization of AI, in conjunction with other tools, will optimize the model-creation process, enabling the modeling of every frame of motion to enhance the accuracy of this analysis. In the meantime, it is intended to leverage the data from these 4DCT scans to explore other joints within the shoulder. This could involve conducting a similar analysis on different shoulder joints or investigating other aspects of the same glenohumeral joint. Currently, our laboratory has already commenced a joint proximity and joint mechanics analysis of the acromioclavicular joint using the same 4DCT data collected during this study.

The data collected for this study included 4DCT scans of four Walch type A1 glenoids. During the initial recruitment phase described in Chapter 3, patients classified as either A1 or B2 were targeted, resulting in a total of 20 B2 patients and only four A1 patients. Future studies should aim to recruit more Walch type A1 patients to facilitate a comparative analysis between different glenoid morphological types. Future research could also extend this analysis to other types of glenoid morphology.

4.4 Significance

Quantifying translation in the glenohumeral joint and establishing if correction of subluxation is possible with a TSA and PAG implants, are essential in advancing shoulder implants, surgical treatments, and overall patient care. This work demonstrates the importance of how precise measurement of glenohumeral joint proximity and translation is critical for improvement in the design and testing of shoulder implants, studying erosion patterns, diagnosing instability (including subluxation and dislocation), and evaluating treatment efficacy. Investigating correction of subluxation in Walch type B2 glenoids after TSA with PAG implants throughout active motion is crucial for determining if it is a successful treatment for patients with posterior glenoid subluxation and erosion. Overall, this thesis contributes to a deeper understanding of dynamic shoulder biomechanics in both healthy individuals and patients with anatomic shoulder implants, ultimately improving shoulder implants, surgical techniques, and enhancing patient health and well-being.

4.5 References

1. Chang LR, Anand P, Varacallo M. Anatomy, Shoulder and Upper Limb, Glenohumeral Joint. In: *StatPearls*. StatPearls Publishing; 2023. Accessed June 13, 2023. http://www.ncbi.nlm.nih.gov/books/NBK537018/

2. Bey MJ, Kline SK, Zauel R, Kolowich PA, Lock TR. In Vivo Measurement of Glenohumeral Joint Contact Patterns. *EURASIP J Adv Signal Process*. 2009;2010(1):1-6. doi:10.1155/2010/162136

3. Bey MJ, Kline SK, Zauel R, Lock TR, Kolowich PA. Measuring dynamic in-vivo glenohumeral joint kinematics: Technique and preliminary results. *J Biomech*. 2008;41(3):711-714. doi:10.1016/j.jbiomech.2007.09.029

4. Friedman RJ. Glenohumeral translation after total shoulder arthroplasty. *J Shoulder Elbow Surg*. 1992;1(6):312-316. doi:10.1016/S1058-2746(09)80058-X

5. Karduna AR, Williams GR, Williams JL, Iannotti JP. Glenohumeral Joint Translations before and after Total Shoulder Arthroplasty. A Study in Cadavera*. *JBJS*. 1997;79(8):1166.

6. Muench LN, Murphey M, Oei B, et al. Elliptical and spherical heads show similar obligate glenohumeral translation during axial rotation in total shoulder arthroplasty. *BMC Musculoskelet Disord*. 2023;24(1):171. doi:10.1186/s12891-023-06273-5

7. Poppen NK, Walker PS. Normal and abnormal motion of the shoulder. *J Bone Joint Surg Am*. 1976;58(2):195-201.

8. Harryman DT, Sidles JA, Clark JM, McQuade KJ, Gibb TD, Matsen FA. Translation of the humeral head on the glenoid with passive glenohumeral motion. *J Bone Joint Surg Am*. 1990;72(9):1334-1343.

9. Warner JJP, Bowen K, Hannafin JA, Arnoczky P, Warren RF. Articular contact patterns of the normal glenohumeral joint. *J Shoulder Elb Surg*. 1998;7(4).

10. Wuelker N, Schmotzer H, Thren K, Korell M. Translation of the glenohumeral joint with simulated active elevation. *Clin Orthop*. 1994;309:193-200.

11. Greis PE, Scuderi MG, Mohr A, Bachus KN, Burks RT. Glenohumeral articular contact areas and pressures following labral and osseous injury to the anteroinferior quadrant of the glenoid. *J Shoulder Elbow Surg*. 2002;11(5):442-451. doi:10.1067/mse.2002.124526

12. Gupta R, Lee TQ. Positional-dependent changes in glenohumeral joint contact pressure and force: Possible biomechanical etiology of posterior glenoid wear. *J Shoulder Elbow Surg*. 2005;14(1, Supplement):S105-S110. doi:10.1016/j.jse.2004.10.005

13. Yu J, McGarry MH, Lee YS, Duong LV, Lee TQ. Biomechanical effects of supraspinatus repair on the glenohumeral joint. *J Shoulder Elbow Surg*. 2005;14(1):S65-S71. doi:10.1016/j.jse.2004.09.019

14. Terrier A, Ston J, Farron A. Importance of a three-dimensional measure of humeral head subluxation in osteoarthritic shoulders. *J Shoulder Elbow Surg*. 2015;24(2):295-301. doi:10.1016/j.jse.2014.05.027

15. Garrigues GE, Quigley RJ, Johnston PS, et al. Early clinical and radiographic outcomes of anatomic total shoulder arthroplasty with a biconvex posterior augmented glenoid for patients with posterior glenoid erosion: minimum 2-year follow-up. *J Shoulder Elbow Surg*. 2022;31(8):1729-1737. doi:10.1016/j.jse.2021.12.047

16. Raniga S, Arenas-Miquelez A, Bokor DJ. Anatomic total shoulder arthroplasty in patients under 50 and over 80 years of age. Part 1. *Obere Extrem*. 2022;17(4):259-266. doi:10.1007/s11678-022-00708-6

17. Lalone EA, McDonald CP, Ferreira LM, Peters TM, King GW, Johnson JA. Development of an image-based technique to examine joint congruency at the elbow. *Comput Methods Biomech Biomed Engin*. 2013;16(3):280-290. doi:10.1080/10255842.2011.617006

18. Besl P, McKay HD. A method for registration of 3-D shapes. IEEE Trans Pattern Anal Mach Intell. *Pattern Anal Mach Intell IEEE Trans On*. 1992;14:239-256. doi:10.1109/34.121791

19. Terrier A, Ston J, Larrea X, Farron A. Measurements of three-dimensional glenoid erosion when planning the prosthetic replacement of osteoarthritic shoulders. *Bone Jt J*. 2014;96-B(4):513-518. doi:10.1302/0301-620X.96B4.32641

20. Choi CH, Kim HC, Kang D, Kim JY. Comparative study of glenoid version and inclination using two-dimensional images from computed tomography and three-dimensional reconstructed bone models. *Clin Shoulder Elb*. 2020;23(3):119-124. doi:10.5397/cise.2020.00220

21. Gerber C, Costouros JG, Sukthankar A, Fucentese SF. Static posterior humeral head subluxation and total shoulder arthroplasty. *J Shoulder Elbow Surg*. 2009;18(4):505-510. doi:10.1016/j.jse.2009.03.003

22. Jacxsens M, Karns MR, Henninger HB, Drew AJ, Van Tongel A, De Wilde L. Guidelines for humeral subluxation cutoff values: a comparative study between conventional, reoriented, and three-dimensional computed tomography scans of healthy shoulders. *J Shoulder Elbow Surg*. 2018;27(1):36-43. doi:10.1016/j.jse.2017.06.005

23. Jacxsens M, Van Tongel A, Willemot LB, Mueller AM, Valderrabano V, De Wilde L. Accuracy of the glenohumeral subluxation index in nonpathologic shoulders. *J Shoulder Elbow Surg*. 2015;24(4):541-546. doi:10.1016/j.jse.2014.07.021

24. Kohan EM, Hendy BA, Kowal LL, et al. Mid- to long-term outcomes of augmented and nonaugmented anatomic shoulder arthroplasty in Walch B3 glenoids. *J Shoulder Elbow Surg*. 2022;31(6, Supplement):S103-S109. doi:10.1016/j.jse.2021.12.016

25. Ma CB, Xiao W, Salesky M, et al. Do glenoid retroversion and humeral subluxation affect outcomes following total shoulder arthroplasty? *JSES Int*. 2020;4(3):649-656. doi:10.1016/j.jseint.2020.04.009

26. Matache BA, Alnusif N, Chaoui J, Walch G, Athwal GS. Humeral head subluxation in Walch type B shoulders varies across imaging modalities. *JSES Int*. 2021;5(1):98-101. doi:10.1016/j.jseint.2020.08.016

27. Neyton L, Falk G, Simon R, Yoshihiro H. Walch B2 glenoids. 2D vs 3D comparison of humeral head subluxation and glenoid retroversion. *JSES Int*. 2022;6. doi:10.1016/j.jseint.2022.01.005

28. Rice RS, Sperling JW, Miletti J, Schleck C, Cofield RH. Augmented Glenoid Component for Bone Deficiency in Shoulder Arthroplasty. *Clin Orthop Relat Res*. 2008;466(3):579. doi:10.1007/s11999-007-0104-4

29. Terrier A, Goetti P, Becce F, Farron A. Reduction of scapulohumeral subluxation with posterior augmented glenoid implants in anatomic total shoulder arthroplasty: Short-term 3D comparison between pre- and post-operative CT. *Orthop Traumatol Surg Res*. 2020;106(4):681-686. doi:10.1016/j.otsr.2020.03.007

30. Graichen H, Stammberger T, Bonel H, Karl-Hans Englmeier, Reiser M, Eckstein F. Glenohumeral translation during active and passive elevation of the shoulder — a 3D open-MRI study. *J Biomech*. 2000;33(5):609-613. doi:10.1016/S0021-9290(99)00209-2

31. Matsui K, Tachibana T, Nobuhara K, Uchiyama Y. Translational movement within the glenohumeral joint at different rotation velocities as seen by cine MRI. *J Exp Orthop*. 2018;5:7. doi:10.1186/s40634-018-0124-x

32. Howell SM, Galinat BJ, Renzi AJ, Marone PJ. Normal and abnormal mechanics of the glenohumeral joint in the horizontal plane. *J Bone Joint Surg Am*. 1988;70(2):227-232.

33. Kozono N, Okada T, Takeuchi N, et al. In vivo kinematic analysis of the glenohumeral joint during dynamic full axial rotation and scapular plane full abduction in healthy shoulders. *Knee Surg Sports Traumatol Arthrosc*. 2017;25(7):2032-2040. doi:10.1007/s00167-016-4263-2

34. Matsuki K, Kenmoku T, Ochiai N, Sugaya H, Banks SA. Differences in glenohumeral translations calculated with three methods: Comparison of relative positions and contact point. *J Biomech*. 2016;49(9):1944-1947. doi:10.1016/j.jbiomech.2016.03.042

35. Matsumura N, Oki S, Fukasawa N, et al. Glenohumeral translation during active external rotation with the shoulder abducted in cases with glenohumeral instability: a 4-dimensional computed tomography analysis. *J Shoulder Elbow Surg*. 2019;28(10):1903-1910. doi:10.1016/j.jse.2019.03.008

36. Massimini DF. *Technique and Application for Quantifying Dynamic Shoulder Joint Kinematics and Glenohumeral Joint Contact Patterns*. Thesis. Massachusetts Institute of Technology; 2014. Accessed August 24, 2023. https://dspace.mit.edu/handle/1721.1/87979

37. Merrill A, Guzman K, Miller SL. Gender differences in glenoid anatomy: an anatomic study. *Surg Radiol Anat*. 2009;31(3):183-189. doi:10.1007/s00276-008-0425-3

Appendices

Appendix A: Additional Joint Proximity Maps

A.1 Results

Chapter 2 of this thesis contained joint proximity maps for one sample participant throughout forward elevation (FE) and internal rotation to the back (IR). This appendix contains the proximity maps for all participants throughout FE (Figure A-1) and IR (Figure A-2). The starting position is shown in the top left and the movement progresses to the right, ending with the terminal position shown in the bottom right. Note: 0mm (red) shows close proximity and 6mm (dark blue) shows far proximity.

Figure A-1: Forward Elevation (FE) Proximity Maps

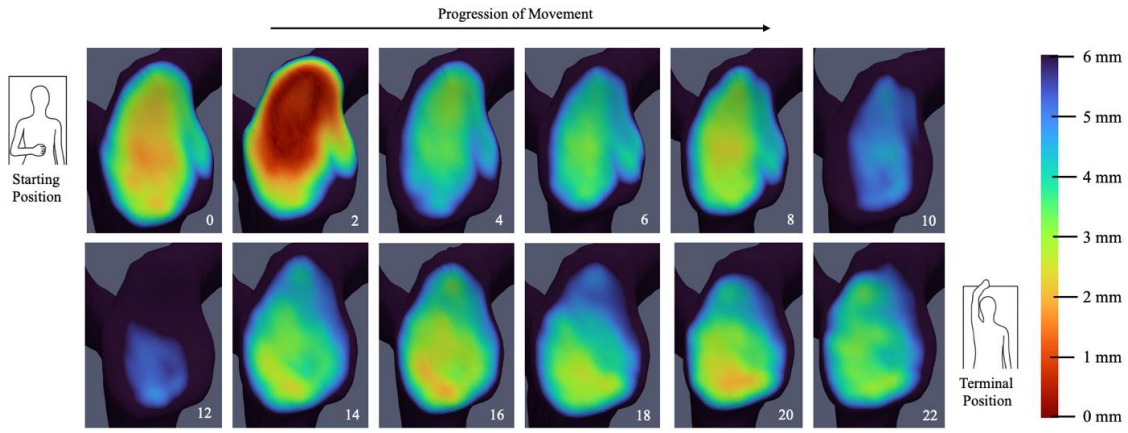

Proximity map for participant Young-1 throughout FE at different reference frames

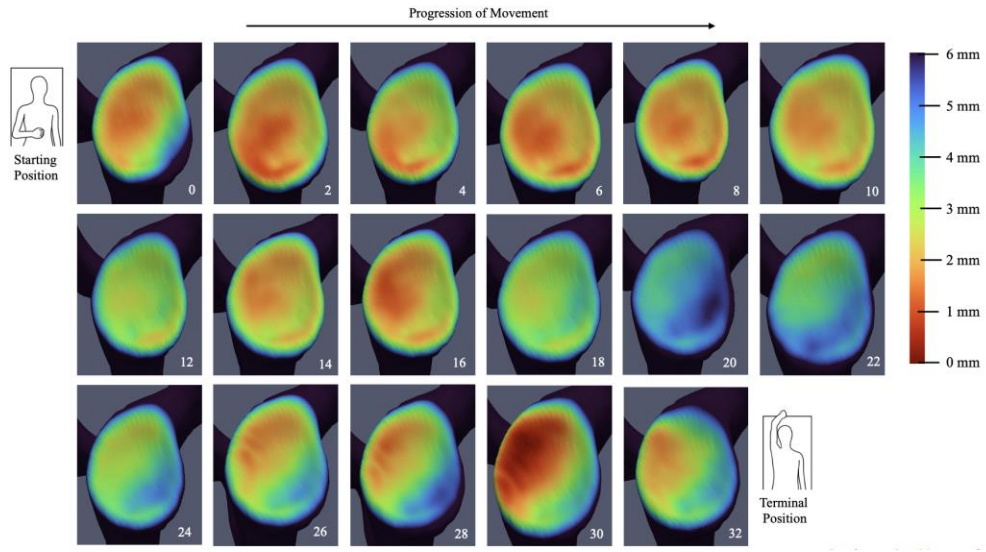

Proximity map for participant Young-2 throughout FE at different reference frames

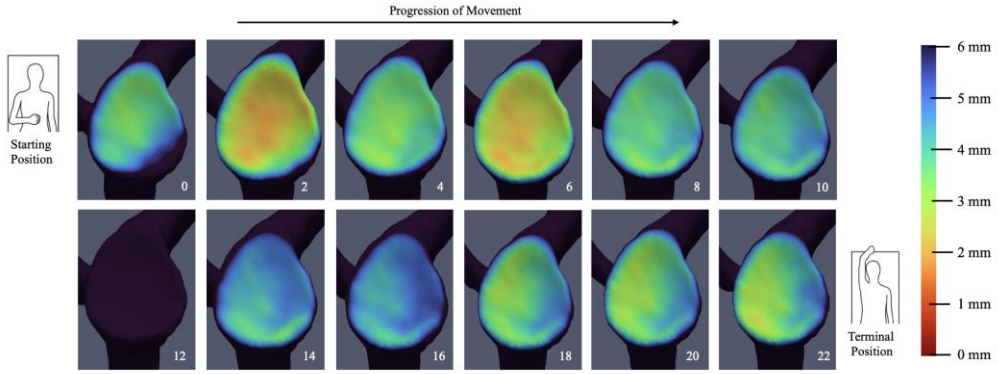

Proximity map for participant Young-3 throughout FE at different reference frames

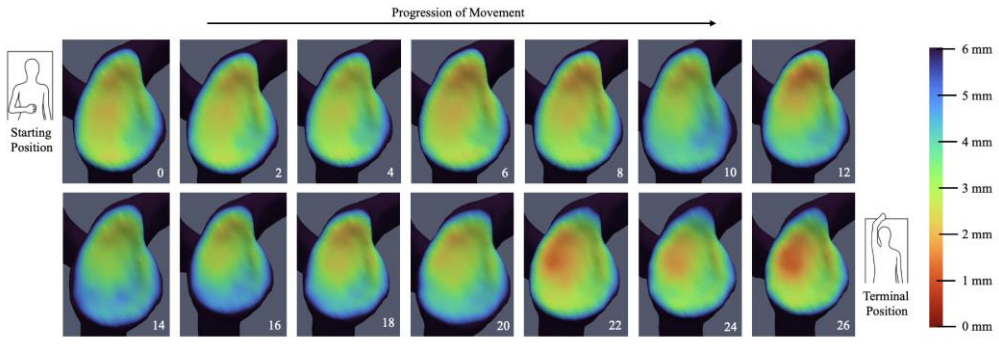

Proximity map for participant Young-4 throughout FE at different reference frames

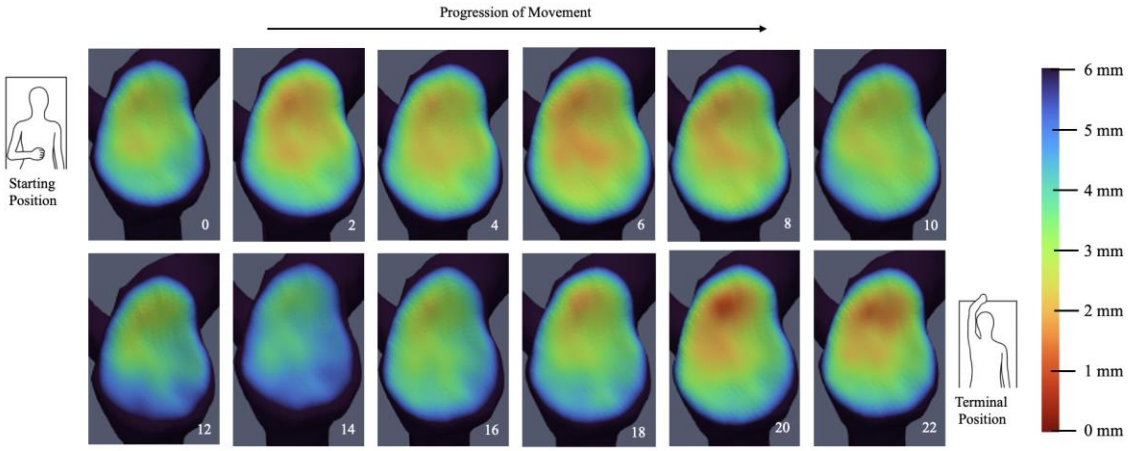

Proximity map for participant Young-5 throughout FE at different reference frames

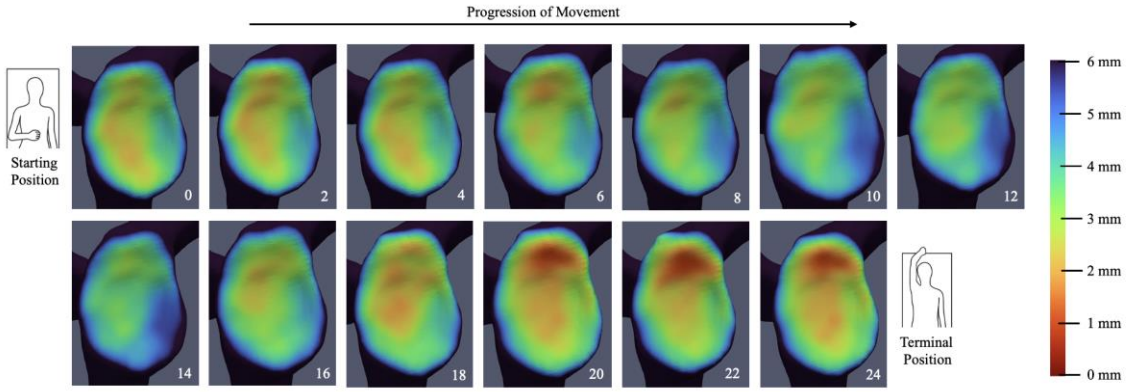

Proximity map for participant Young-6 throughout FE at different reference frames

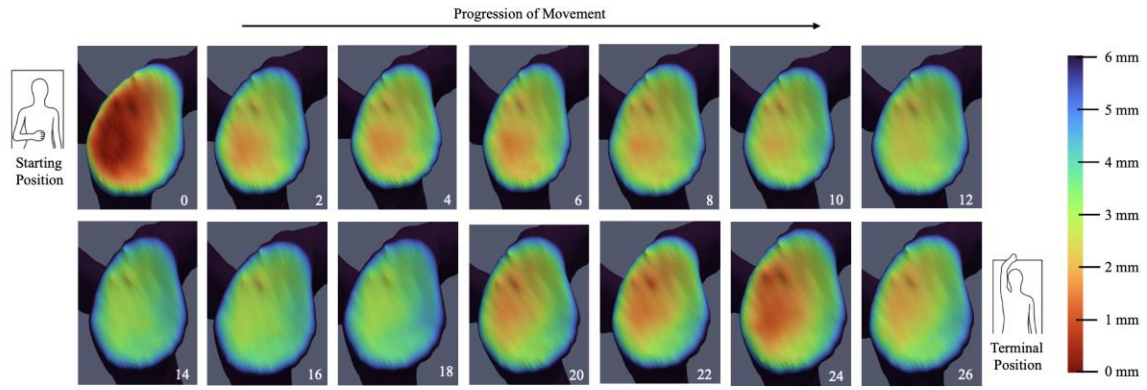

Proximity map for participant Young-7 throughout FE at different reference frames

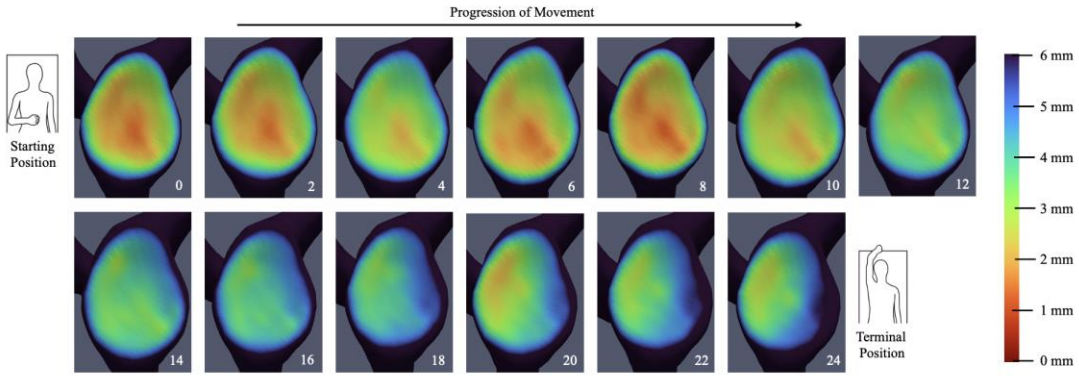

Proximity map for participant Young-8 throughout FE at different reference frames

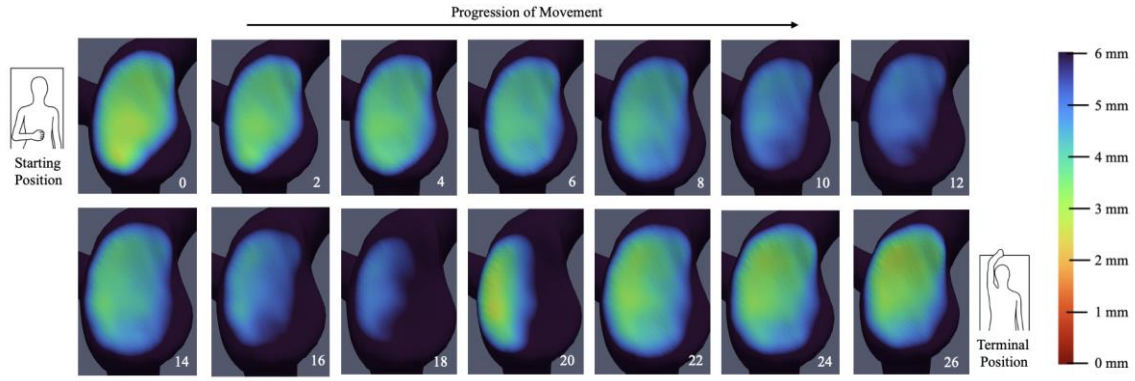

Proximity map for participant Young-9 throughout FE at different reference frames

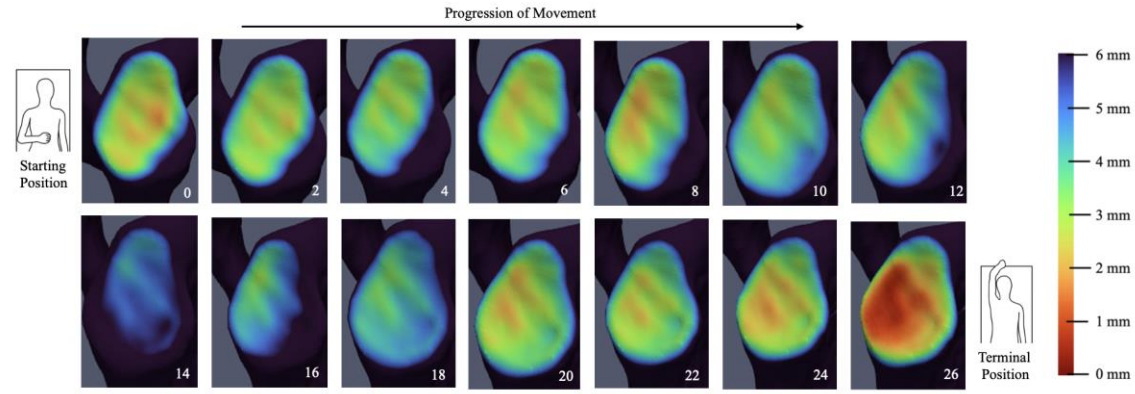

Proximity map for participant Young-10 throughout FE at different reference frames

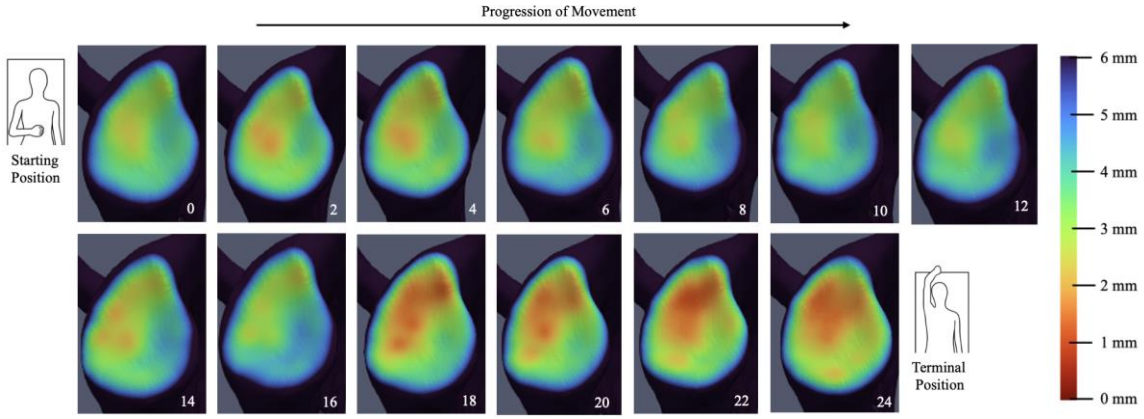

Proximity map for participant Young-11 throughout FE at different reference frames

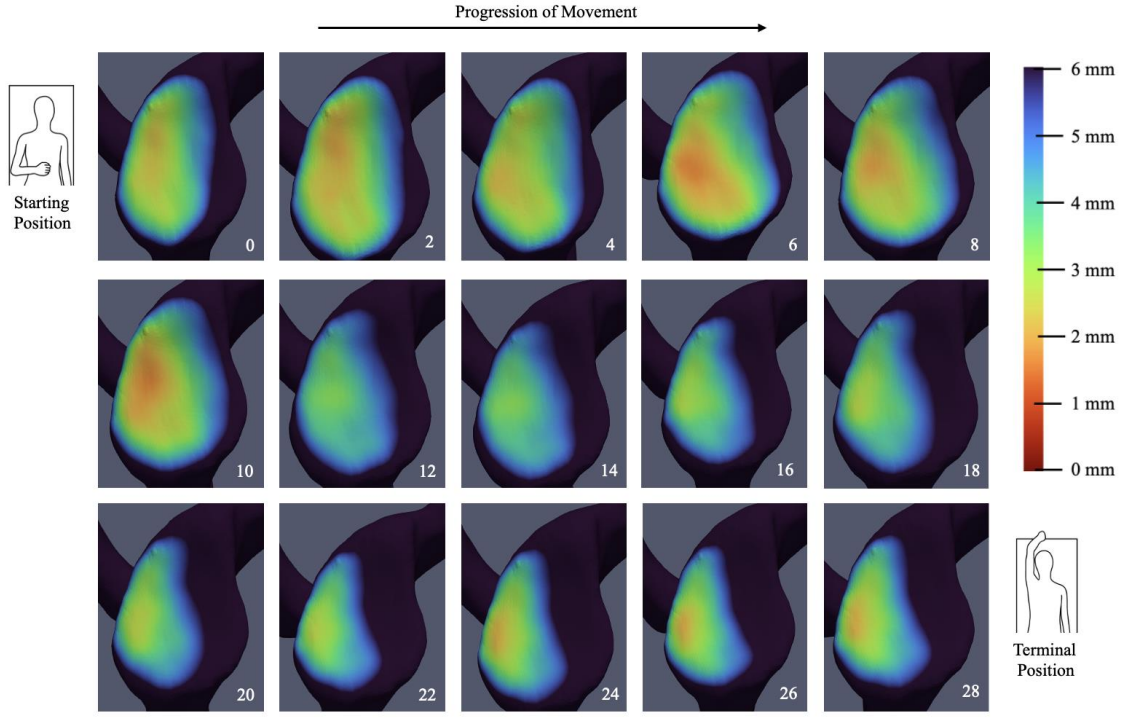

Proximity map for participant Young-12 throughout FE at different reference frames

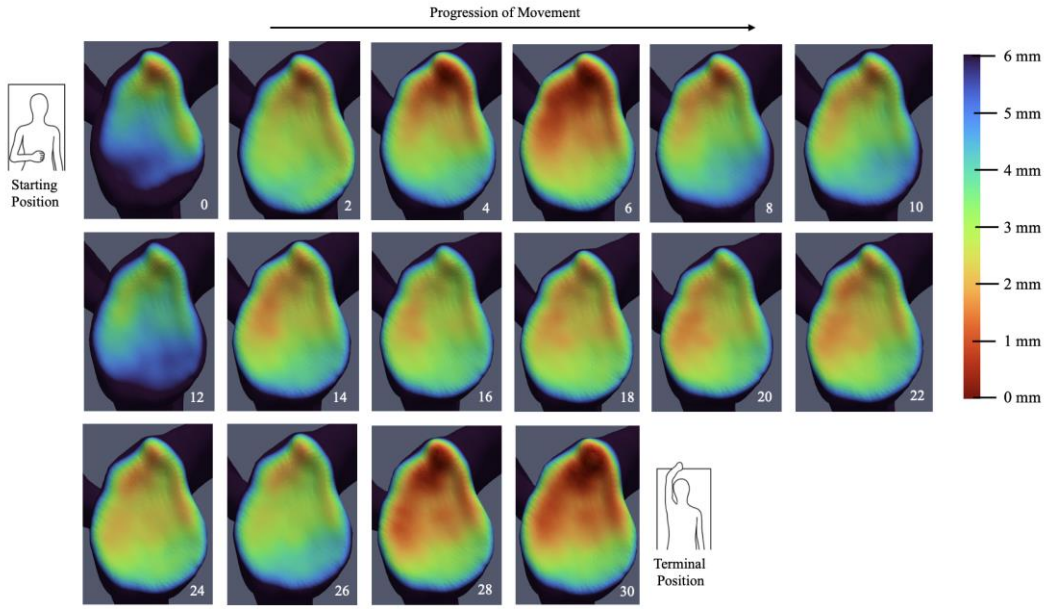

Proximity map for participant Old-1 throughout FE at different reference frames

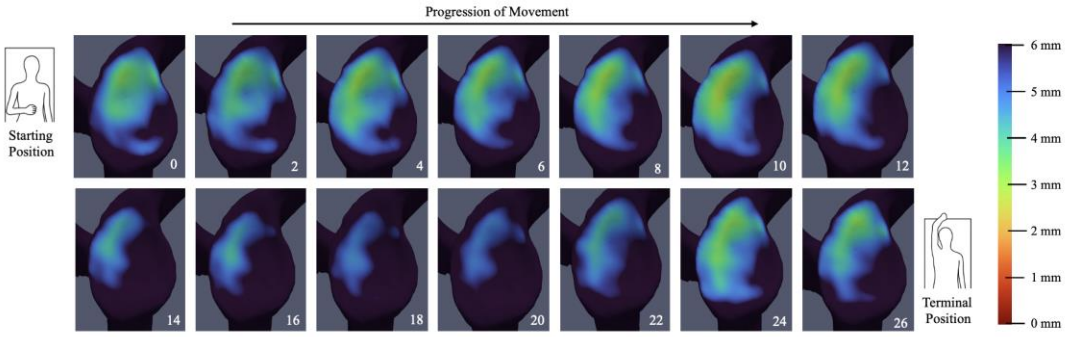

Proximity map for participant Old-2 throughout FE at different reference frames

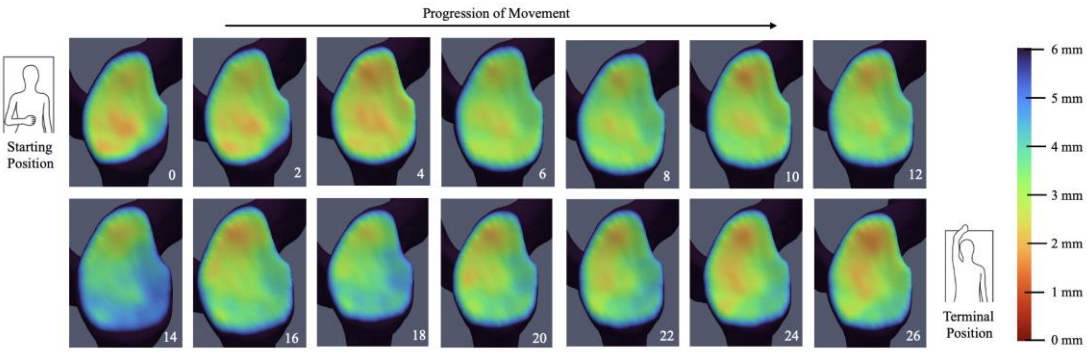

Proximity map for participant Old-3 throughout FE at different reference frames

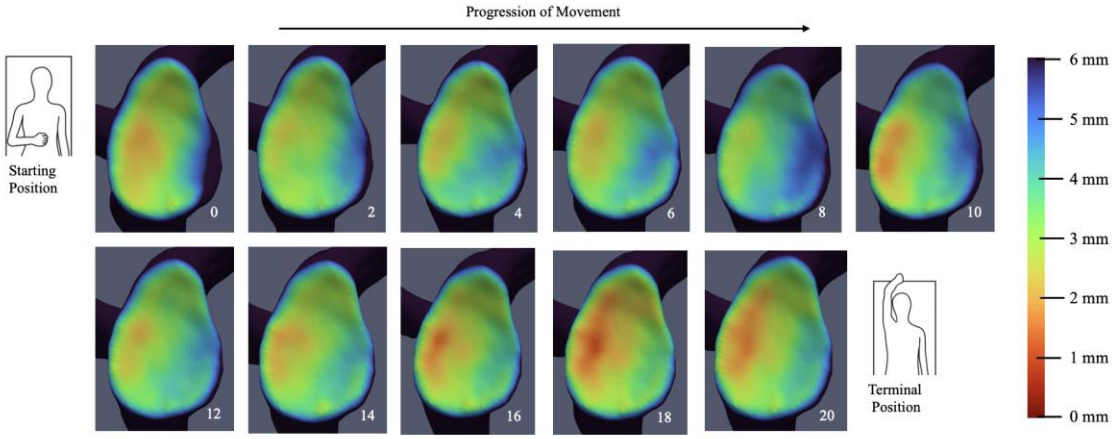

Proximity map for participant Old-4 throughout FE at different reference frames

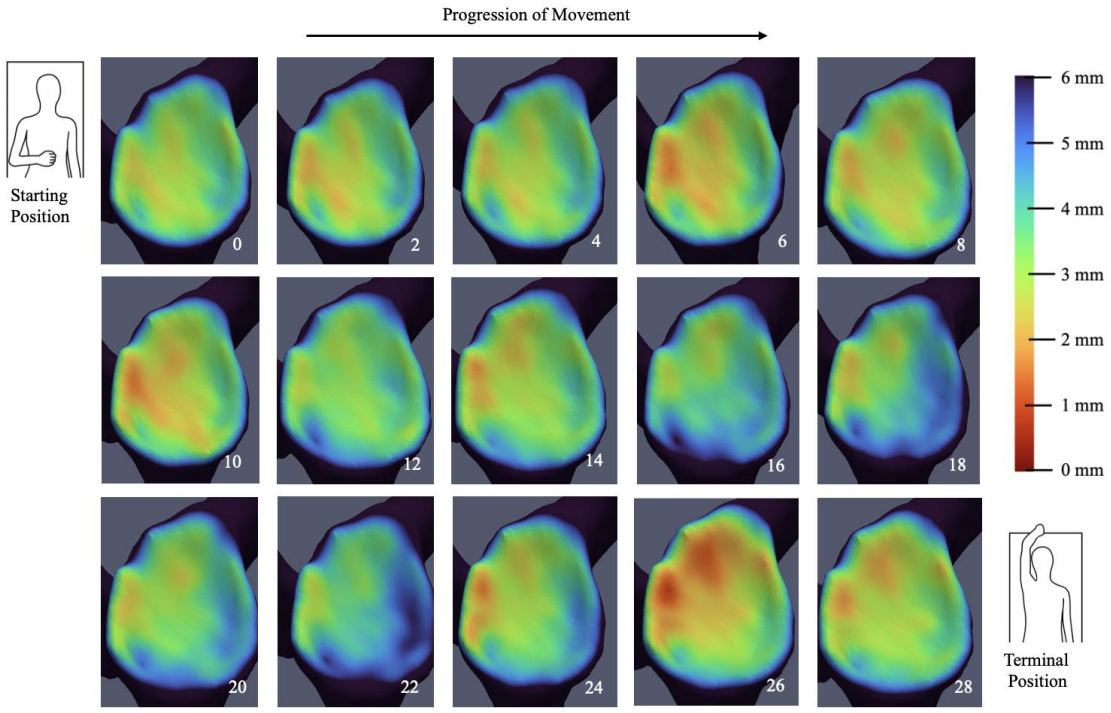

Proximity map for participant Old-5 throughout FE at different reference frames

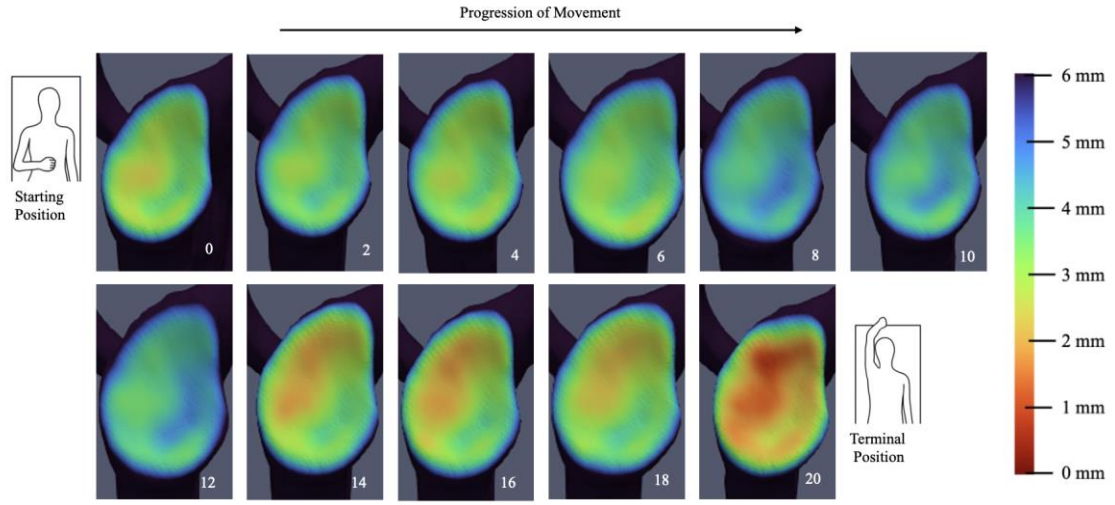

Proximity map for participant Old-6 throughout FE at different reference frames

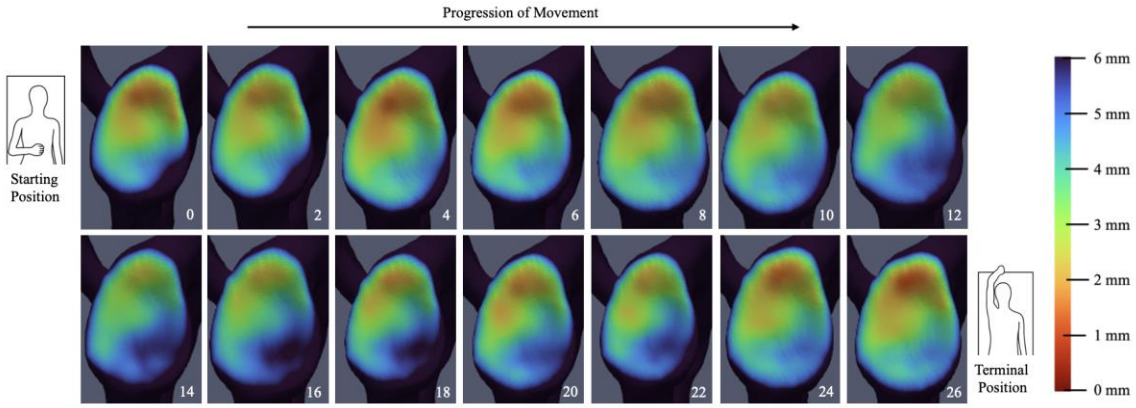

Proximity map for participant Old-7 throughout FE at different reference frames

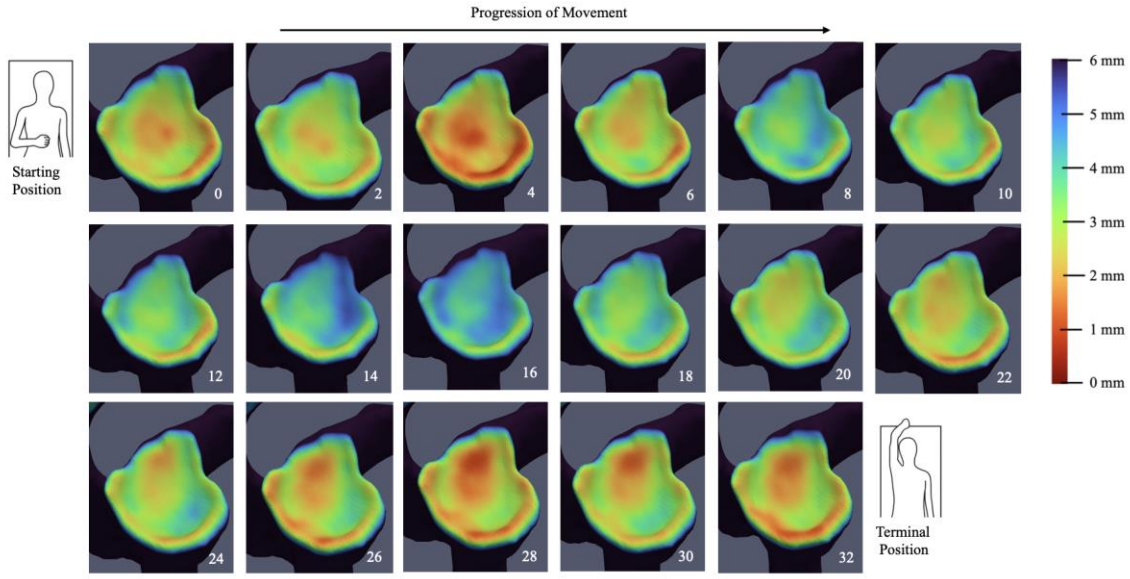

Proximity map for participant Old-8 throughout FE at different reference frames

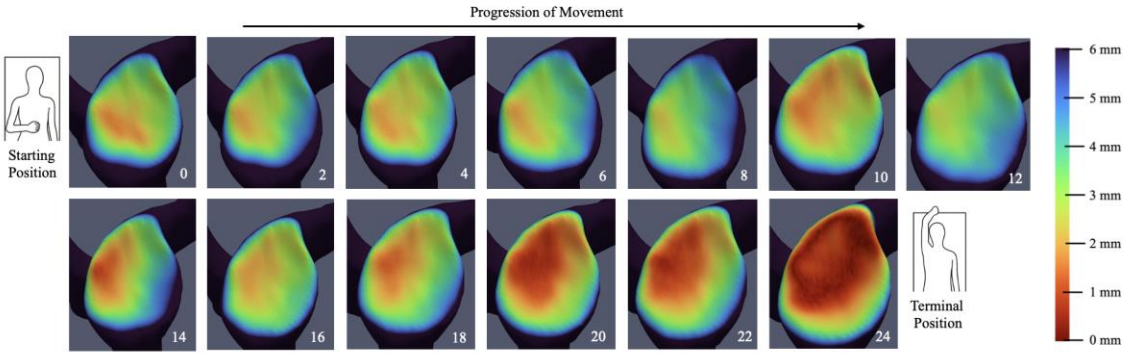

Proximity map for participant Old-9 throughout FE at different reference frames

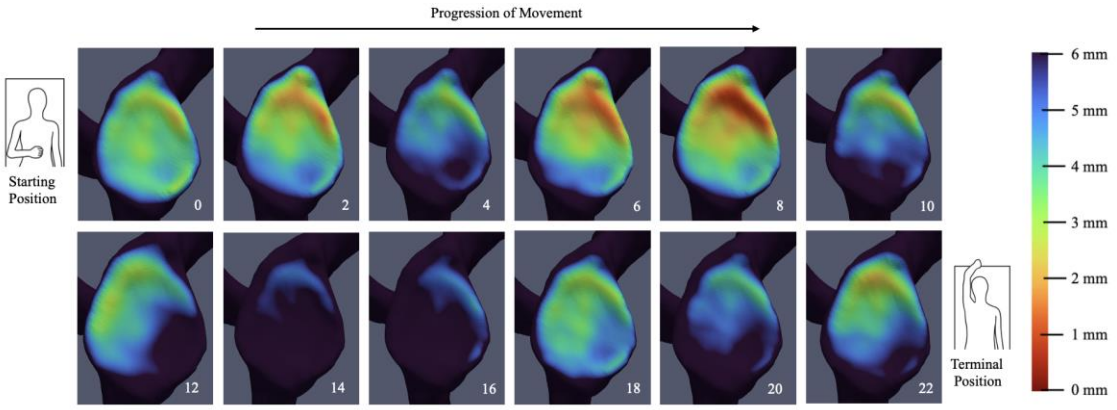

Proximity map for participant Old-10 throughout FE at different reference frames

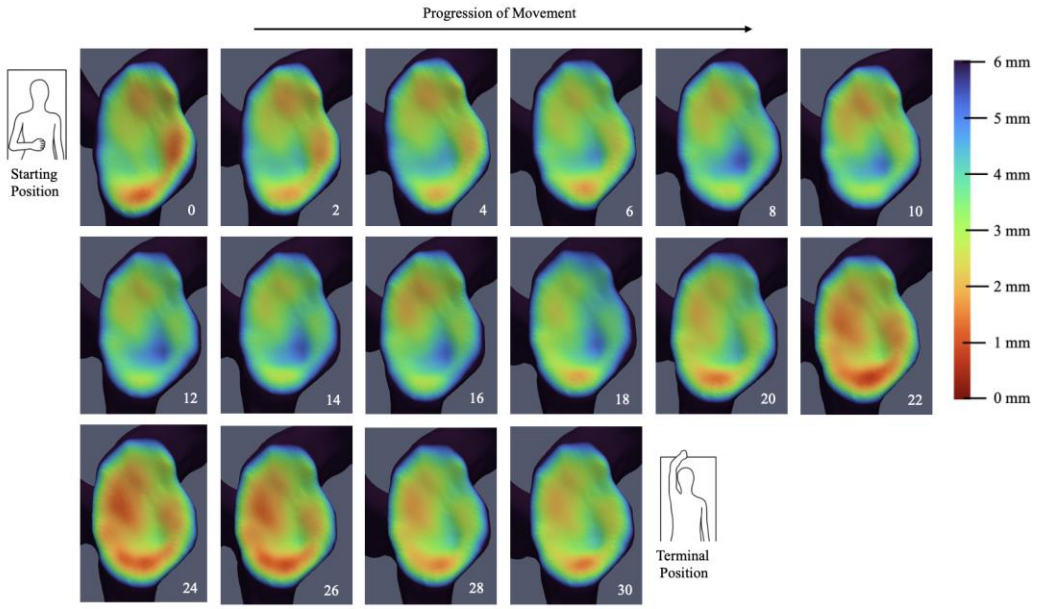

Proximity map for participant Old-11 throughout FE at different reference frames

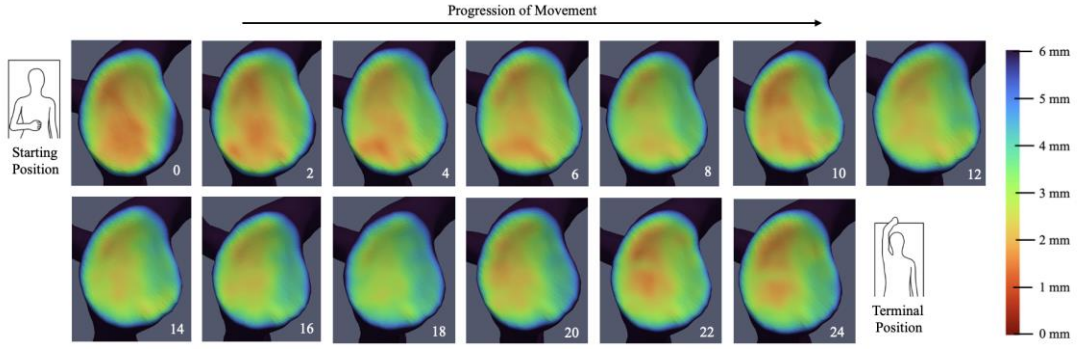

Proximity map for participant Old-12 throughout FE at different reference frames

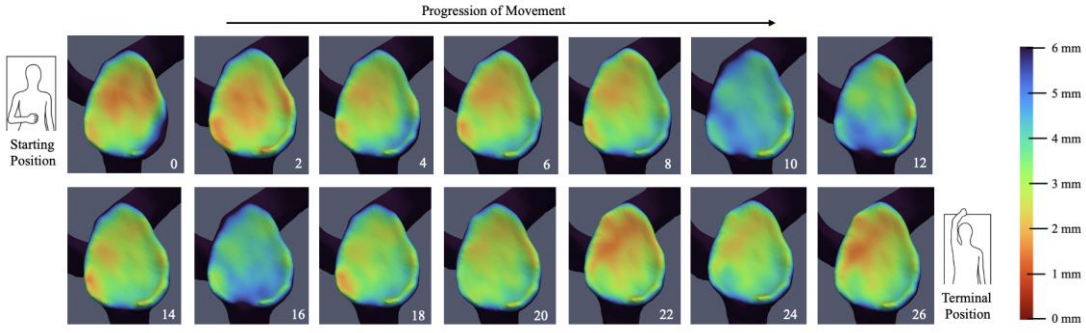

Proximity map for participant Old-13 throughout FE at different reference frames

Figure A-2: Internal Rotation to the Back (IR) Proximity Maps

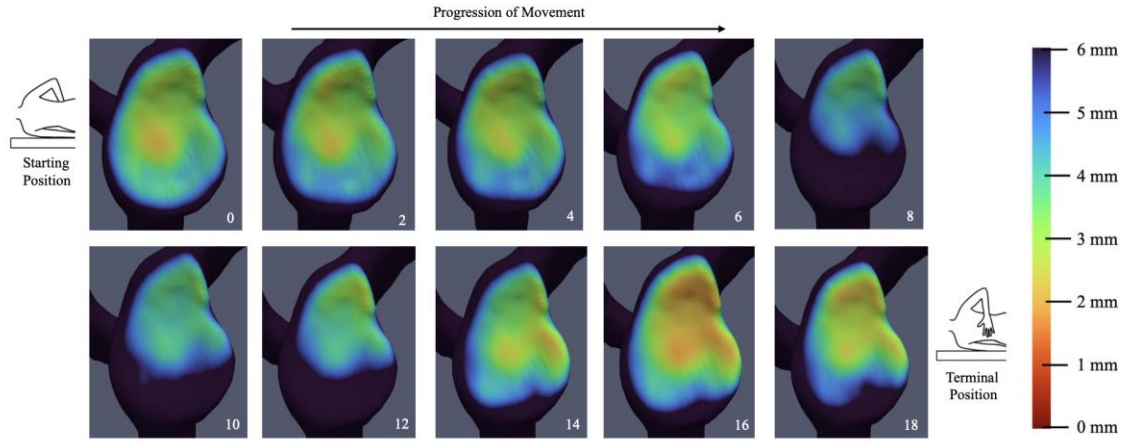

Proximity map for participant Young-1 throughout IR at different reference frames

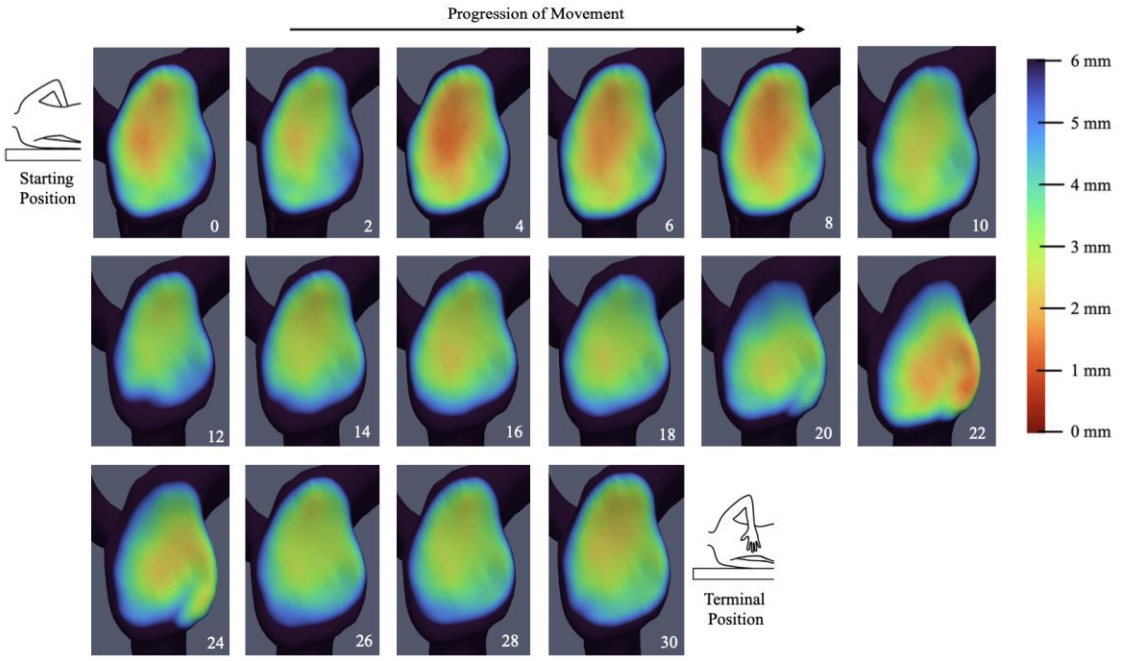

Proximity map for participant Young-2 throughout IR at different reference frames

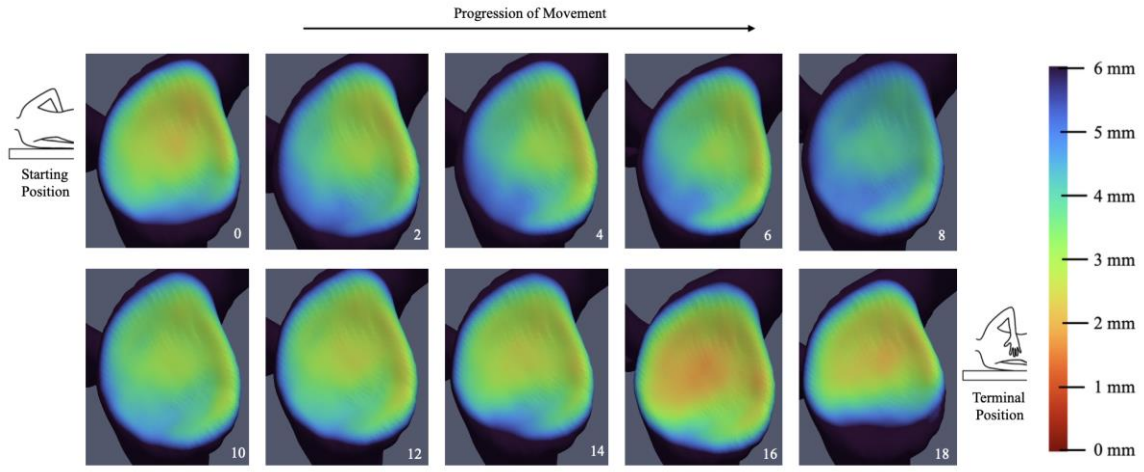

Proximity map for participant Young-3 throughout IR at different reference frames

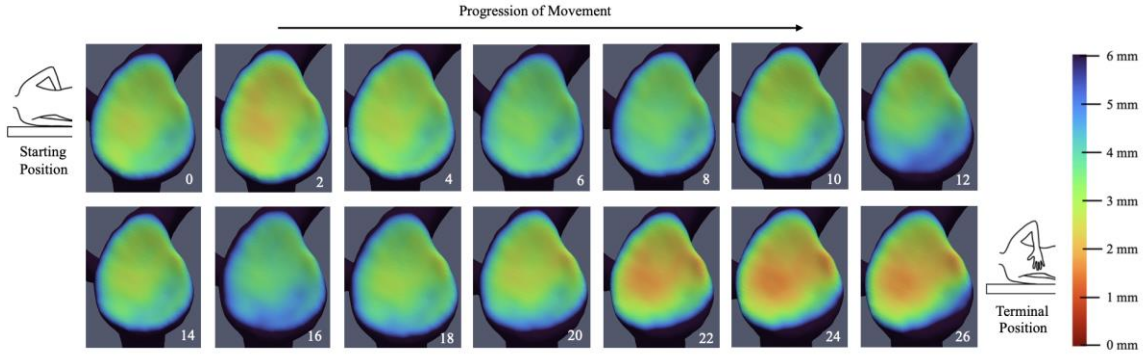

Proximity map for participant Young-4 throughout IR at different reference frames

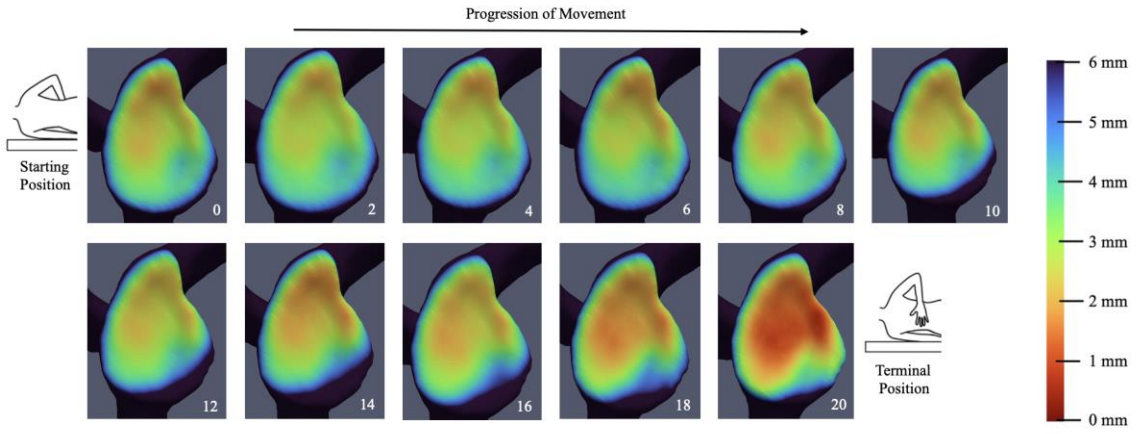

Proximity map for participant Young-5 throughout IR at different reference frames

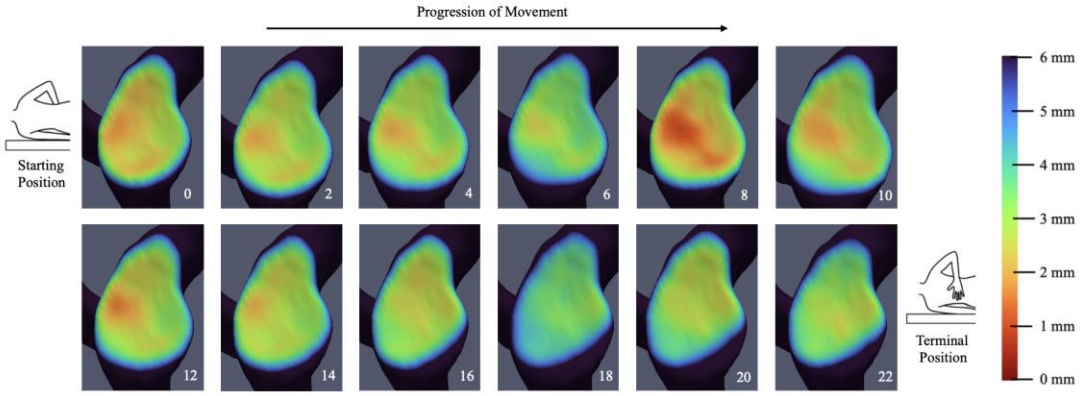

Proximity map for participant Young-6 throughout IR at different reference frames

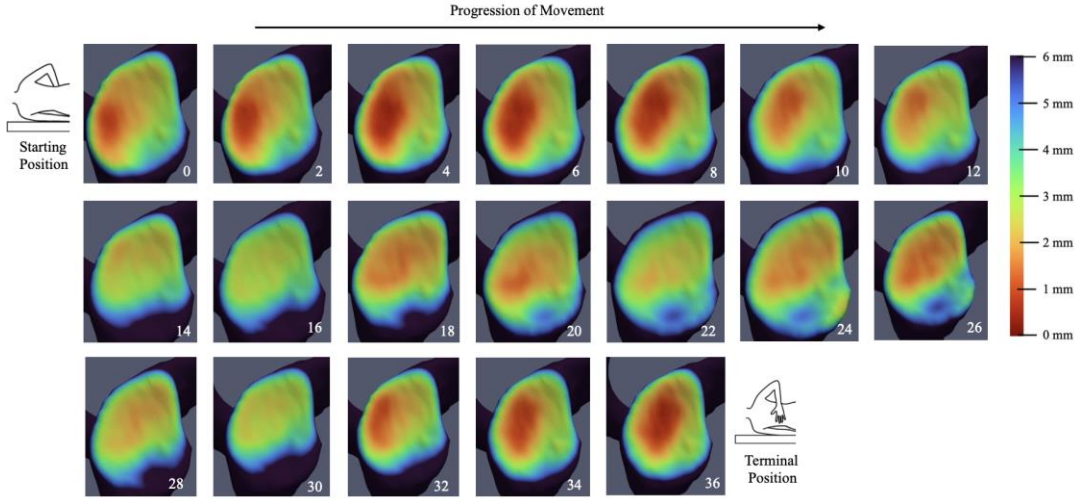

Proximity map for participant Young-7 throughout IR at different reference frames

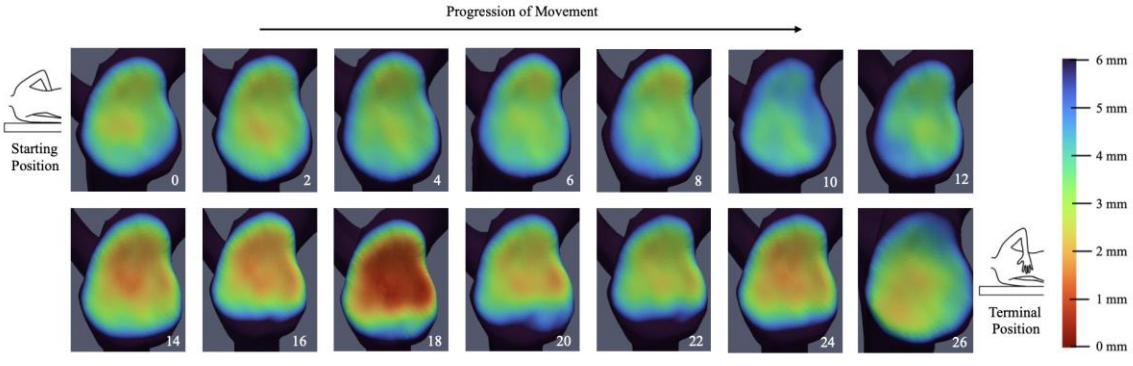

Proximity map for participant Young-8 throughout IR at different reference frames

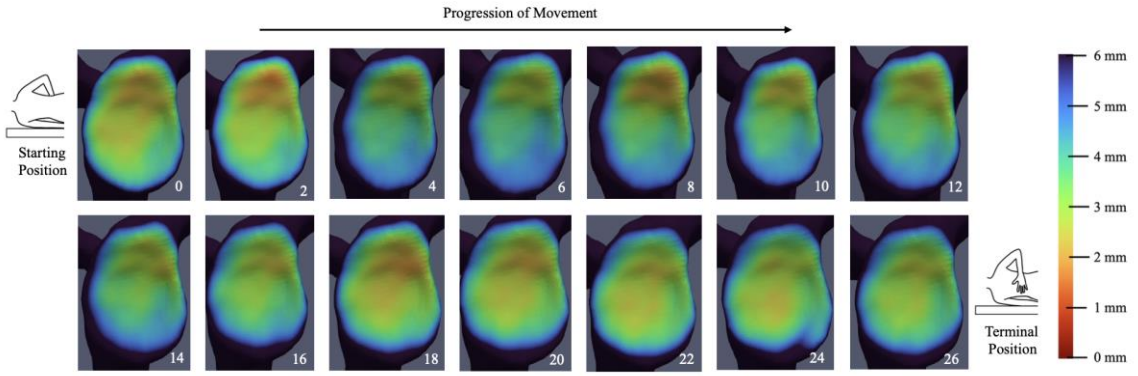

Proximity map for participant Young-9 throughout IR at different reference frames

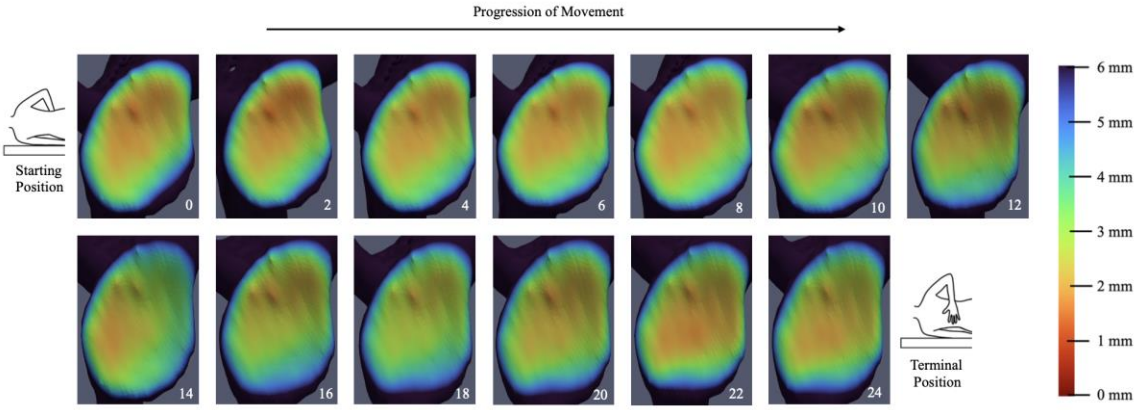

Proximity map for participant Young-10 throughout IR at different reference frames

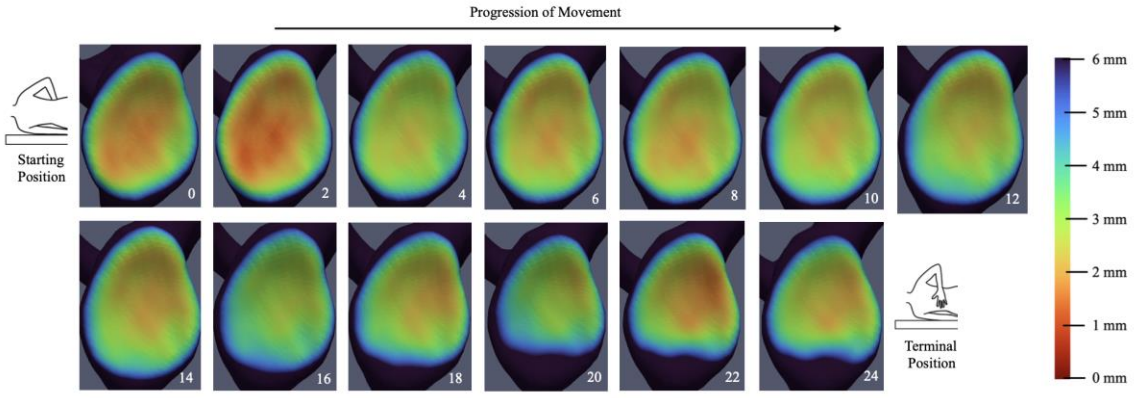

Proximity map for participant Young-11 throughout IR at different reference frames

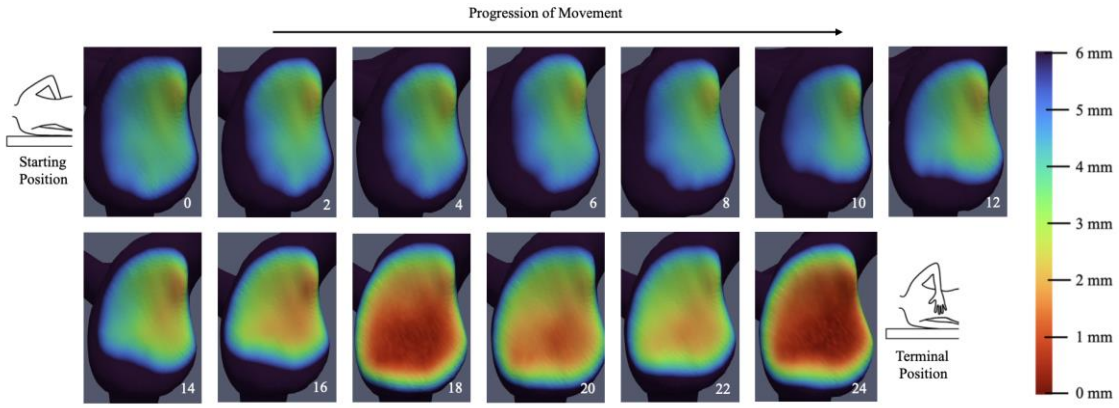

Proximity map for participant Young-12 throughout IR at different reference frames

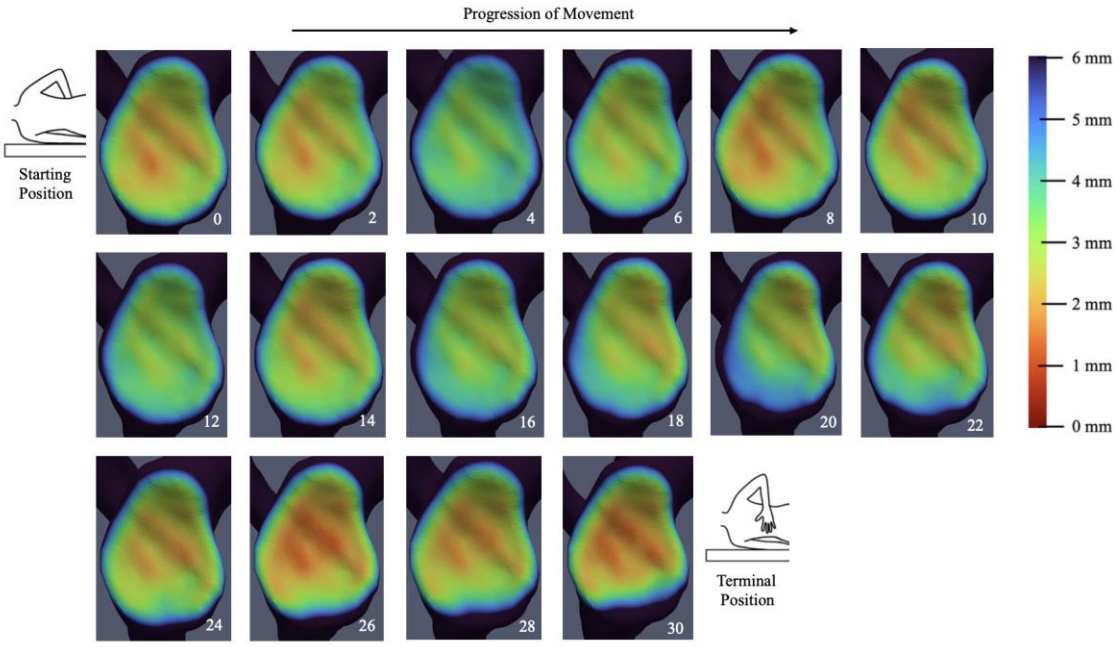

Proximity map for participant Young-13 throughout IR at different reference frames

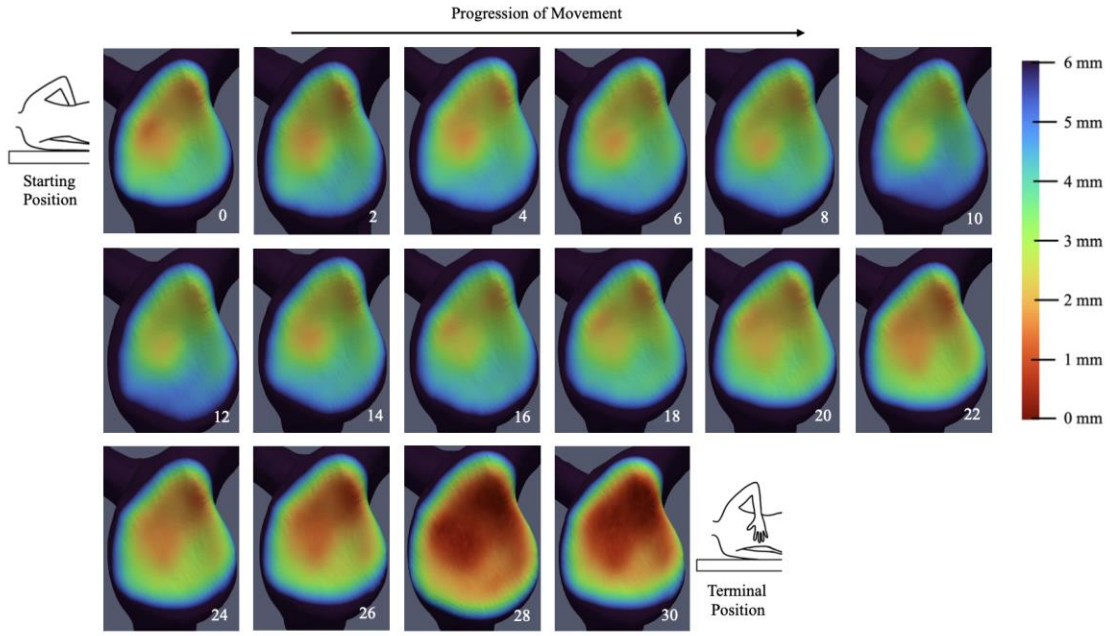

Proximity map for participant Young-14 throughout IR at different reference frames

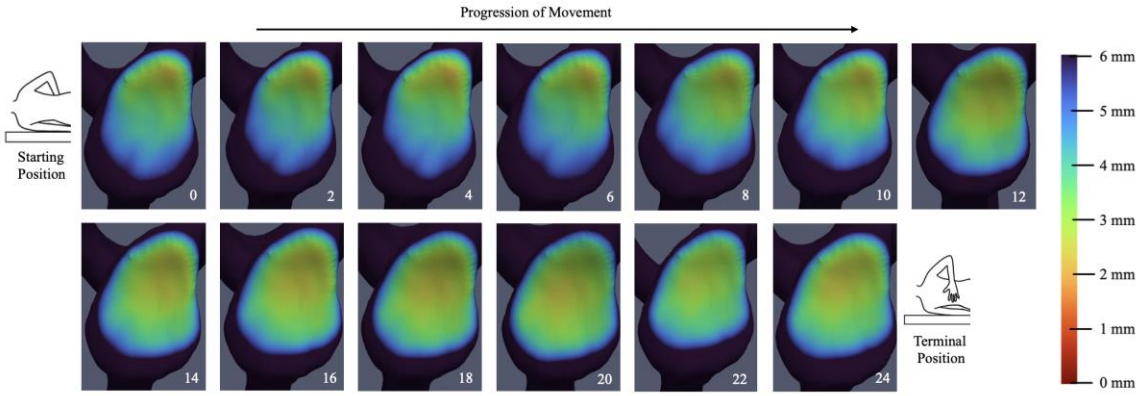

Proximity map for participant Young-15 throughout IR at different reference frames

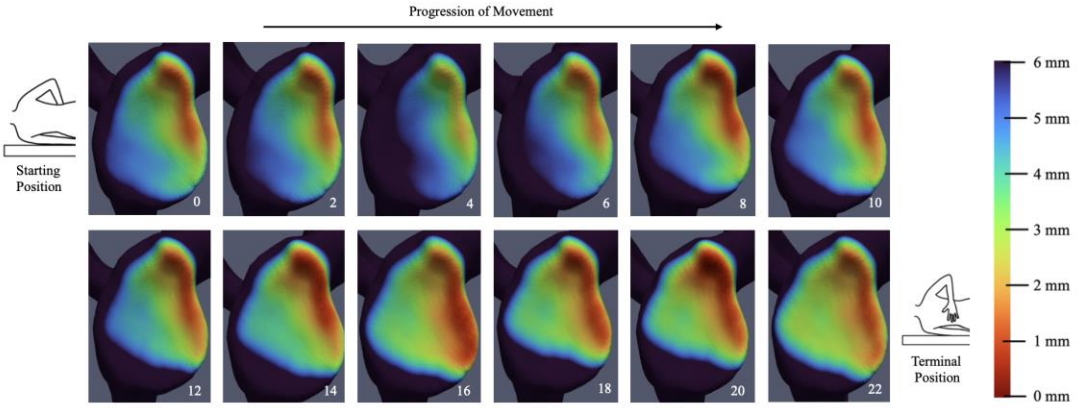

Proximity map for participant Old-1 throughout IR at different reference frames

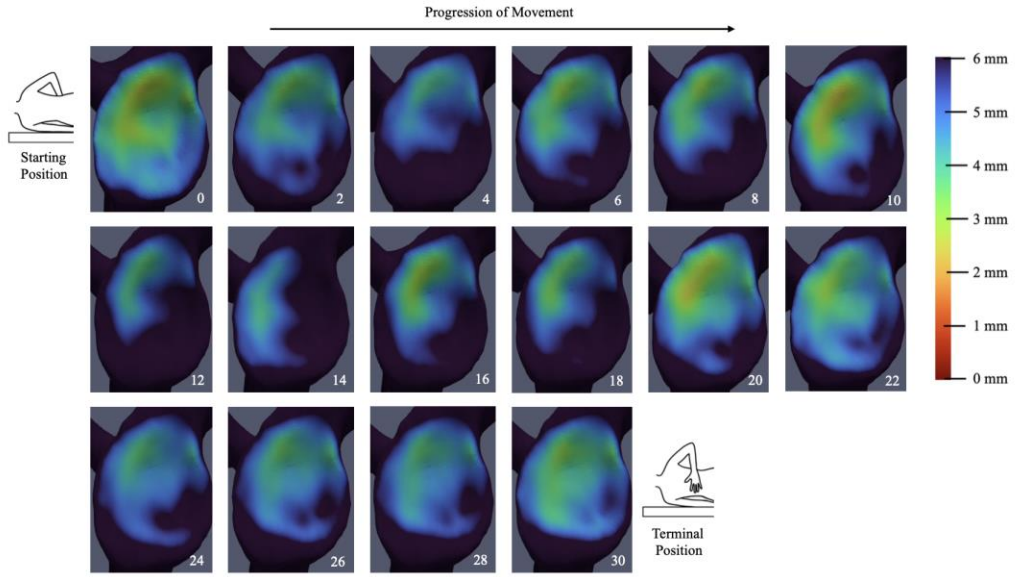

Proximity map for participant Old-2 throughout IR at different reference frames

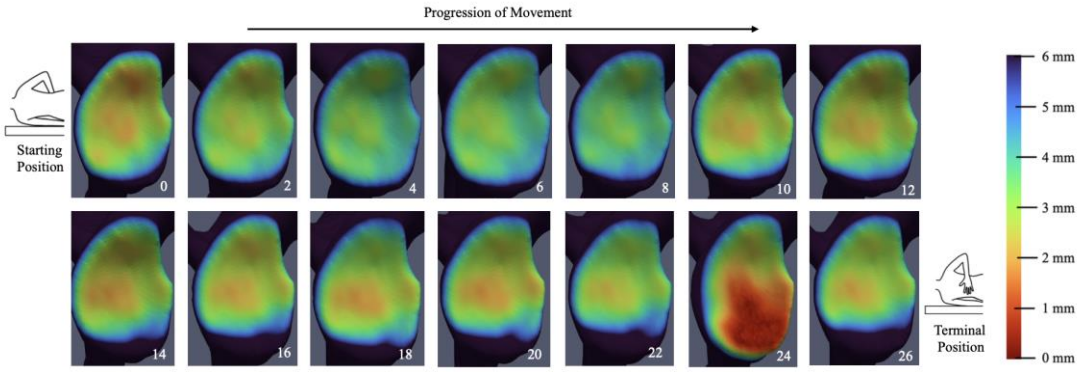

Proximity map for participant Old-3 throughout IR at different reference frames

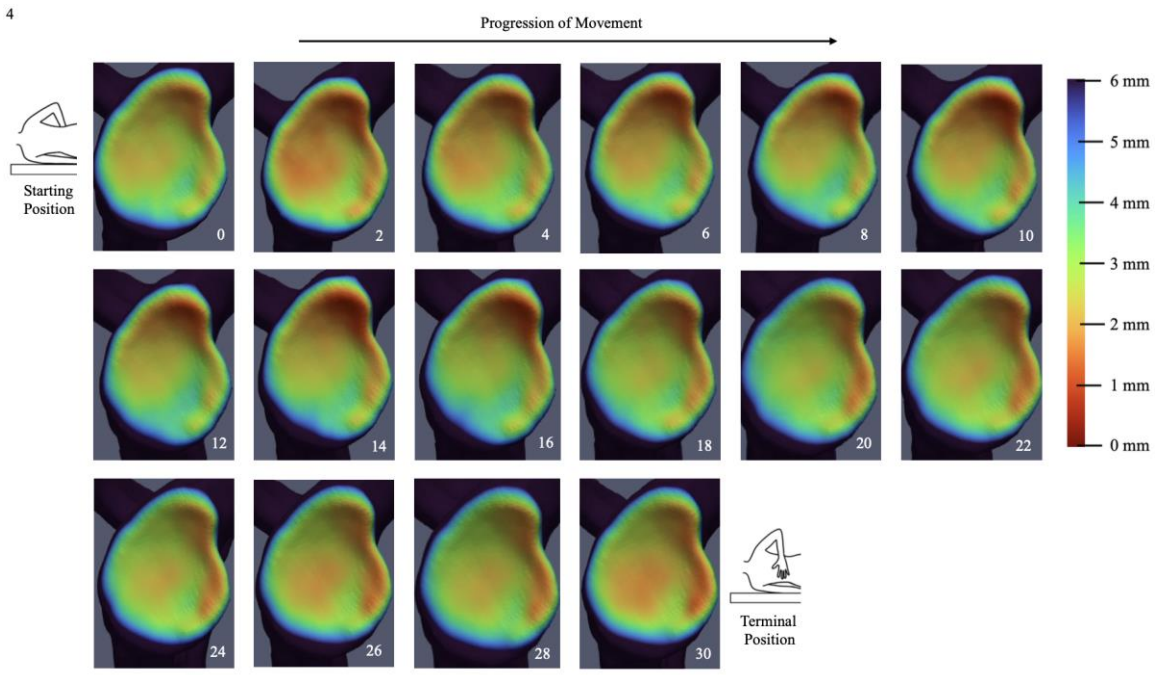

Proximity map for participant Old-4 throughout IR at different reference frames

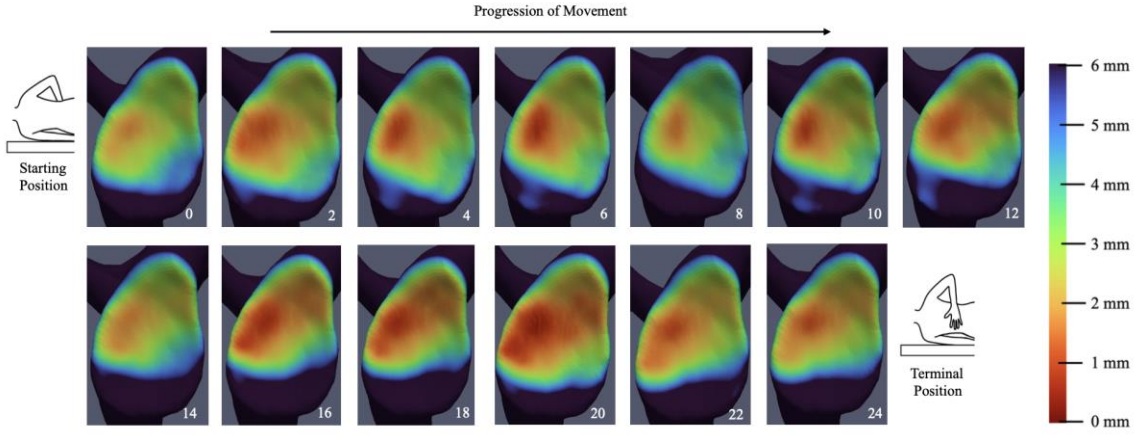

Proximity map for participant Old-5 throughout IR at different reference frames

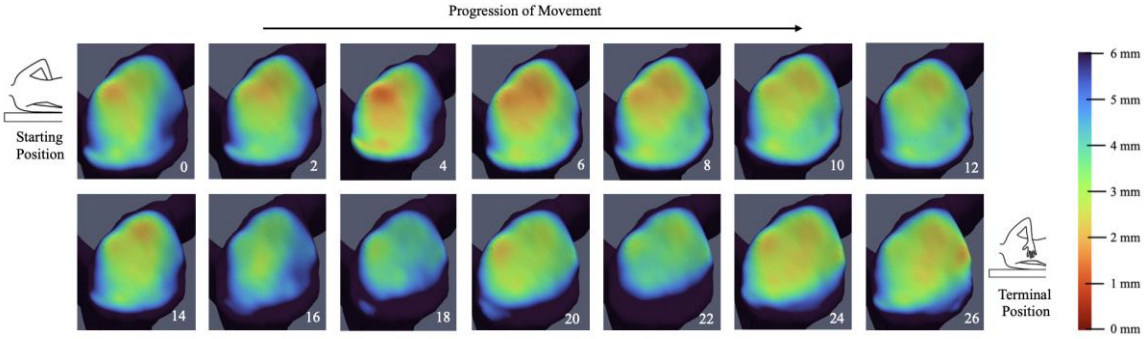

Proximity map for participant Old-6 throughout IR at different reference frames

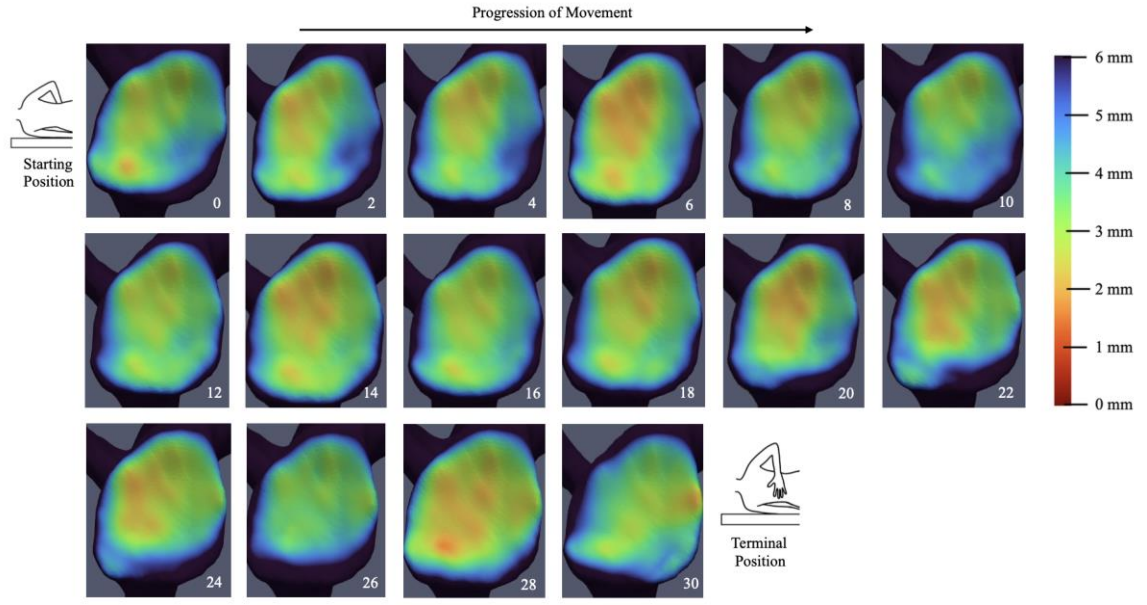

Proximity map for participant Old-7 throughout IR at different reference frames

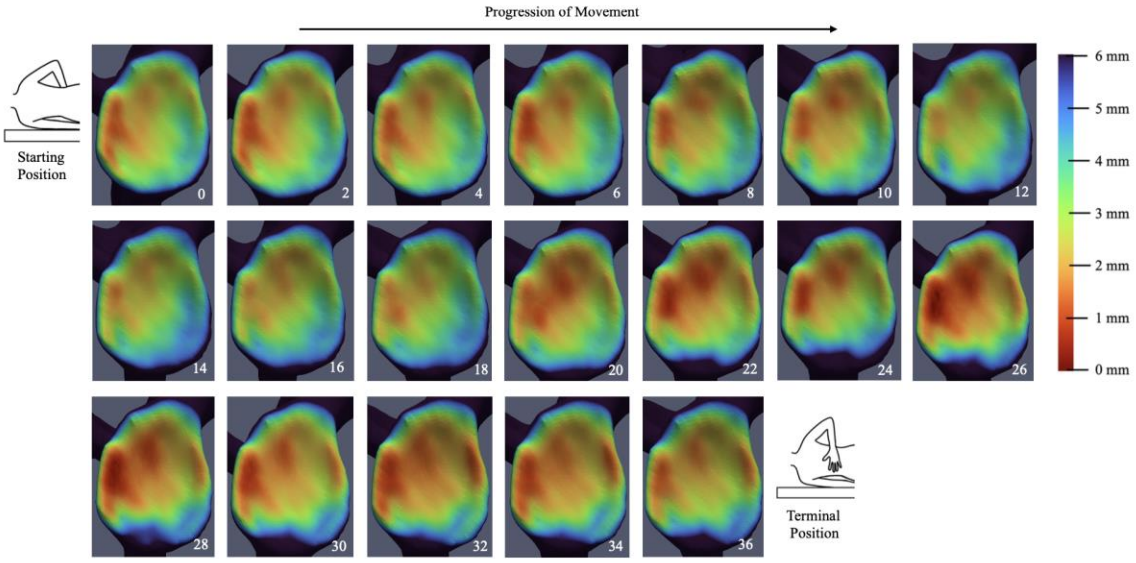

Proximity map for participant Old-8 throughout IR at different reference frames

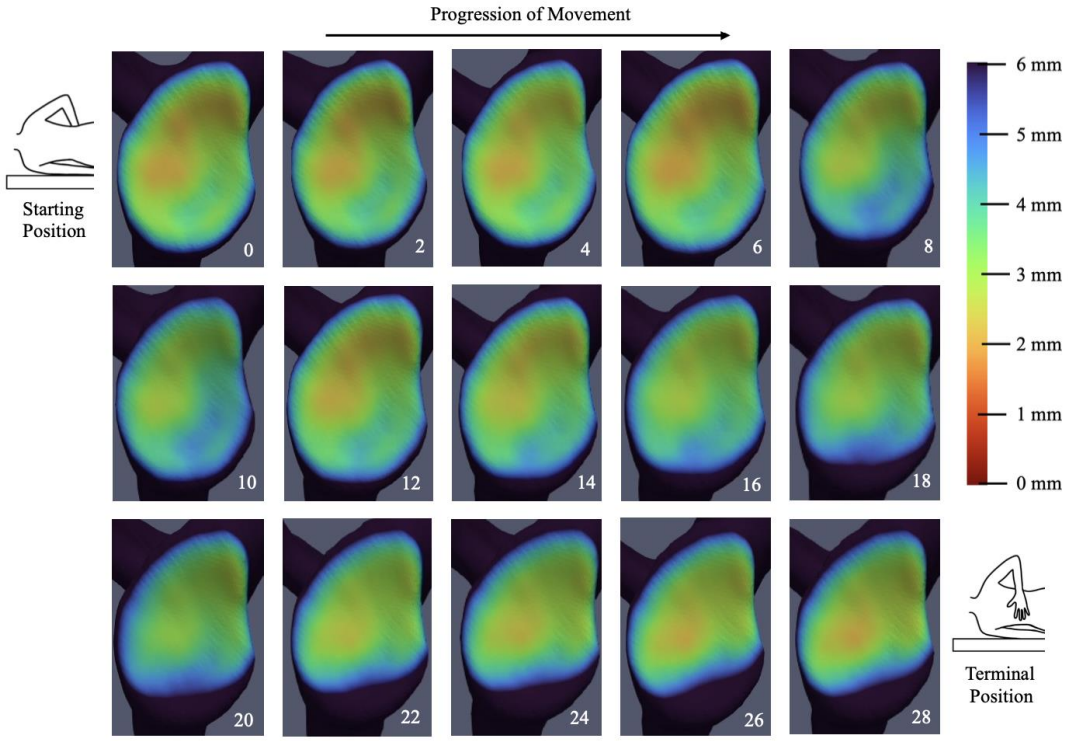

Proximity map for participant Old-9 throughout IR at different reference frames

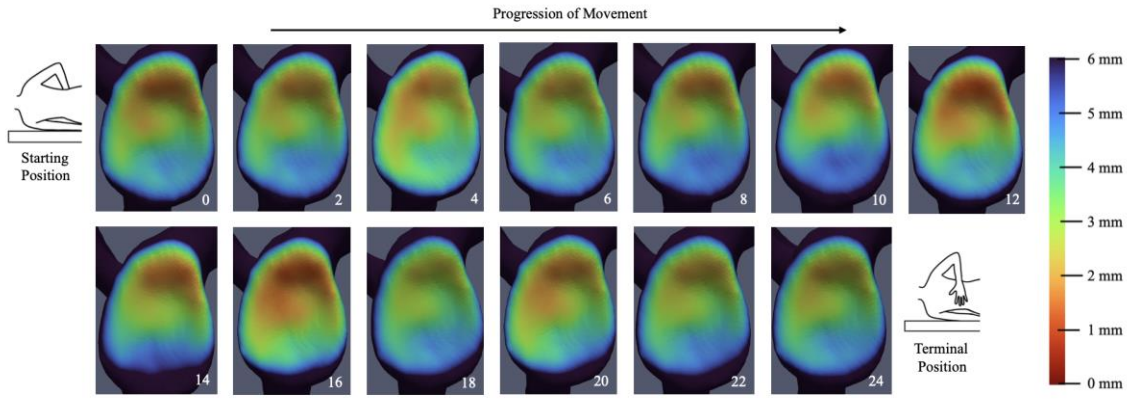

Proximity map for participant Old-10 throughout IR at different reference frames

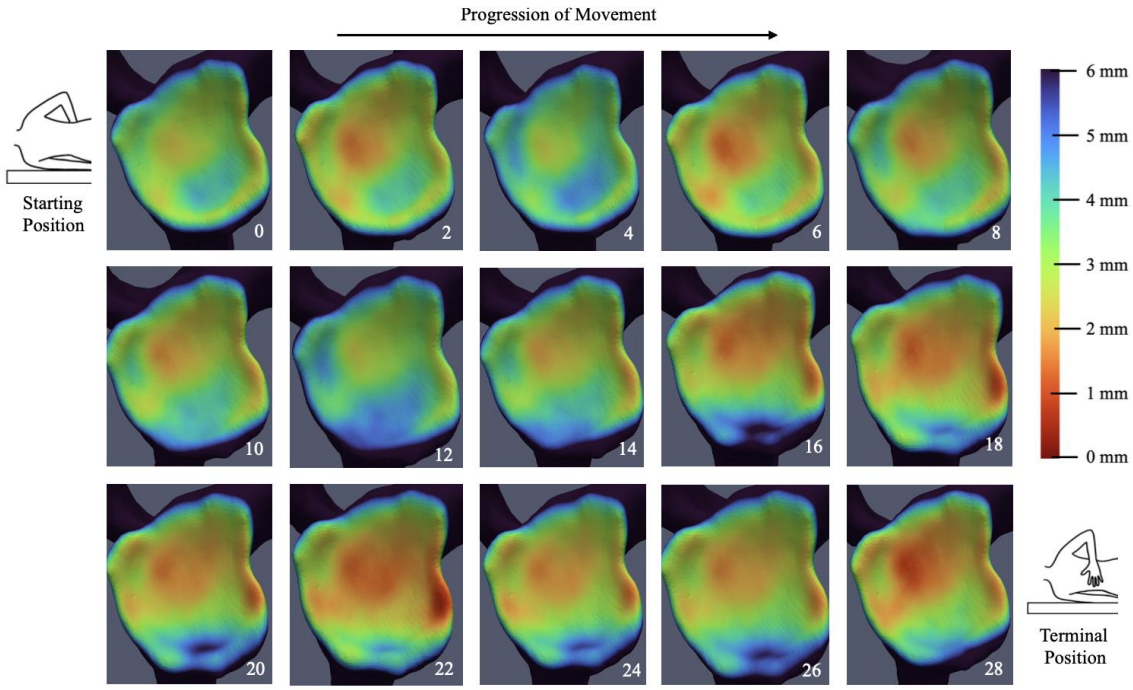

Proximity map for participant Old-11 throughout IR at different reference frames

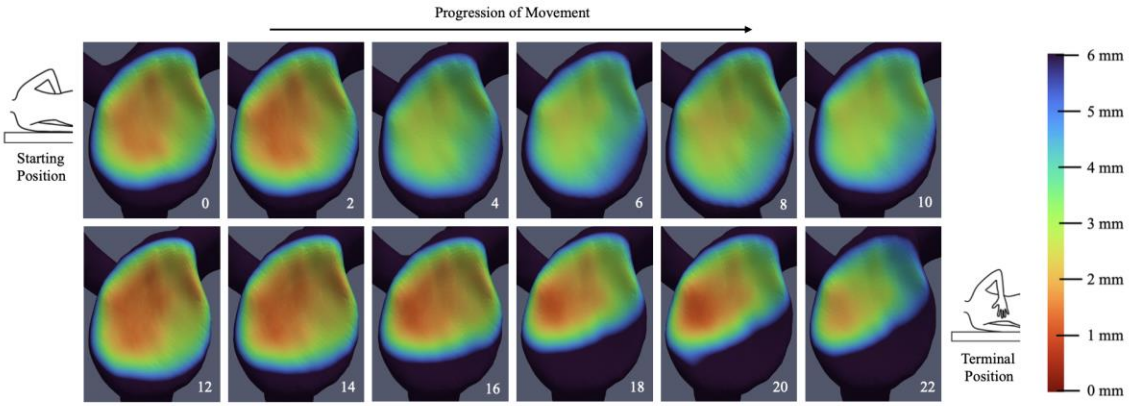

Proximity map for participant Old-12 throughout IR at different reference frames

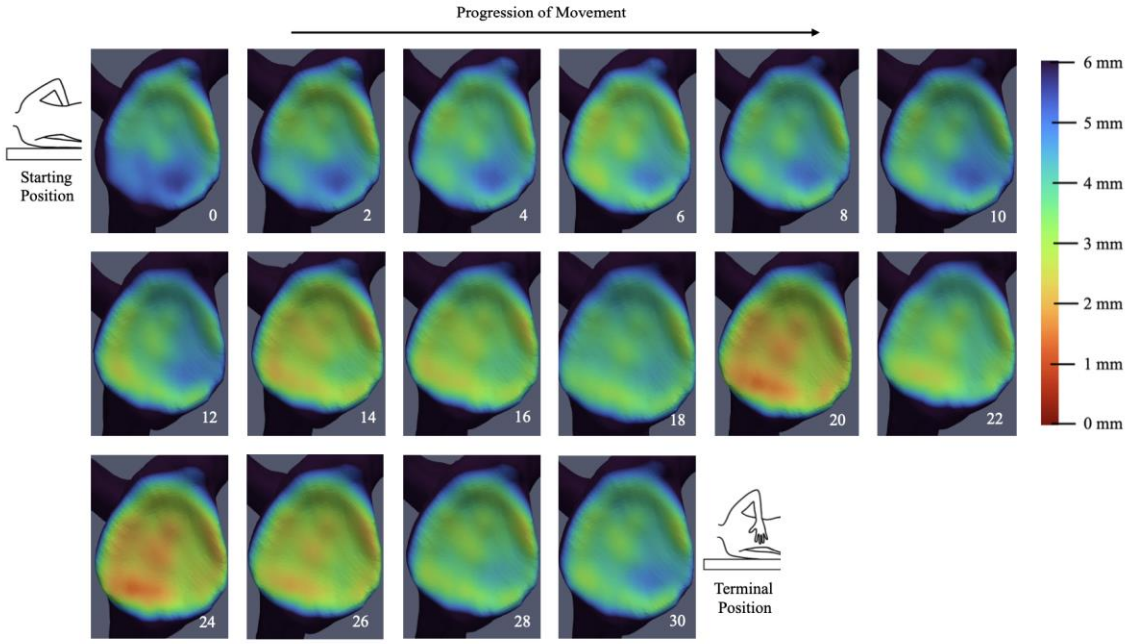

Proximity map for participant Old-13 throughout IR at different reference frames

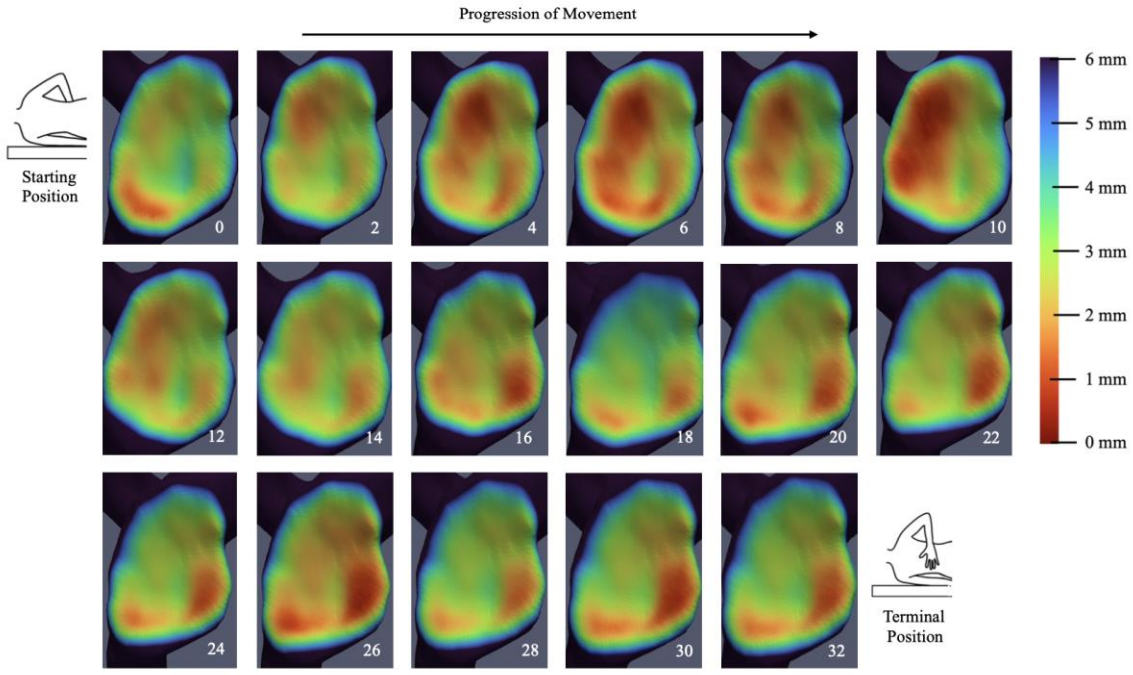

Proximity map for participant Old-14 throughout IR at different reference frames

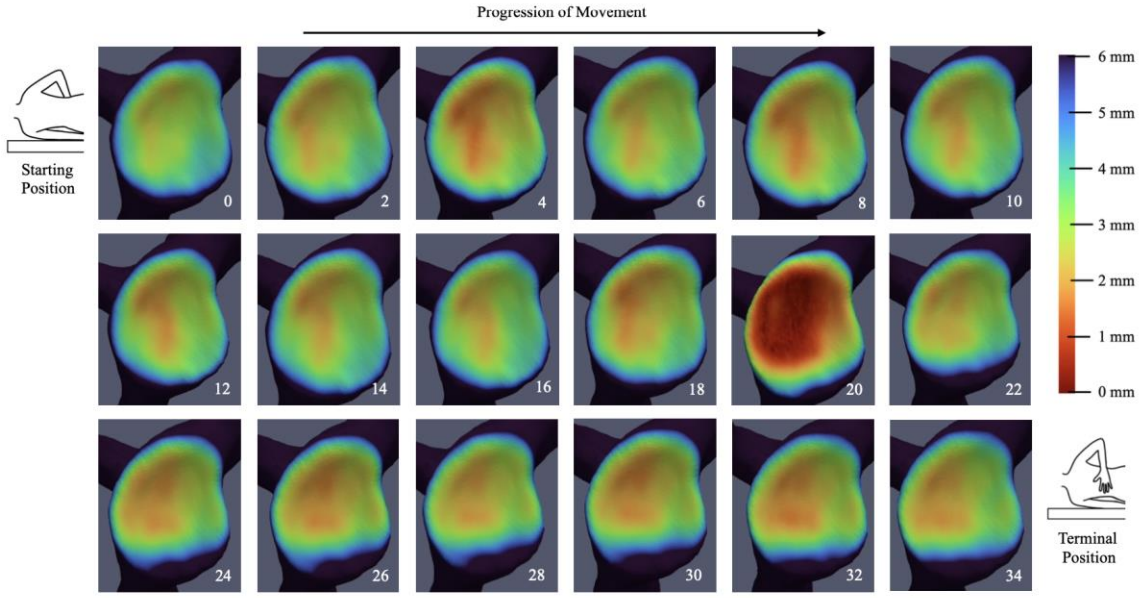

Proximity map for participant Old-15 throughout IR at different reference frames

Appendix B: Glenohumeral Joint Tracking (Translation) Using Surface Contact Point Versus Humeral Head Centre Point

B.1 Introduction

As previously mentioned in Chapter 2 of this thesis, historically, most studies have used the centre of the humeral head to track the translation at the glenohumeral joint.[1–10] However, in Chapter 2 of this thesis, the actual surface contact point between the humeral head and the glenoid was used to track glenohumeral translation. This is thought to provide a much more accurate representation of what is happening at the joint surfaces because it is taking into account exactly how the joint surfaces are moving relative to one another.

Therefore, the objective of this appendix was to determine if there was a correlation between using the surface contact point (that was used in Chapter 2 of this thesis) and the humeral head centre point (historically used) for quantifying glenohumeral translation. The hypothesis was that there would be a weak correlation between the two points. Thus, implying that the centre of the humeral head is not the most accurate way to measure glenohumeral translation at the joint.

B.2 Methods

The same methods that were described in Chapter 2 of this thesis were used to find the surface contact point between the humeral head and the glenoid. To find the humeral head centre point, a sphere of best fit was fitted onto the humeral head and the centre of the sphere was recorded. The surface contact point and the humeral head centre point were then compared by graphing the surface contact point versus the humeral head centre point for both the y-coordinate (S/I direction) and z-coordinate (A/P direction) of the point. A line of best fit was added to the graph and the R^2 value was found to determine the correlation between the two points in space. R^2 value meanings are as follows: 0.00-0.19 is considered a very weak correlation, 0.20-0.39 is considered a weak correlation, 0.40-0.59 is considered a moderate correlation, 0.60-0.79 is considered a strong correlation, 0.80-1.00 is considered a very strong correlation.

Additionally, the actual translation at the glenohumeral joint for both methods were found by taking the difference between the maximum and the minimum values in both the S/I and A/P direction. For example, translation in the S/I direction was the difference between the max and min y-plane values, and the translation in the A/P direction was the difference between the max and min z-plane values. The translation differences between the two different methods were found by subtracting the translation (mm) found using the humeral head centre point from the translation (mm) found using the surface contact point.

B.3 Results

A sample graph for one healthy participant can be seen in Figure B-1 and Figure B-2. Figure B-1 (blue) shows the y-coordinate (S/I direction) of the surface contact points throughout each frame of movement compared to the y-coordinate (S/I direction) of the centre of the humeral head points throughout each frame of movement. Figure B-2 (orange) shows the z-coordinate (A/P direction) of the surface contact points throughout each frame of movement compared to the z-coordinate (A/P direction) of the centre of the humeral head points throughout each frame of movement. An ideal plot would show a linear line because that would indicate that the y and z coordinates of the surface contact points would be aligned with each y and z coordinates of humeral head centre points. In the figures below you can see that $R^2 = 0.15$ for the S/I direction, and $R^2 = 0.06$ for the A/P direction.

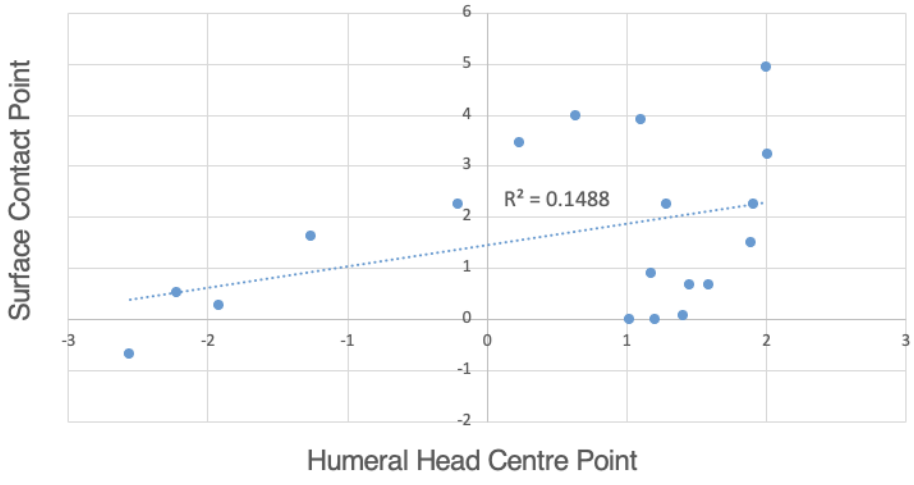

Figure B-1: Y-coordinate (S/I) of surface contact point versus humeral head centre point for all frames of IR motion

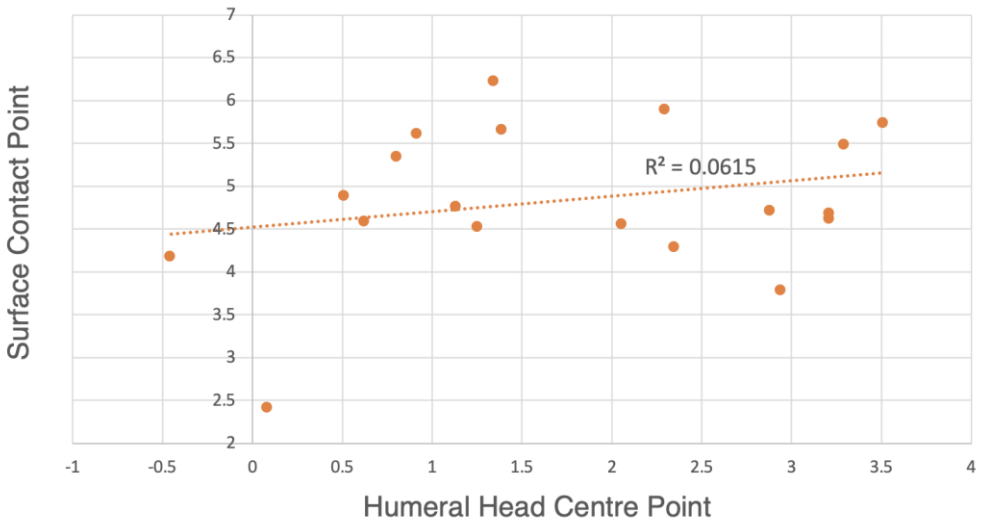

Figure B-2: **Z-coordinate (A/P) of surface contact point versus humeral head centre point for all frames of IR motion**

These graphs were made for all healthy participants that completed the IR movement (Young: n=15, and Old: n=15). Once all the graphs were made, the average R^2 values were found for each participant in both directions (S/I and A/P). The mean R^2 values for both cohorts in each direction were found. Figure B-3 is a summary of the findings. For the younger cohort, a moderate correlation was found for translation in S/I direction ($R^2 = 0.46$) and a strong correlation for translation in A/P direction ($R^2 = 0.63$). For the older cohort, a weak correlation was found for translation in the S/I direction ($R^2 = 0.28$) and a moderate correlation for translation in A/P direction ($R^2 = 0.45$). Overall, a stronger correlation was seen in the A/P direction for both younger and older cohorts. As well, a stronger correlation was seen overall for the young participants.

	Y - S/I	**Z - A/P**
R^2 – Young	0.46	0.63
R^2 – Old	0.28	0.45

Figure B-3: Summary of R^2 values for the younger and older cohorts in S/I and A/P direction

The difference in translation using both methods was found, and a summary of the average glenohumeral translation difference for both the younger and older cohorts for the S/I and A/P direction can be seen in Figure B-4.

	Translation Difference	
	Y - S/I (mm)	**Z - A/P (mm)**
Young	2.2	-0.4
Old	2.0	1.3

Figure B-4: Translation difference using the surface contact point versus the humeral head centre point

Note that a positive value means that the surface contact point translation is greater than the humeral head centre point translation, and a negative value means the surface contact point translation is less than humeral head centre point translation. For the younger cohort, the mean glenohumeral translations were found to be 2.2mm greater (S/I direction) and 0.4mm less (A/P direction) when using the surface contact point than when using the humeral head centre point. For the older cohort, the mean glenohumeral translations were found to be 2.0mm greater (S/I direction) and 1.3mm greater (A/P direction) when using the surface contact point than when using the humeral head centre point.

Appendix C: Validation of Proximity Maps

C.1 Introduction

To validate the method utilized in Chapter 2 of this thesis for determining the joint proximity of the glenohumeral joint, a cadaveric shoulder in conjunction with a jig and a Tekscan pressure sensor was employed to compare the joint proximity and contact area in both cases. The Tekscan system is an effective instrument for precisely measuring and analyzing interface pressure between two surfaces, using a thin and flexible sensor, which can be seen in Figure C-1. It has been used in numerous past studies to investigate joint contact and pressure throughout various positions, however, it is also known to introduce a lot of error into the system if not set up and calibrated correctly.

Therefore, the objective of this appendix was to validate the patient-specific bone models and the inter-bone distance algorithm that were used to determine glenohumeral joint proximity in Chapter 2 of this thesis, by using a cadaveric shoulder with a jig and a Tekscan pressure sensor.

C.2 Methods

Cadaver Prep

The use of one fresh-frozen shoulder cadaver specimen was used for this analysis. The dissection of the humerus and scapula from the shoulder specimen was completed by an orthopaedic resident in training. The removal of all soft tissues was completed so that the humeral head and glenoid fossa could be separated from one another. Articular cartilage on the bone surfaces remained. The humerus and glenoid were then potted into PVC piping using dental cement. Once this was complete, the humerus and glenoid were then placed back into the freezer.

3D Printing

Custom fit jig components were designed on SolidWorks and then printed using a 3D printer. Two components were made for the jig, one for the top and one for the bottom.

The bottom component was printed on the desired angle (either 0° or 10°) and placed within the columns to hold the potted glenoid in place within the jig. The top component was printed to hold the potted humeral head in place within the jig.

CT scan

The specimen was taken out of the freezer around 2 hours prior to the CT scans. The glenoid and humeral head were fit snug into the jig via the 3D-printed components, first setting the shoulder into the jig via the 0° component. Next, the correct force was applied to the jig (20N), which in this case was just the weight of the jig. The entire jig, including the glenoid and humeral head components, was then placed into the CT scanner. The same was repeated for the 10° position (Figure C-2)

A total of two CT scans of the shoulder (one at 0° and one at 10°) were obtained after the scanning was complete. These two CT scans were then used to make patient-specific models of the glenoid and humeral head. The same methods as described in Chapter 2 were used to make these bone models. After the 3D bone models were made, the same method employed in Chapter 2 was used to make the joint proximity maps of the shoulder in each position. A summary of these results can be seen in Figure C-5.

Tekscan

The same setup that was used for the CT scan was repeated for this analysis, but Tekscan was used for the tracking of the contact area and pressure. First, the pressure sensor was set up while the jig was in the 0° position (Figure C-3). Next, the acquisition parameteres were defined: Moving Frames = 5, Frequency = 1, Period =1, Duration = 5 sec. The correct force was applied to the jig (20N), which in this case was just the weight of the jig. A Tekscan recording was taken to obtain outcomes including centroid, contact area, and pressure. The same steps were repeated but with the jig in the 10° position (Figure C-4). Measurements were repeated again in the same positions so two trials could be obtained. Lastly, reprosil was used as the experimental cast material. In each position (0° and 10°) with the 20N weight of the jig, the reprosil was placed on the glenoid face and the jig was dropped into place. Around 6 minutes later, once the cast was solidified it was removed from the jig.

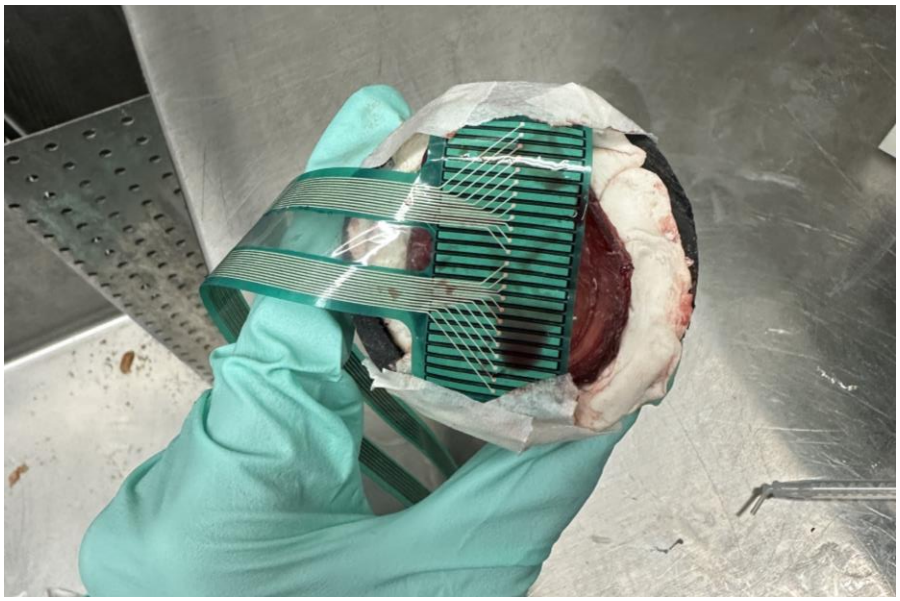

Figure C-1: Tekscan Overlayed on Glenoid Surface

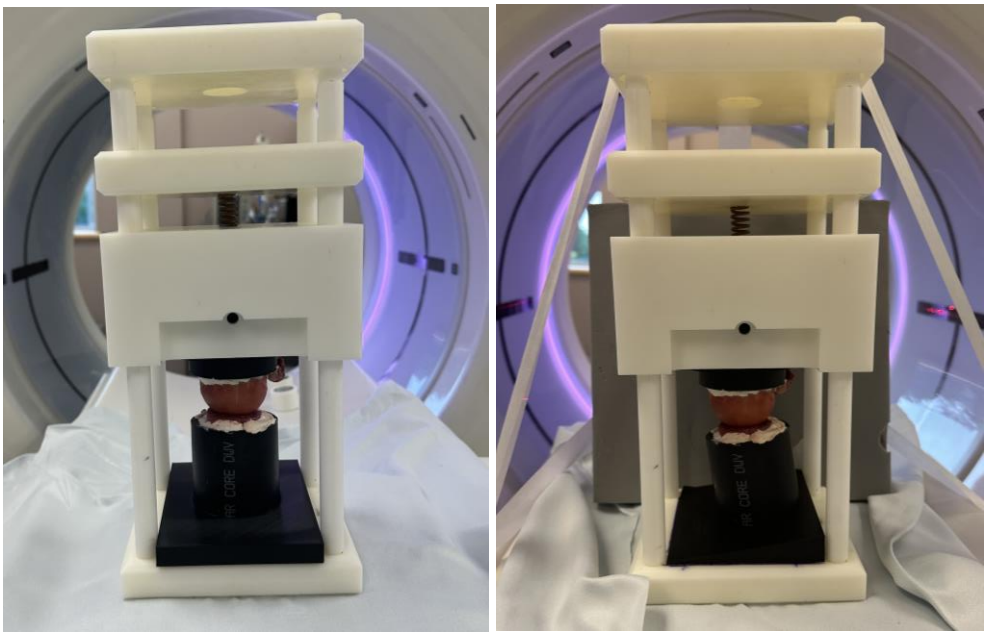

Figure C-2: Jig setup of cemeted glenoid and humeral head for 0° (left) and 10° (right) for CT scan

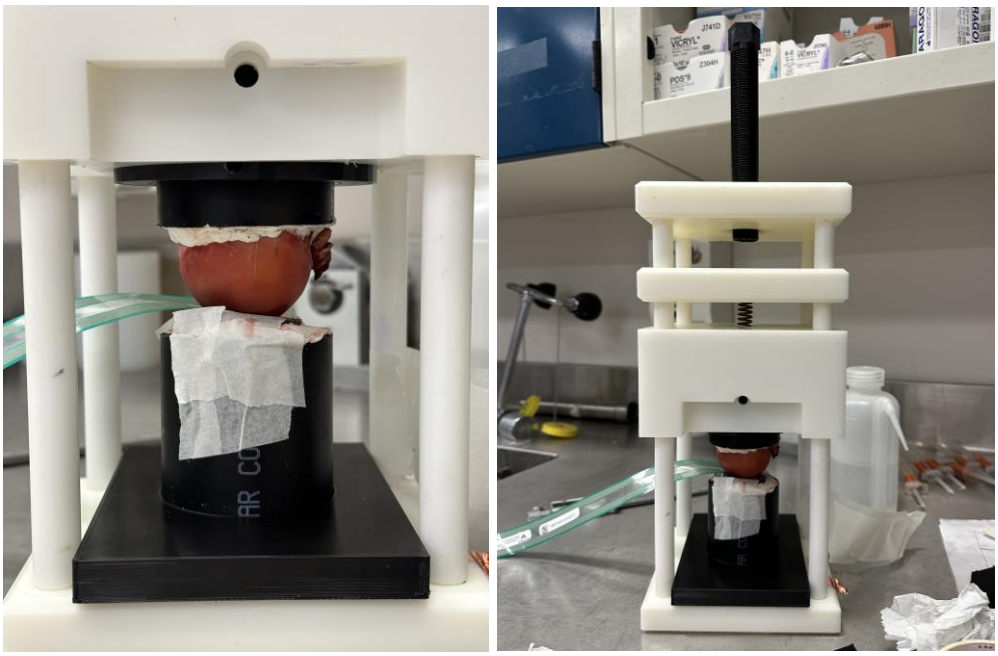

Figure C-3: Jig setup of cemeted glenoid and humeral head for 0° with Tekscan

Note: Closeup view of the joint surfaces in jig (left) and entire jig setup (right).

Figure C-4: Jig setup of cemeted glenoid and humeral head for 10° with Tekscan

Note: Closeup view of the joint surfaces in jig (left) and entire jig setup (right).

C.3 Results:

The proximity maps found for the 0° and 10° CT scans can be seen in Figure C-5. Note that 0mm (red) shows close proximity and 6mm (dark blue) shows far proximity.

The experimental casting that was placed between the cadaver joint surfaces during the Tekscan testing for 0° and 10° can also be seen in Figure C-5. Note that 0mm (see-through cast) shows close proximity and 2.5mm (dark orange) shows far proximity.

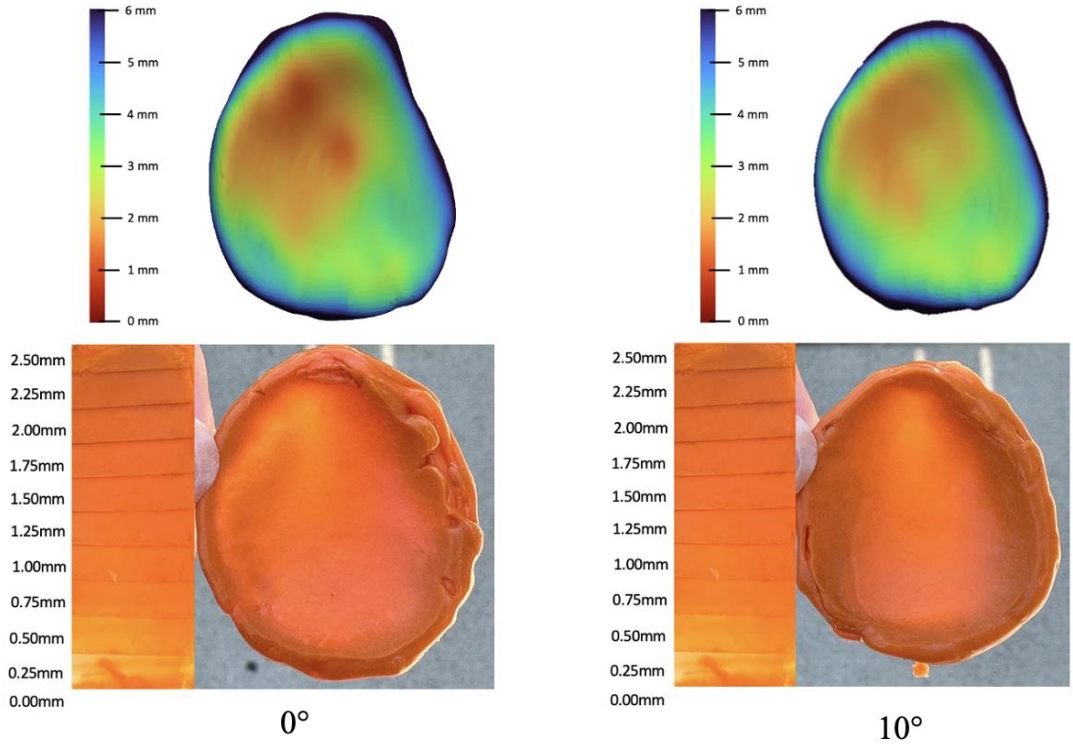

Figure C-5: Comparison of proximity maps (top) versus experimental casting (bottom) for 0° (left) and 10° (right)

A summary of the contact area found for both the CT scan and the Tekscan can be seen in Figure C-6. The total contact area (mm^2) for the 0° CT scan was found to be $796mm^2$ and for the 10° CT scan was found to be $736mm^2$. The total contact area (mm^2) for the 0° Tekscan was found to be $530mm^2$ and for the 10° CT scan was found to be $442mm^{2.}$ The percent errors were found to be 33% and 40% for the 0° and 10° setup, respectively.

	Contact Area (mm^2)		
	CT scan	**Tekscan**	**% Error**
0°	796	530	33%
10°	736	442	40%

Figure C-6: Contact Area Found Using CT Scan and Tekscan

C.4 Limitations

This biggest limitation to the work done in this appendix is that the CT scan and Tekscan were completed on different days. Although the 3D-printed components were printed to ensure the bones would be aligned exactly the same during both scans, due to the fact that the bones were taken out of the jig and placed back in the jig on a different day, introduces a lot of error in the exact positioning of the bones. This difference in bone positioning can be seen in Figure C-5 through the differences seen in contact on the proximity maps versus the experimental casting (which was taken the day of Tekscan).

Additionally, during the Tekscan testing, it appeared that the Tekscan pressure sensor did not fully cover the width of the glenoid. This could explain why the contact area found through Tekscan was a lot lower than the contact area found through the CT scans. As well, the Tekscan pressure sensor creased when the pressure of the bones was applied in the jig, distorting the contact that was picked up through the sensor. Both of these reasons may have caused the pressure sensor to not accurately capture the contact area, which could explain the high percent error seen between the CT scan and Tekscan.

Appendix D: Walch Type A1 Subluxation

D.1 Methods

In Chapter 3 of this thesis, an analysis was conducted on 20 Type B2 patients. Additionally, data from four Type A1 patients was also collected. However, this data was excluded from the final analysis due to the insufficient number of Type A1 patients recruited, which prohibited drawing robust conclusions about this cohort. The results for these four Type A1 patients will be highlighted in this appendix.

The same methods that were described in Chapter 3 of this thesis were used to complete the analysis on these four Type A1 patients (n=4).

D.2 Results

The mean subluxation postoperatively (51.3%) was similar to the mean subluxation preoperatively (50.5%) (Figure D-1 and Figure D-2).

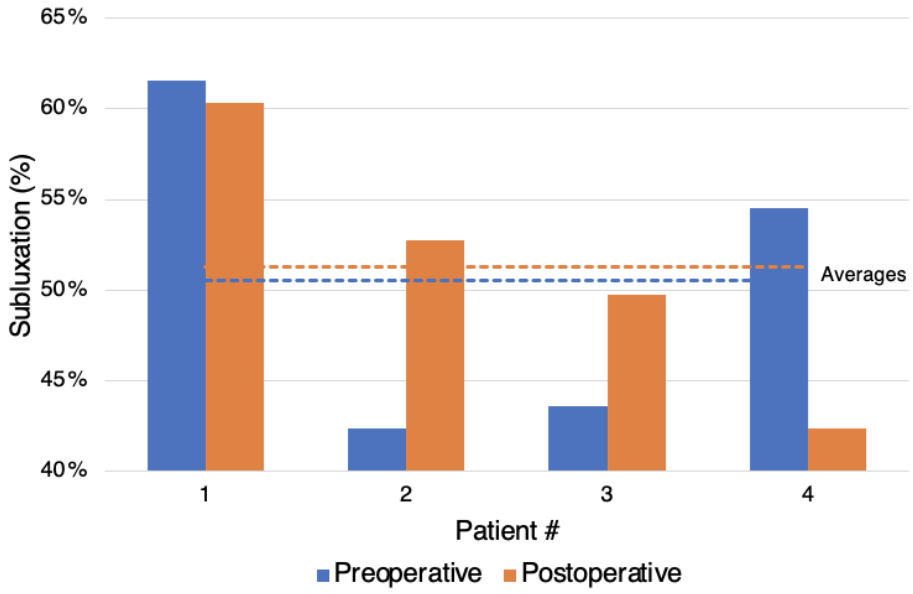

Figure D-1: Subluxation (%) preoperatively (static) versus postoperatively (dynamic) per patient

The mean preoperative subluxation (50.5%) is indicated by the blue dashed line and mean postoperative subluxation (51.3%) is indicated by the orange dashed line.

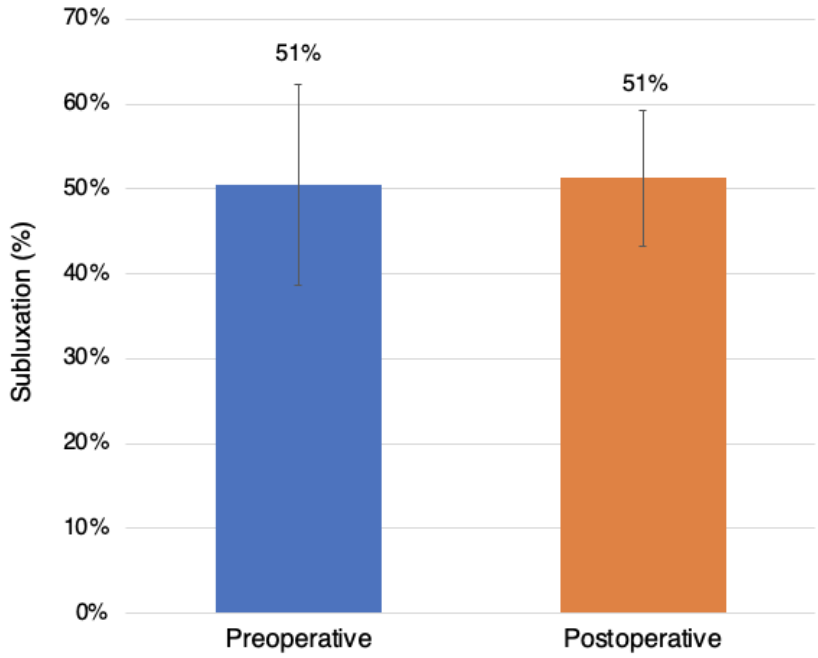

Figure D-2: Mean subluxation (%) preoperatively (static) versus postoperatively (dynamic) for all Walch type A1 patients

On average for all patients postoperatively, subluxation ranged from 50% to 54% throughout active IR, indicating that a minimal change in subluxation was present throughout the entire movement (Figure D-3).

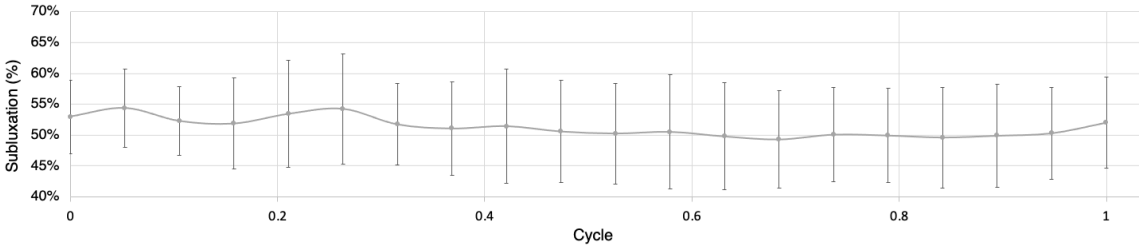

Figure D-3: Subluxation during active internal rotation for all Walch type A1 patients

Standard deviations are shown by the lines at each time point throughout the cycle.

Below is a look at a summary of all 24 patients that were analyzed. This includes the four Type A1 patients in addition to the 20 Type B2 patients (n=24). The mean subluxation postoperatively (54%) was an improvement to the mean subluxation preoperatively (63%) (Figure D-4 and Figure D-5).

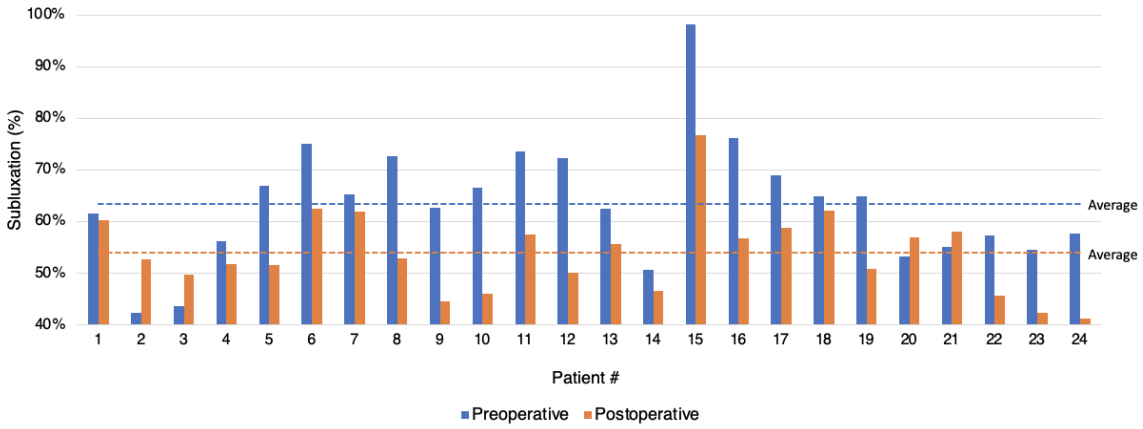

Figure D-4: Subluxation (%) preoperatively (static) versus postoperatively (dynamic) per patient.

The mean preoperative subluxation (63%) is indicated by the blue dashed line and mean postoperative subluxation (54%) is indicated by the orange dashed line.

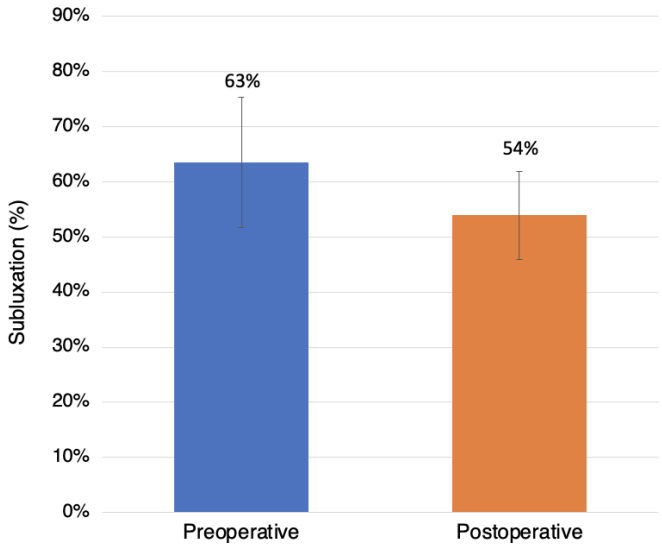

Figure D-5: Mean subluxation (%) preoperatively (statically) versus postoperatively for all patients (Type A1 and Type B2)

On average for all patients postoperatively, subluxation ranged from 53% to 55% throughout active IR, indicating that a minimal change in subluxation was present throughout the entire movement (Figure D-6).

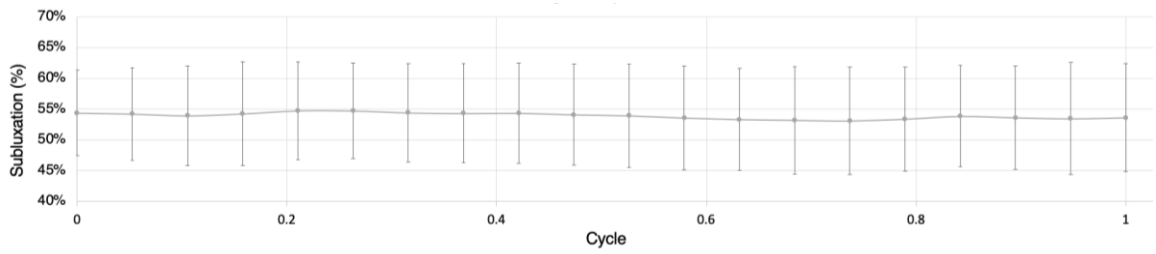

Figure D-6: Subluxation during active internal rotation for all patients (Type A1 and Type B2)

Standard deviations are shown by the lines at each time point throughout the cycle.

As stated before in Chapter 2 of this thesis, the range of motion (ROM) was documented for each patient when they performed IR during the preoperative scan and grouped into two cohorts based on a previously established IR vertebral range[11]: good ROM and limited ROM. The good ROM cohort included thirteen patients (n=13), and the limited ROM cohort included 11 patients (n=11). The subluxation preoperatively and postoperatively for patients in both the good ROM and limited ROM cohorts can be seen below in Figure D-7. The good ROM cohort were subluxated 66% preoperatively, and 56% postoperatively (10% subluxation correction). The limited ROM cohort were subluxated 60% preoperatively, and 52% postoperatively (8% subluxation correction). Both cohorts were able to be corrected on average from being posteriorly subluxated (66% for good ROM and 60% for limited ROM patients), to having nearly centred humeral heads (56% for good ROM and 52% for limited ROM patients).

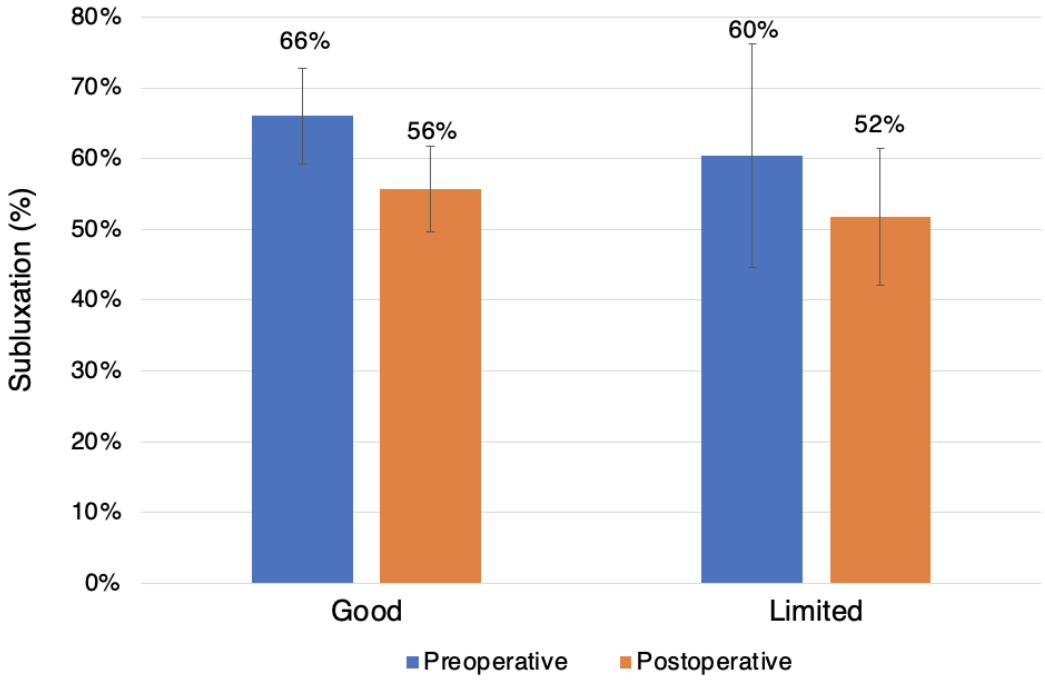

Figure D-7: Subluxation for patients with good ROM (n=13) versus limited ROM (n=11)

Appendix E: Glenohumeral Implant Mismatch

E.1 Introduction

When patients undergo a total shoulder arthroplasty (TSA), they are required to take a preoperative CT scan as a part of the preoperative planning protocol for the surgery. From this scan, the surgeon decides on a specific glenoid size and humeral head size based on the shape and size of the patient's anatomy. Stryker's Aequalis™ Perform™ + glenoid has been designed to be compatible with the Simpliciti™, Aequalis™, Affiniti™ and Ascend™ humeral head systems in certain combinations. Each combination has a specific diametrical mismatch that is recorded in millimeters.

E.2 Methods

All 24 patient (Type A1 and Type B2) mismatches were found by finding the difference in the radius of curvature between the humeral head implant component and the glenoid implant component. This mismatch (mm) was then used to compare to subluxation (%) to see if there was any correlation between the amount of subluxation postoperatively (throughout IR) and the implant mismatch the patient received. A plot of the mean subluxation postoperatively (throughout IR) versus glenohumeral implant mismatch (mm) was made and a line of best fit was added (Figure E-1).

E.3 Results

From the line of best fit, an $R^2 = 0.04$ was found. This displays that there is a very weak correlation between the implant mismatch received and subluxation, which implies that the type of implant mismatch did not affect the subluxation seen within the glenohumeral joint for the patients analyzed.

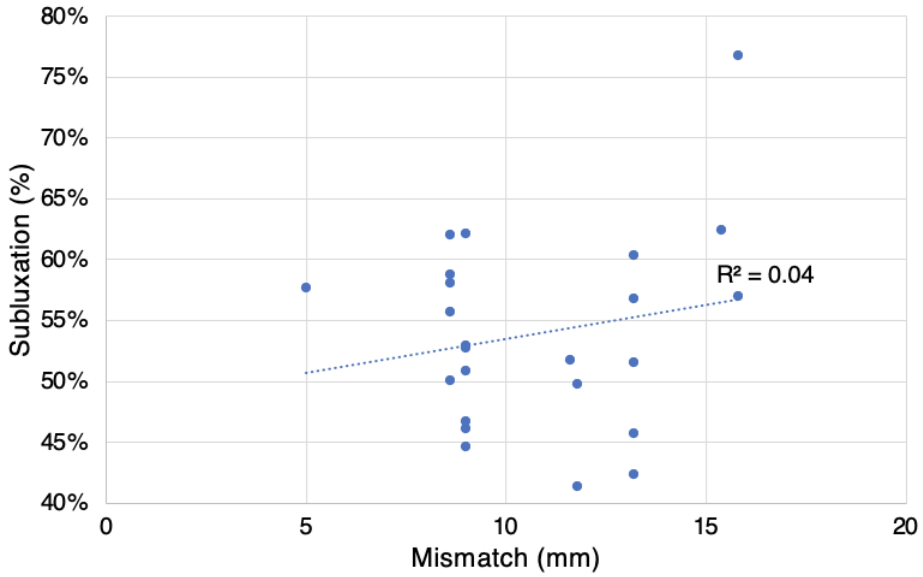

Figure E-1: Subluxation (%) postoperatively (throughout IR) versus implant mismatch (mm)

Appendix F: ASES Shoulder Score Survey

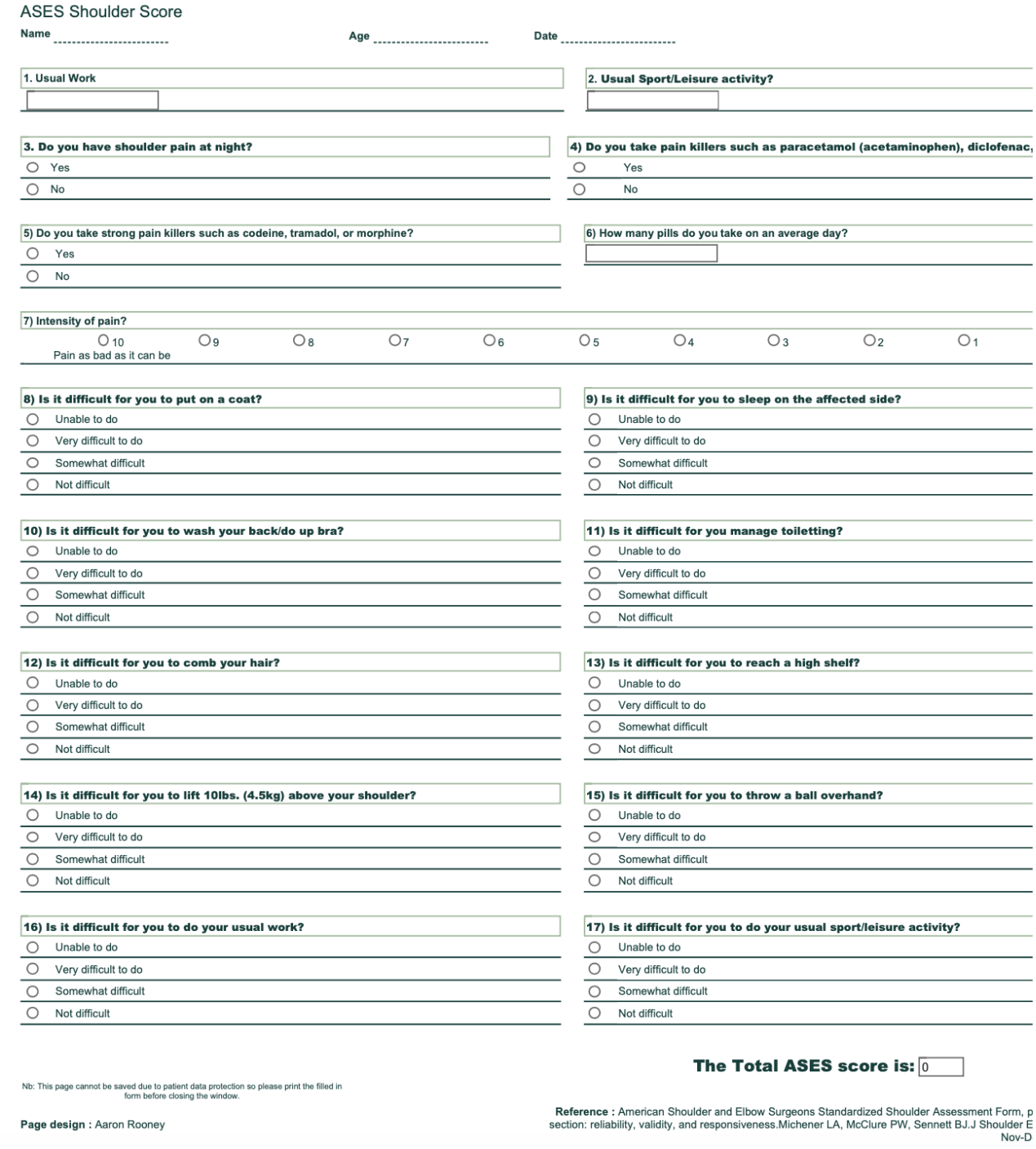

ASES Shoulder Score

Name ..... Age ..... Date .....

1. Usual Work

2. Usual Sport/Leisure activity?

3. Do you have shoulder pain at night?
- ○ Yes
- ○ No

4) Do you take pain killers such as paracetamol (acetaminophen), diclofenac,
- ○ Yes
- ○ No

5) Do you take strong pain killers such as codeine, tramadol, or morphine?
- ○ Yes
- ○ No

6) How many pills do you take on an average day?

7) Intensity of pain?

○10 ○9 ○8 ○7 ○6 ○5 ○4 ○3 ○2 ○1

Pain as bad as it can be

8) Is it difficult for you to put on a coat?
- ○ Unable to do
- ○ Very difficult to do
- ○ Somewhat difficult
- ○ Not difficult

9) Is it difficult for you to sleep on the affected side?
- ○ Unable to do
- ○ Very difficult to do
- ○ Somewhat difficult
- ○ Not difficult

10) Is it difficult for you to wash your back/do up bra?
- ○ Unable to do
- ○ Very difficult to do
- ○ Somewhat difficult
- ○ Not difficult

11) Is it difficult for you manage toiletting?
- ○ Unable to do
- ○ Very difficult to do
- ○ Somewhat difficult
- ○ Not difficult

12) Is it difficult for you to comb your hair?
- ○ Unable to do
- ○ Very difficult to do
- ○ Somewhat difficult
- ○ Not difficult

13) Is it difficult for you to reach a high shelf?
- ○ Unable to do
- ○ Very difficult to do
- ○ Somewhat difficult
- ○ Not difficult

14) Is it difficult for you to lift 10lbs. (4.5kg) above your shoulder?
- ○ Unable to do
- ○ Very difficult to do
- ○ Somewhat difficult
- ○ Not difficult

15) Is it difficult for you to throw a ball overhand?
- ○ Unable to do
- ○ Very difficult to do
- ○ Somewhat difficult
- ○ Not difficult

16) Is it difficult for you to do your usual work?
- ○ Unable to do
- ○ Very difficult to do
- ○ Somewhat difficult
- ○ Not difficult

17) Is it difficult for you to do your usual sport/leisure activity?
- ○ Unable to do
- ○ Very difficult to do
- ○ Somewhat difficult
- ○ Not difficult

The Total ASES score is: 0

Nb: This page cannot be saved due to patient data protection so please print the filled in form before closing the window.

Page design : Aaron Rooney

Reference : American Shoulder and Elbow Surgeons Standardized Shoulder Assessment Form, p section: reliability, validity, and responsiveness.Michener LA, McClure PW, Sennett BJ.J Shoulder E Nov-D

Figure F-1: ASES Shoulder Score Survey

Appendix G: References

1. von Eisenhart-Rothe RMO, Jäger A, Englmeier KH, Vogl TJ, Graichen H. Relevance of Arm Position and Muscle Activity on Three-Dimensional Glenohumeral Translation in Patients with Traumatic and Atraumatic Shoulder Instability. *Am J Sports Med*. 2002;30(4):514-522. doi:10.1177/03635465020300041101

2. Friedman RJ. Glenohumeral translation after total shoulder arthroplasty. *J Shoulder Elbow Surg*. 1992;1(6):312-316. doi:10.1016/S1058-2746(09)80058-X

3. Graichen H, Stammberger T, Bonel H, Karl-Hans Englmeier, Reiser M, Eckstein F. Glenohumeral translation during active and passive elevation of the shoulder — a 3D open-MRI study. *J Biomech*. 2000;33(5):609-613. doi:10.1016/S0021-9290(99)00209-2

4. Harryman D, Sidles J, Clark J, McQuade K, Gibb T, Matsen F. Translation of the humeral head on the glenoid with passive glenohumeral motion. *J Bone Joint Surg Am*. 1990;72:1334-1343. doi:10.2106/00004623-199072090-00009

5. Howell SM, Galinat BJ, Renzi AJ, Marone PJ. Normal and abnormal mechanics of the glenohumeral joint in the horizontal plane. *J Bone Joint Surg Am*. 1988;70(2):227-232.

6. Karduna AR, Williams GR, Iannotti JP, Williams JL. Kinematics of the glenohumeral joint: Influences of muscle forces, ligamentous constraints, and articular geometry. *J Orthop Res*. 1996;14(6):986-993. doi:10.1002/jor.1100140620

7. Karduna AR, Williams GR, Williams JL, Iannotti JP. Glenohumeral Joint Translations before and after Total Shoulder Arthroplasty. A Study in Cadavera*. *JBJS*. 1997;79(8):1166.

8. Kozono N, Okada T, Takeuchi N, et al. In vivo kinematic analysis of the glenohumeral joint during dynamic full axial rotation and scapular plane full abduction in healthy shoulders. *Knee Surg Sports Traumatol Arthrosc*. 2017;25(7):2032-2040. doi:10.1007/s00167-016-4263-2

9. Massimini DF, Boyer PJ, Papannagari R, Gill TJ, Warner JP, Li G. In-vivo glenohumeral translation and ligament elongation during abduction and abduction with internal and external rotation. *J Orthop Surg*. 2012;7:29. doi:10.1186/1749-799X-7-29

10. Matsumura N, Oki S, Fukasawa N, et al. Glenohumeral translation during active external rotation with the shoulder abducted in cases with glenohumeral instability: a 4-dimensional computed tomography analysis. *J Shoulder Elbow Surg*. 2019;28(10):1903-1910. doi:10.1016/j.jse.2019.03.008

11. Triplet JJ, Everding NG, Levy JC, Moor MA. Functional internal rotation after shoulder arthroplasty: a comparison of anatomic and reverse shoulder arthroplasty. *J Shoulder Elbow Surg*. 2015;24(6):867-874. doi:10.1016/j.jse.2014.10.002

Curriculum Vitae

Name: Kylie Kiera Paliani

Post-secondary Education and Degrees

Master of Engineering Science (MESc) in Biomedical Engineering (Biomechanics)
University of Western Ontario
London, Ontario, Canada
2022-2024

- Collaborative Specialization in Musculoskeletal Health Research (CMHR)

Bachelor of Engineering Science (BESc) in Mechanical Engineering with Professional Internship
University of Western Ontario
London, Ontario, Canada
2016-2021

- Graduated with Distinction and with the CSME Gold Medal Award (2021) for a graduating student with outstanding academic achievement

Related Work Experience

Graduate Teaching Assistant (TA)
University of Western Ontario
London, Ontario, Canada
2022-2024

Courses Included:
MME4470 - Medical and Assistive Devices
MME2202 - Mechanics of Materials
ES1050 - Foundations of Engineering Practice

Medical Device Designer of a Surgical Mechanism for Rotational Osteotomies
ADEISS and University of Western Ontario
London, Ontario, Canada
2020-2021

Co-Founder, Co-President, and VP External of Western Engineering Biomedical Club (WEBMC)
University of Western Ontario
London, Ontario, Canada
2017-2021

Other Related Work Experience

Communications Lead for Trainee Leadership Committee
Western Bone and Joint Institute
London, Ontario, Canada
2023-2024

Honours and Awards

Western Graduate Research Scholarship | 2022-2024

- Awarded to a full-time graduate student that has the motivation, commitment, and conscientious understanding of academic study in the Faculty of Engineering that is consistent with their expectations and aspirations ($32,500)

Graduation with Distinction | 2021

- Awarded to graduating students who have achieved an overall average of 80% or more (i.e. Dean's Honour List) in every year of study after first year

Dean's Honour List | 2016-2021

- Awarded to students who have achieved an overall average of 80% or more

Canadian Society of Mechanical Engineering (CSME) Gold Medal Award | 2021

- Awarded to a graduating student for outstanding academic achievement (Gold Medal Pendant)

Ontario Professional Engineers Foundation for Education Scholarship | 2018

- Awarded to an undergraduate student with outstanding academic achievement and demonstrated leadership skills as a major participant in an organization or activity related to engineering ($1500)

Professional Engineers of Ontario (PEO) Chapter Scholarship | 2016

- Awarded for excellence in academics, extra-curricular activities, community service and interest in pursuing a career in Engineering as a licensed professional Engineer ($500)

Publications

Paliani, K., Hunter, J., Johnson, J. Lee, T-Y., Athwal, G., Lalone, E. Posterior Augmented Polyethylene Glenoid Implants Correct Posterior Subluxation and Maintain Joint Reduction during Active Motion. *In the process of being submitted to the Journal of Shoulder and Elbow Surgery (JSES).*

Paliani, K., Hunter, J., Johnson, J. Lee, T-Y., Athwal, G., Lalone, E. Analysis of Healthy Glenohumeral Arthrokinematics using Four-Dimensional Computed Tomography throughout Internal Rotation and Forward Elevation. *Accepted to be published in the Journal of Shoulder and Elbow Surgery (JSES) International.*

Presentations at Scientific Meetings

Paliani, K., Hunter, J., Johnson, J. Lee, T-Y., Athwal, G., Lalone, E. (2024) Analysis of Healthy Glenohumeral Arthrokinematics using Four-Dimensional Computed Tomography throughout Internal Rotation and Forward Elevation. *Canadian Orthopaedic Research Society (CORS),* Halifax, Nova Scotia, Canada**.**

Paliani, K., Hunter, J., Johnson, J. Lee, T-Y., Athwal, G., Lalone, E. (2024) Analysis of Healthy Glenohumeral Arthrokinematics using Four-Dimensional Computed Tomography throughout Internal Rotation and Forward Elevation. *Ontario Biomechanics Conference,* Toronto, Ontario, Canada.

Paliani, K., Hunter, J., Johnson, J. Lee, T-Y., Athwal, G., Lalone, E. (2023) Analysis of Healthy Glenohumeral Arthrokinematics using Four-Dimensional Computed Tomography throughout Internal Rotation and Forward Elevation. *Ontario Biomechanics Conference,* Waterloo, Ontario, Canada.